Comprehensive Summaries of Uppsala Dissertations
from the Faculty of Science and Technology 756

Non-Orthogonality and Electron Correlations in Nanotransport

Spin- and Time-Dependent Currents

BY

JONAS FRANSSON

ACTA UNIVERSITATIS UPSALIENSIS
UPPSALA 2002

Non-Orthogonality and Electron Correlations in Nanotransport

Spin- and Time-Dependent Currents

BY

JONAS FRANSSON

Dissertation for the Degree of Doctor of Philosophy in Physics presented at Uppsala University in 2002

Abstract

Fransson, J. 2002. Non-orthogonality and electron correlations in nanotransport. Spin- and time-dependent currents. Acta Universitatis Upsaliensis. *Comprehensive Summaries of Uppsala Dissertations from the Faculty of Science and Technology* 756. 101 pp. Uppsala. ISBN 91-554-5418-6.

The concept of the transfer Hamiltonian formalism has been reconsidered and generalized to include the non-orthogonality between the electron states in an interacting region, e.g. quantum dot (QD), and the states in the conduction bands in the attached contacts. The electron correlations in the QD are described by means of a diagram technique for Hubbard operator Green functions for non-equilibrium states.

It is shown that the non-orthogonality between the electron states in the contacts and the QD is reflected in the anti-commutation relations for the field operators of the subsystems. The derived formula for the current contains corrections from the overlap of the same order as the widely used conventional tunneling coefficients.

It is also shown that kinematic interactions between the QD states and the electrons in the contacts, renormalizes the QD energies in a spin-dependent fashion. The structure of the renormalization provides an opportunity to induce a spin splitting of the QD levels by polarizing the conduction bands in the contacts and/or imposing different hybrizations between the states in the contacts and the QD for the two spin channels. This leads to a substantial amplification of the spin polarization in the current, suggesting applications in magnetic sensors and spin-filters.

Jonas Fransson, Department of Physics, Uppsala University, Box 530, SE-751 21 Uppsala, Sweden

© Jonas Fransson 2002

ISSN 1104-232X
ISBN 91-554-5418-6

Printed in Sweden by Eklundshofs Grafiska AB, Uppsala 2002

To my flowers, one, two, three

List of publications

I. On the non-orthogonality problem in the description of quantum devices
J. Fransson, O. Eriksson, B. Johansson, and I. Sandalov,
Physica B **272**, 28 (1999).

II. Effects of non-orthogonality in the time-dependent current through tunnel junctions
J. Fransson, O. Eriksson, and I. Sandalov,
Physical Review B, Brief Reports **64**, 153403 (2001).

III. Effects of non-orthogonality and electron correlations in the time-dependent current through quantum dots
J. Fransson, O. Eriksson, and I. Sandalov,
Physical Review B (2002) *(accepted).*

IV. Time-dependent transport in quantum dot systems
J. Fransson,
Submitted to Int. J. Quantum Chem (2002)

V. Many-body approach to spin-dependent transport in quantum dot systems
J. Fransson, O. Eriksson, and I. Sandalov,
Physical Review Letters **88**, 226601 (2002).

Erratum: Many-body approach to spin-dependent transport in quantum dot systems [Phys. Rev. Lett. 88, 226601 (2002)
J. Franssson, O. Eriksson, and I. Sandalov,
Physical Review Letters (2002) *(accepted).*

VI. Theory of spin-filtering through Fe-Pd-Fe nano-structures
J. Fransson, E. Holmström, O. Eriksson, and I. Sandalov,
In manuscript.

VII. Cluster approach to transport through complex nanostructures
I. Sandalov, O. Eriksson and J. Fransson,
Submitted to Physical Review B (2002)

Comment: The Erratum to **Paper V** provides corrections of two typos in the paper. However, the calculations and the conclusions of the paper are unaffected.

Publication not included in this thesis

A non-Kondo description of the experimentally observed "Kondo resonances" in quantum dots
J. Fransson and I. Sandalov,
in *Kondo effect and dephasing in low-dimensional metallic systems*, ed. V. Chandrasekhar, C. Van Haesendonck, and A. Zawadowski, **NATO Science Series**, Kluwer Academic Publishers, Dordrecht, The Netherlands (2001).

Comments on my participation

In all contributed papers I have participated in formulating the problems, I have carried out most of the derivations leading to the presented results and performed all numerical computations except for parts of the computations in **Paper VI**. In addition, I have written all manuscripts but **Paper I** and **Paper VII**, which I have co-authored, and **Paper VI**, which I have written the major parts of.

CONTENTS

List of publications i

Publication not considered in the thesis ii

Comments on my participation ii

Om elektrisk ström och kvantprickar 1

Introduction 7

1 Electric current 11
1.1 General formulation of charge current 11
1.2 Tunneling phenomenon 14
1.2.1 Penetration of a barrier 14
1.2.2 Transmission resonances 16

2 Transport in mesoscopic systems 19
2.1 Boltzmann equation 19
2.2 Kubo formula 22
2.3 Landauer formula 25

3 Transfer Hamiltonian formalism 29
3.1 Generalization of the formalism 30

4 Current through quantum dots 35
4.1 Non-equilibrium Green function approach 36
4.2 Non-orthogonality and many-body states 40
4.2.1 Commutation relations 42
4.2.2 Dynamics of the conduction electrons 42
4.3 Current in the non-orthogonal framework 43

5 Focusing on the quantum dot **49**
5.1 Single-particle picture 50
5.1.1 Non-interacting resonant level 51
5.1.2 Weak-coupling mean-field approximation 52
5.1.3 Further perturbation expansion 52
5.1.4 Simple model of a Coulomb island 53
5.1.5 The retarded and lesser quantum dot Green functions 54
5.2 Many-body picture 55
5.2.1 Diagram technique in brief 57
5.2.2 Hubbard I approximation 60
5.2.3 Loop correction 61
5.2.4 The retarded and lesser quantum dot Green functions 66
5.3 Non-orthogonality in the many-body picture 67
5.3.1 The retarded and lesser quantum dot Green functions 71
5.4 Comparison of the different approaches 72

6 Some recent results **81**
6.1 Alternative opportunity to induce spin-dependent transport 81
6.2 Cluster approach to transport in nanostructures 83

Summary **87**
What's next? 89

Appendix **90**

A Diagram technique **91**

Acknowledgments **95**

Bibliography **97**

Om elektrisk ström och kvantprickar

För den som inte haft lyckan att studera fysik ter sig titeln på den här avhandlingen, tillika titeln på föreliggande avsnitt, möjligen något eländig. De flesta har antagligen en vag uppfattning om vad elektrisk ström är men vad är en kvantprick? I denna inledning skall vi söka reda ut en del begrepp som förekommer i de följande kapitlen, vilka lätt kan framstå som en sörja av matematisk rotvälska med symboler och beteckningar som icke-fysiker/matematiker inte vill kännas vid. Avsikten är att göra det möjligt för fler än fysiker och matematiker att känna sig välkomna till det som tillhandahålls och som ett löfte skall det inte användas någon matematik i denna inledning.

För oss, som lever i den "moderna" västvärlden, är elektrisk ström något som tas för givet, vare sig man vill veta vad det handlar om eller inte. Vi trycker

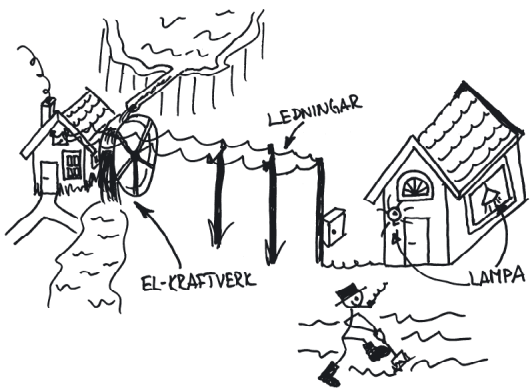

Figure 1: Vid vattenkraftverket (El-kraftverk) genereras en elektrisk ström som förs via ledningarna till lampan. Lampan tänds/släcks med en strömbrytare i huset.

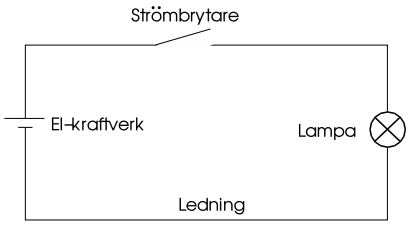

Figure 2: Schemastisk bild över den slutna kretsen bestående av kraftverket, ledningarna strömbrytaren och lampan.

på strömbrytaren till kökslampan och ljuset tänds. För att en elektrisk ström skall kunna uppstå måste det finnas ett slutet system, eller en så kalled sluten krets. I fallet med kökslampan består systemet av elkraftverket, ledningarna till och från lampan samt lampan själv, jämför Fig. 1 och 2. När vi trycker på strömbrytaren sluts systemet och *laddningar* börjar att röra sig i kretsen. I kretsen utgörs laddningarna av *elektroner*, små partiklar som vanligtvis kretsar runt *atomkärnor*. Ibland kan de dock röra sig någorlunda fritt i ett material, vilket är fallet när de utgör en elektrisk ström. Elektroner bär mängder av, i det närmaste fantasifulla, egenskaper som "synligörs" vid olika tillfällen. De kretsar t.ex. runt atomkärnorna i stabila banor med bestämda energier. (Jämförelsevis kretsar inte satelliter runt jorden med samma stabilitet. De tappar hela tiden något av sin energi och närmar sig långsamt jorden, för att till sist krascha på jordytan. Förhoppningsivs då i ett hav långt bort från alla människor.)

De väl bestämda energierna, *energikvantiseringen*, som elektronerna har i sina banor runt atomkärnorna, kan utnyttjas i flera sammanhang. Den stora tillämpning i dagens värld är i första hand inom elektronikindustrin. I TV-apparater, datorer, mobiltelefoner, bilar, båtar, flygplan, raketer m.m. m.m. finns den elektronik som ständigt drar nytta av elektroners energikvantisering. På 1950-talet lanserades den s.k. *transistorradion* och trots att inte så många då brydde sig om vad en transistor var, har ordet fastnat i svenskan. En transistor är en elektronisk komponent som byggs av ett *halvledarmaterial*. Ordet halvledare kommer från att materialet ibland leder ström och ibland inte, beroende på omgivningen. Lite mer komplicerat är det att beskriva hur en transistor fungerar. Emellertid, i gränsskiktet mellan de delar som kallas *kollektor* och *emitter* bildas en *två-dimensionell elektrongas* vilken spelar en väsentlig roll i moderna transistorer, se Fig. 3 på sida 3.[1] Den två-dimensionella elektrongasen bildas i en så kallad *kvantbrunn* i vilken elektronerna tillåts röra sig fritt i två riktningar men där rörelsen i den tredje begränsas av energikvantisering i kvantbrunnen. Det innebär i sin tur att de energinivåer som kvantiseringen ger upphov till, bara kan besättas av ett givet antal elektroner.När de är besatta kan det inte komma in fler elektroner i kvantbrunnen. Antag nu att en elektrisk *spänning* sätts över kollektor/emitter-övergången.

[1]Beskrivningen avser en MOSFET (Metal Oxide Semiconductor Field Effect Transistor/Metall-Oxid-Halvledar-Fält-Effekt-Transistor) som är en modernare och energisnålare variant av den ursprungliga transistorn.

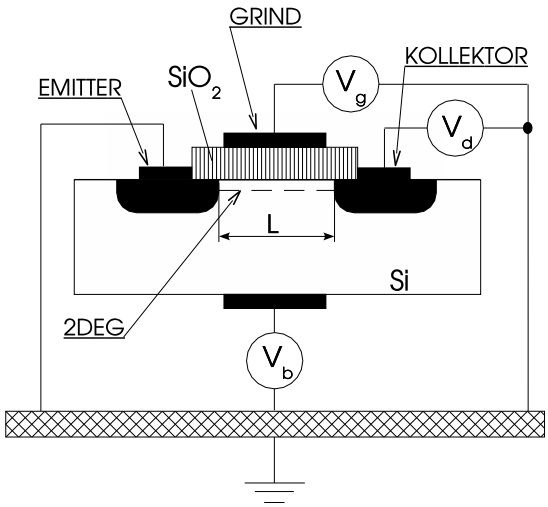

Figure 3: Schematisk skiss över en MOSFET uppbyggd av en bit kisel (Si) på vilken ett isolerande kiseldioxid-skikt (SiO_2) läggs mellan emittern och kollektorn. På oxid-skiktet placeras ett kisel-skikt, grinden, till vilken en spänning kopplas. Mellan emittern och kollektorn finns en två-dimensionell elektrongas (2DEG) med de energinivåer som strömmen drivs genom.

Då kan man med hjälp av det som kallas *grinden*, jämför Fig. 3, kontrollera om det skall gå en ström genom tranistorn eller inte. Transistorn fungerar alltså som en elektronisk strömbrytare. Storleksordningen på de transistorer som idag används kommersiellt ligger på mellan 1-1000 μm.[2]

I detta sammanhang kan vi komma in på kvantprickar. En skiss över en experimentell kvantprick kopplad till ledningar återfinns i Fig. 4 på sida 4. Som ett exempel på storleksordningen kan nämnas att lagret märkt SiO_2, Fig. 4, inte är mer än ungefär 3 nm tjockt.[3] Kvantpricken dimensioner är därmed cirka $3\times3\times3$ nm^3 (kubiknanometer). Det visar sig nu att om man gör de elektroniska komponenterna så mycket mindre, i storleksordningar mellan 1-1000 nm, kan de beräkningsformler och regler som används för transistorer inte längre kan tillämpas. Således har den *makroskopiska* (stora) världens regler lämnats bakom och den *mikroskopiska* (lilla) världens lagar har tagit överhanden. Ofta benämns komponenterna i denna storleksordning som *mesoskopiska*, där mesoskopisk förstås som en luddig gräns mellan det mikro- och makroskopiska. Det är dock inte bara storleken som skiljer en kvantprick från en vanlig transistor. De vanliga transistorerna innehåller en två-dimensionell elektrongas och den utnyttjas även i samband med kvantprickar. Emellertid avskärmas kvantbrunnen som bär elektrongasen ytterligare, till att bli *noll-dimensionell*, d.v.s. att energinivåerna i kvantbrunnen blir sådana att elektronernas rörelser begränsas i rummets alla tre riktningar.

[2] 1 μm (mikrometer) är en miljondels meter, eller 0,000 001 m.
[3] 1 nm (nanometer) är en miljarddels meter, eller 0,000 000 001 m.

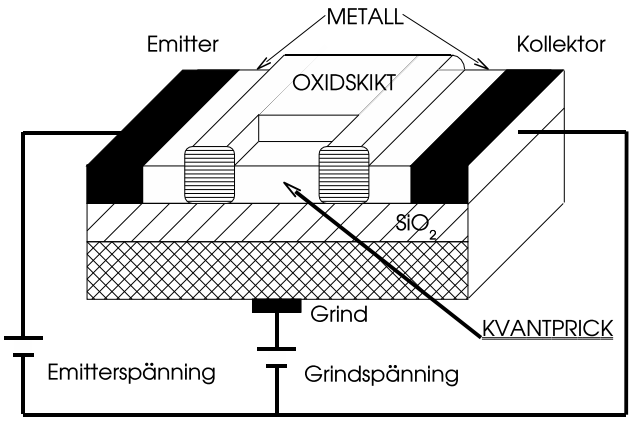

Figure 4: Skiss över en experimentell kvantprick. Emittern och kollektorn är separerade från kvantpricken medelst oxidskiktet som utgör tunnlingsbarriärer.

Kvantprickar erhålles också genom att man skapar t.ex. metallkulor i nanometerstorlek. Detta exempel visar tydligt vad som är avgörande för om man har att göra med en kvantprick eller inte. Vi gör en jämförelse. Antag att man inuti en fotboll har en lös stenkula. Stenkulan kan då röra sig i rummets alla tre riktningar, d.v.s. åt alla håll inuti bollen. Antag nu att vi drar en tråd genom stenkulan, som råkade ha ett hål rakt genom, och knyter fast stenkulan i tråden. Om vi därefter fäster tråden diametralt i bollen, begränsas stenkulans rörelser till två riktninar inuti bollen, den kan fritt svänga framåt och bakåt och i sidled men inte vare sig upp eller ner eftersom stenkulan är fastknuten i tråden, jämför Fig. 5 a). Detta motsvarar i någon mening den två-dimensionella elektrongasen. Om vi drar ytterligare en tråd genom stenkulan och fäster den, så att trådarna bildar ett kors i bollen, medför det att stenkulan endast kan svänga i en riktning, Fig.

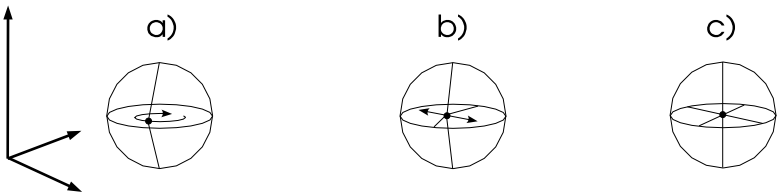

Figure 5: Stenkulan i fotbollen. I a) är en tråd dragen genom kulan och dess rörelser begränsas till två riktningar - kan ge upphov till en cirkulär rörelse. När två trådar dras genom kulan, b), kan kulan endast röra sig i en riktning och med tre trådar, alla vinkelräta mot varandra, kan kulan inte röra sig i någon riktning. Rummet beskrivs med de tre riktningar som koordinatsystemet utpekar (längst till vänster).

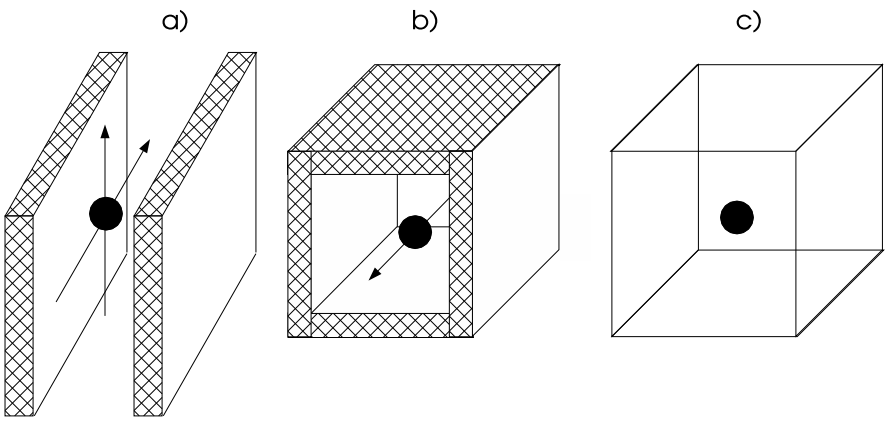

Figure 6: Rumslig kvantisering av en elektron. För en elektron som placeras mellan två oändligt stora plan, a), kvantiseras energierna i en dimension medan dess tillåtna energier i de två övriga riktningarna är obegränsat många. Om rummet avskärmas i två riktningar, b), tillåts elektronen fria energier endast i en riktning samtidigt som de kvantiseras i de två övriga. En elektron som är innesluten i en låda, c), har kvantiserade energier i alla rummets riktningar. För denna typ av kvantisering bör lådan vara i nanometer-storlek.

5 b). Med hjälp av en tredje tråd genom stenkulan, som fästs vinkelrät mot de två övriga, kan stenkulan inte röra sig fritt i någon riktning, Fig. 5 c). Stenkulans rörelser har blivit tre-dimensionellt begränsade, vilket är detsamma som att dess rörelserymd har blivit noll-dimensionell. Omvandlat till elektroner och kvantbrunnar, så motsvaras stenkulans rörelserymd av elektronernas energikvantisering. Intuti den nanometerstora metallkulan, kvantpricken, kvantiseras elektronernas tillgängliga energinivåer i alla rummets riktningar. Om det finns en elektron i kvantpricken, har den en given energi och ingen annan, jämför Fig. 6.

Ett fenomen hos elektroner som är avgörande inom min forskning är deras möjlighet att gå genom material på ett sätt som synes vara en inbillning. Antag att vi har ett bollplank och skjuter en boll mot det, se Fig. 7. De enda sätten för bollen att komma till andra sidan av bollplanket är antingen att skjuta bollen över planket eller, mer dramatiskt, skjuta bollen så hårt mot planket att det går sönder och bollen far rakt genom. Den sistnämnda möjligheter är mindre önskvärd, ty då har bollplanket mist sin funktion för senare bruk. Vi bortser från detta alternativ. För en elektron finns ett alternativ till att skjutas över en *potentialbarriär*, vilket är den kvantmekaniska motsvarigheten till bollplanket. Den kan nämligen gå genom barriären utan att barriären förstörs. Elektronen sägs *tunnla* genom barriären. Detta kan tyckas vara tämligen akademiskt men faktum är att dessa potentialbarriärer finns på många håll i den värld vi befinner oss. I samband med elektroniska tillämpningar består potentialbarriärerna av gränskikt mellan olika material, som t.ex. ledningarna till och från kvantprickar. När det går en elektrisk ström genom kvantpricken, tunnlar en elektron först från ena ledningen in i kvantpricken. Därefter tunnlar elektronen vidare, från kvantpricken till den

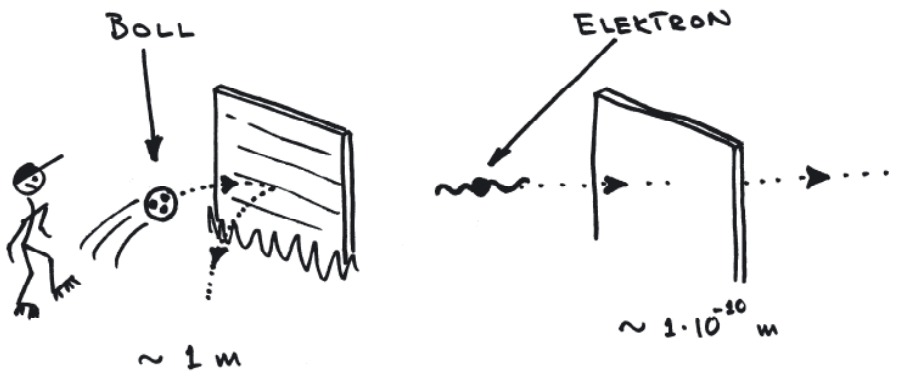

Figure 7: En boll som skjuts mot en vägg studsar tillbaka. En elektron som skjuts mot en barriär kan *antingen* studsa tillbaka (reflekteras) *eller* gå rakt genom (tunnla).

andra ledningen. Potentialbarriärerna mellan kvantpricken och ledningarna, är nödvändiga för att kvantpricken skall bibehålla sina egenskaper som kvantprick.

Som alltså nämnts, handlar kvantprickar om mycket små elektronikkomponenter. Eventuellt skall dessa kunna användas för att ge oss mångfaldigt mycket snabbare och mer minnesspäckade datorer, mobiltelefoner m.m. Vad man än kan tycka om tillämpningarna innehåller kvantprickarna en hel del intressant att sysselsätta sig med, som att utveckla teorier för hur de fungerar och för hur de skall kunna användas. Med hjälp av kvantprickar har en hel rad *kvantmekaniska* fenomen har kunnat renodlas och studeras. Det är åt utvecklingen om förståelsen av några utav dessa som jag ägnar denna avhandling. De metoder som jag använt är en del av den teoretiska fysikerns vardag, nämligen att med matematiska metoder söka beskriva det som observeras i experiment. Trots att innehållet i Kap. 1 - 5 kan synas vara ett sätt att briljera och visa min förträfflighet i att excellera med matematiska beräkningar, handlar det självfallet inte om det, bara lite;-) Att begå överdrivna excesser i matematiska härledningar av fysikaliska formler är min stora perversion i livet och kanske ett uttryck för min önskan att njuta av mitt arbete. Lite förnumstigt skulle man säga att det är vägen och inte målet som är det viktiga, men faktiskt, resultaten skulle inte betyda någonting om det inte vore för alla de våndor, all ångest över att inte begripa någonting, de aha-upplevelser som någon gång emellanåt ger sig tillkänna och allt trasslande med ekvationer, summor och integraler. Det handlar istället om att det matematiska språket har visat sig vara överlägset för att finna grunden för de fenomen som söks. Det ger en enkel (tro det eller ej) och, i slutändan, kortfattad beskrivning av det observerbara.

Introduction

A QUANTUM DOT IS, in a sense, the ultimate limit of what mankind has been able to manufacture that resembles an atom or a molecule. In fact, in all those devices called quantum dots, one of the most remarkable features is that the energy levels available for electrons, in the quantum dot, are very clearly discretized in all three spatial directions. One talks about that the quantum dots are quasi zero-dimensional, since the electrons in the dots experience a three dimensional confinement. Being a result of shrinking the size of a piece of matter, it is natural that the larger quantum dots can contain more electrons than the smaller ones. Indeed, the smallest possible quantum dot, which should be of any technical interest, contains a single electron. Thus, such a device would be a very nice manifestation of a controllable single spin-moment. In the state of the art technology of today, it is possible to make quantum dots out of very small metallic grains with sizes down to 4-5 nm. For such quantum dots, the separation between the energy levels is sufficiently large that single-electron transistors can be constructed, where the quantum dot plays the role of the active component in the device. When the quantum dot is coupled to contact leads, a single level can be tuned in to become conducting for rather a large bias voltage regime. However, in order to construct effective single-electron devices one does not have to have such small quantum dots. On the other hand, these smallest devices illustrate the beautiful and attractive possibilities that may be found in nature when ones mind is not restricted to common sense and rules.

Although quantum dots by themselves display interesting physics, they become even more attractive when two, or more, conducting leads are attached to them. Because of the energy discretization in the quantum dots, they show a very distinct onset of the current through the system, as one level becomes conducting when the source-drain voltage is increased. Such a behaviour is attractive, for instance, in digital electronics applications, where a clear distinction between the 0- and 1-state is desirable. However, an even more fascinating prospect the single-electron devices invite to is the observation of the magnetic moment of the quantum dot. In the simplest case, the quantum dot with a single available energy level, the magnetic moment of the quantum dot is zero when it is unoccupied by an electron. When an electron populates the quantum dot, the magnetic moment becomes one Bohr magneton. The difference of these magnetic moments

is experimentally observable and therefore also technically applicable.

The opportunity of changing the magnetic moment in the quantum dot by observing whether an electron occupies the quantum dot or not, is pleasant. However, suppose that the quantum dot is occupied by an electron and suppose that its spin state is up. Then, by a magnetic field applied over the quantum dot, the spin of the electron may be switched to the down state. Then, after terminating the magnetic field, the spin of the electrons remains in the down state, however, eventually the electron spin will change its character due to spin-lattice relaxations and exchange correlations in the quantum dot. Nevertheless, without leading any charge current through the system, one yet has changed the structure of the system. Talking about digital applications, then the 0- and 1-states would be represented by the spin projections up and down of the electron. By a combination of driving a charge current through the system and by manipulating the spin projection of the electrons in the quantum dot one would, in principle, be able to construct technical applications far beyond todays single-minded electronics.

Let us now discuss some scientific hardware. Electronics based on semiconductor devices have been around, at least, since the 1950s. Since then, a considerable amount of people have put their efforts into the understanding of the physics of these devices and the technological implications that may be drawn. Has not all the details of semi-conductor physics been discovered then? Is there anything new to be found, even if one developed new theoretical and experiment techniques that, maybe, puts everything into another shade of light? The answer is quite simply no. Why? For instance, in 1943 Zener proposed the interband tunneling effect [95] but it had to wait until the beginning of the 1950s until the first diode manifesting the Zener tunneling was constructed. Further years elapsed and in 1958 Esaki suggested the so-called Esaki resonant tunneling diode [22], exhibiting negative differential resistance (NDR) due to Zener tunneling between the conduction and the valence bands in a heavily doped p-n junction diode. In the beginning of the 1970s Esaki and Tsu predicted that the NDR should also be found in GaAs/Al_xGa_{1-x} double and multiple barrier structures [87, 14], or superlattices. However, it took more than ten years before high quality quantum well (double barrier) samples exhibiting NDR could be fabricated [85]. Actually, the first observation of NDR in a superlattice was reported in 1990 [81]. During this time, the technical improvements in fabricating quantum well structures had become overwhelming. Actually, it was made possible to confine electrons in also two and three spatial directions, thus, the ability of making quantum wells had been improved by also making quantum wires and quantum dots. This is where we are today.

It is seen that some of the great discoveries were made before the technical abilities to realize these phenomena were achieved. However, the progress also takes the other way around, that is, the technical improvements lie far beyond the theoretical understanding. The size of the fabricated devices had, in the end of the 1980s, become far smaller than what the usual (macroscopic) theories allowed for a good interpretation and prediction of the inherited effects. Thus, one had to say goodbye to the classical or semi-classical theories that were previously used and by adopting (non-equilibrium) quantum mechanics new under-

standing of the physics in the fabricated devices was achieved. However, the whole theme started by considering steady-state phenomena, but rather soon the need for actual non-equilibrium techniques was realized by many. Based on a microscopic foundation, new theories evolved and are yet evolving. For example, even though many features concerning tunneling currents, which become important for small devices, are understood, there are several issues that have to be resolved before calculations of transport without any adjustable parameters can be performed. Almost all first principles calculations schemes of today, are based upon equilibrium situations. Thus, since transport by definition is a non-equilibrium phenomenon, equilibrium methods cannot be satisfactory in this case. Such methods may be relevant only if the deviations from equilibrium are very small. Another issue that has to be solved is how the new devices respond to very high frequency, in the order of THz or higher, bias and gate voltages. In such regimes, one cannot even find qualitative answers by using equilibrium methods or macroscopical approaches. What happens if we apply magnetic fields to the devices? The spin-degeneracy of the energy levels in a quantum dot is naturally lifted, at least eventually as the strength of the magnetic field is increased. On the other hand, what happens with the degeneracy of the quantum dot levels if the couplings between the quantum dot and its attached contacts are different for the two spin channels? One desired achievement with mesoscopic physics is to construct highly spin-polarized currents in the systems, something that may be used for quantum computing, magnetic sensors and memory storage etc. What is the theoretical limit of a spin-polarized current and how well does this limit correspond to the realistic devices of today? There are many more open questions concerning electronics design based upon mesoscopic physics.

The present text is by no means intended to give an answer to all these question. However, the questions be themselves open a large area for physicists to work in and being one of the community, I have chosen certain tasks to investigate. Quantum dots are small objects with rather a small concentration of electron states, and for this reason effects from strong correlations between the states should be important in the current flowing through the quantum dot system. This is actually one of the main issues that motivated to work on transport theory in quantum dots. However, since the macroscopic transport theories are not satisfactory and the existing quantum mechanical transport theories suffers from one or another problem, there was yet another motive to investigate the reliability and consistency of transport theory, mainly used in connection with strongly correlated quantum dot states. Finally, the non-equilibrium Green functions technique used for the present work, is probably one of the best candidates for studying transport phenomena in mesoscopic physics. The framework provides a natural and simple enough description of the physics considered.

Chapter 1

Electric current

In general, electric current can be viewed as a motion of charged particles, such as electrons and/or ions. With this basic definition of electric current, it is then a rather simple task to provide a mathematically formulated theory from which further calculations can be performed, although the mathematics itself does not have to be simple at all.

1.1 General formulation of charge current

For an understanding of the fundamental processes involved, it is preferable to approach the problem in a field theoretical manner. For instance, by applying an electric field $\mathbf{E}(\mathbf{r}, t)$, which depends on the spatial and temporal coordinates $\mathbf{r}$ and t, to a conducting system a net current $\mathbf{J}(\mathbf{r}, t)$ through the system can be observed. In contrast, if there is no electric but a magnetic field $\mathbf{H}(\mathbf{r}, t)$ applied to the system, there will also be a current as a result. Actually, for the charged particles flowing in the system there is no real distinction between the fields, a fact which is resolved by introducing the vector potential $\mathbf{A}(\mathbf{r}, t)$. This potential has the property that

$$\begin{aligned} \nabla \times \mathbf{E} &= -\frac{\partial}{\partial t} \nabla \times \mathbf{A} \\ \mathbf{H} &= \nabla \times \mathbf{A}, \end{aligned} \tag{1.1}$$

where $\nabla = (\partial/\partial x, \partial/\partial y, \partial/\partial z)$. In terms of the vector potential, the electric current becomes a question of determining the response of the potential's variation in a system. Formalizing, let the energy of a system be described by the Hamiltonian operator H. Then, the electric current density $\mathbf{j}(\mathbf{r}, t)$ in this system is given

by the equation [55]

$$\delta H = -\frac{1}{c}\int \mathbf{j}\cdot\delta\mathbf{A}\mathrm{d}V, \tag{1.2}$$

where c is the speed of light and V is the volume in which the current flows. Physically, Eq. (1.2) determines the change of the charge and field distributions in the Hamiltonian system when the vector potential varies.

A simple example is given by considering free charged particles in space with no outer constraints. Then, the Hamiltonian consists of the kinetic energy operator of the particles

$$H = \frac{1}{2m}\int \psi^{\dagger}\left(\mathbf{p}-\frac{e}{c}\mathbf{A}\right)^{2}\psi\mathrm{d}V,$$

where m and e are the particles mass and charge, respectively, the momentum operator $\mathbf{p} = -i\hbar\nabla$ and ψ is a particle-field operator. Effecting the variation yields

$$\delta H = \frac{1}{2m}\int \psi^{\dagger}\left[-\frac{e}{c}[\mathbf{p}\cdot\delta\mathbf{A}+\delta\mathbf{A}\cdot\mathbf{p}]+\left(\frac{e}{c}\right)^{2}\mathbf{A}\cdot\delta\mathbf{A}\right]\psi\mathrm{d}V \tag{1.3}$$

and integration by parts on $\mathbf{p}\cdot\delta\mathbf{A}$ results in

$$\int \psi^{*}\mathbf{p}\cdot\delta\mathbf{A}\psi\mathrm{d}V = -i\hbar\int\psi^{\dagger}\nabla(\delta\mathbf{A}\cdot\psi)\mathrm{d}V = i\hbar\int\delta\mathbf{A}\cdot(\nabla\psi^{\dagger})\psi\mathrm{d}V, \tag{1.4}$$

since the surface integral vanishes. Putting the last expression in Eq. (1.4) into Eq. (1.3) gives the equation

$$\delta H = -i\frac{e\hbar}{2mc}\int\delta\mathbf{A}\cdot[(\nabla\psi^{\dagger})\psi-\psi^{\dagger}\nabla\psi]\mathrm{d}V+\frac{e^{2}}{mc^{2}}\int\mathbf{A}\cdot\delta\mathbf{A}\psi^{\dagger}\psi\mathrm{d}V$$

from which we extract the current density operator

$$\mathbf{j} = i\frac{e\hbar}{2m}[(\nabla\psi^{\dagger})\psi-\psi^{*}\nabla\psi]-\frac{e^{2}}{mc}\mathbf{A}\psi^{\dagger}\psi. \tag{1.5}$$

Here one may worry that this expression is not single valued because of the explicit appearance of the vector potential, which is defined up to a gauge transformation

$$\mathbf{A}\to\mathbf{A}+\nabla f,\ \phi\to\phi-\frac{1}{c}\frac{\partial f}{\partial t},$$

where ϕ is a scalar potential and $f = f(\mathbf{r},t)$ is an arbitrary scalar function. However, any such gauge transformation has to be accompanied by changing the field operator

$$\psi\to\psi e^{ief/\hbar c},$$

which therefore makes the current density (1.5) unique.

From Eq. (1.5) one can derive the equation of continuity

$$\frac{\partial\rho}{\partial t}+\nabla\cdot\mathbf{j} = 0, \tag{1.6}$$

where $\rho(\mathbf{r},t) \equiv e\langle\psi^\dagger\psi\rangle$ is the charge density in the system. This equation relates back to the point where we started in this chapter, namely to regard electric current as a motion of charge, and this equation will be the starting point in our exploration of the transport properties of mesoscopic systems. In words Eq (1.6) means, *the rate of change of the charge density in a unit volume of the system equals the net out flux (divergence) of the current density per unit volume in the system.*

Later on in this thesis we will concentrate very much in electronics devices on a mesoscopic length scale. Therefore, it is desirable to point out a distinction between macroscopic, mesoscopic and microscopic views of the electric phenomena. The first problem one encounters is the fact that in todays macroscopic electronics, the current-voltage ($J-V$) relations are, with some exceptions, linear or Ohmic, whereas the $J-V$ characteristics of molecules are evidently shown to be non-linear [53], in general. The different behaviour is actually more or less a matter of size. Indeed, there are three characteristic length scales working as a boundary between the macro- and microscopics and these are the *de Broglie wave length*, the *mean free path* and the *phase relaxation length*.

- The **de Broglie wave length**, or the particles wave length, $\lambda = 2\pi/k$ is related to its wave vector k and sets a lower limit of where macroscopic, or classical, physics may be used for an accurate description of the physics. Any system which is smaller than λ requires a quantum mechanical description. At low temperatures the current is mainly driven by electrons with energy close to the chemical potential and therefore the relevant length scale is the Fermi wave length, typically around 35 nm [16].

- The **mean free path** is defined through the momentum relaxation time τ_m, interpreted as the time it takes before the electron has lost its initial momentum. It is not identical with the collision time τ_c since if at each collision the electron is scattered only a small angle, then very little of the momentum is lost. The momentum relaxation time is therefore, in this case, much longer than the collision time. The mean free path L_m is given by the relation $L_m = v_F\tau_m$, where $v_F = \hbar k_F/m$ and k_F are the Fermi velocity and momentum, respectively. The Fermi velocity is typically around $3\cdot 10^7$ cm/s for $\lambda_F \sim 35$ nm. Thus, assuming a momentum relaxation time about 100 ps the mean free path is around 35 μm [16].

- The **phase relaxation length** L_ϕ is defined as the average distance the electron can move before its phase memory is destroyed. The implications of this is that if we want to measure interference phenomena, L_ϕ must be larger than the size of the system. Phase relaxation, phase randomizing or phase decoherence, it neither equivalent with elastic nor inelastic scattering, although there are cases where they appear simultaneously. For example, electron-electron interaction is an important phase randomizing scattering. Electrons scatter off other electrons due to Coulomb repulsion. However, apart from some cases, e.g. Umklapp processes, the mean free path remains unaffected since there is no loss in the net momentum. Another example of phase relaxation is scattering on magnetic impurities which has an internal degree if freedom, the spin, which fluctuates with time. In general it is the fluctuating scatterers that cause phase relaxation while stationary do not.

A system which is of the size on the order of atoms is microscopic and whenever the system is larger than the three length scales described above, it is macroscopic. A system in the size between these two limit cases is identified as mesoscopic. One realizes that the definition of the mesoscopic regime is somewhat floating but on the other hand there is no need of a very precise interpretation of the concept. For those who are keen on numbers one may say that devices ranging from perhaps tens of Ångströms to 1-2 μm can be classified as mesoscopic. However, numbers are actually determined by the strength of the scattering processes and should always be treated with care.

1.2 Tunneling phenomenon

The phenomenon of tunneling can popularly be described as *the ability of electrons to penetrate 'walls' which intuitively are non-penetrable*. By *walls* we mean potential barriers and by *intuitively* we mean our physical understanding founded on classical physics. Thus, the walls should be regarded as non-penetrable by classical particles. Considering electrons as classical particles leads to a contradiction in the statement above, however, electrons can not be described by classical physics[1]. The tunneling phenomenon is thoroughly discussed in, for example, *Quantum Theory* by D. Bohm [11].

Now, someone may wonder what tunneling has to do with electric current. The answer, however, is simply that in many electric circuits there are interfaces between different materials and devices. Interfaces between different materials can be responsible for creation of potential barriers through which the charge have to pass. Some electronic devices, such as diodes and transistors, also have interfaces between different materials and some of their properties are actually constructed such the tunneling phenomenon plays an essential ingredient in their function. Thus, the phenomenon of tunneling is a natural concept in connection with electric current.

1.2.1 Penetration of a barrier

An example which, mathematically, very well describes the tunneling behaviour of electrons is given by studying the one dimensional potential

$$V(x) = \begin{cases} V_0 & \text{if } x \in (0, x_0) \\ 0 & \text{otherwise,} \end{cases}$$

shown in Fig. 1.1. Assume that an electron is incident from the left with energy $\varepsilon < V_0$. By treating electrons as classical objects the result behaviour in this system is that the electron bounces into the barrier and returns to wherever it came from. However, treating electrons within quantum mechanics their motion have

[1] Often electrons are described as being *both* particles and waves depending on the circumstances. In my opinion though, electrons should be regarded as neither particles nor waves. They show both particle and wave properties, which is far from being either. Comparison with (semi-) classical physics only leads to confusions in the interpretation of quantum mechanics

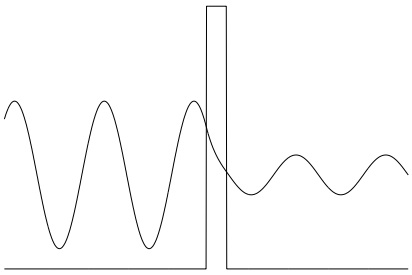

Figure 1.1: Potential barrier of height V_0 and width x_0.

to satisfy the time-independent Schrödinger equation

$$-\frac{\hbar^2}{2m}\nabla^2\phi(x) + V(x)\phi(x) = \varepsilon\phi(x)$$

where the wave function $\phi(x)$ contains all properties about the electron but its charge. Here $\hbar$ is Planck's constant, m is the effective electron mass and ε is the energy eigenvalue of the equation. To the left of the barrier the wave function is

$$\phi(x) = Ae^{ikx} + A'e^{-ikx},$$

with the wave vector $k = \sqrt{2m\varepsilon/\hbar^2}$. The first and second term can be interpreted as the *incident* and *reflected* part, respectively. Proceeding in the same manner we find the wave function inside the barrier , *i.e.* in the interval $(0, x_0)$, as

$$\phi(x) = Be^{i\kappa x} + B'e^{-i\kappa x},$$

where $\kappa = \sqrt{2m(\varepsilon - V_0)/\hbar^2} = i\sqrt{2m(V_0 - \varepsilon)/\hbar^2}$. Thus, the exponents are real is this case. The electron was assumed to be incident from the left, hence, the wave function to the right of the barrier is just

$$\phi(x) = Ce^{ikx}.$$

The wave function should describe the electron in all of the interval $(-\infty, \infty)$ which is fulfilled by requiring it to be continuously differentiable everywhere. From these constraints the constants A, A', B, B' can be determined in terms of C. The *reflectance* $R = |A'/A|^2$, defined as the probability that the electron is reflected at the barrier, is then given by

$$R = \frac{1}{1 + \left[\frac{2\kappa k}{(\kappa^2+k^2)\sinh\kappa x_0}\right]^2}$$

and the *transmittance (tunneling)* $T = |C/A|^2$, the probability that the electron passes through the barrier, is

$$T = \frac{1}{1 + \left[\frac{\kappa^2+k^2}{2\kappa k}\sinh\kappa x_0\right]^2}.$$

By conservation of probability $T + R = 1$, which is easily seen to be satisfied by the quantities in our case.

The interesting physics is that the transmittance T is not identically zero which implies that although the electron energy is less than the barrier height, it is able to penetrate the classically forbidden region. If the barrier is thin enough it also escapes out to the right of the barrier. The tunneling probability strongly depends on the barrier's width and height and we shall not further discuss its dependence on the potential shape. The wave function typically looks like in Fig. 1.1. Most of the wave function is reflected, but a small part is transmitted through the barrier.

The α-decay of a radioactive nuclei, such as uranium, is one example of barrier penetration. The theory is based on the idea that the α-particle is held inside the nucleus by a large nuclear attraction. This attraction is very short ranged, such that it is negligible unless the α-particle is inside the nucleus. Both α-particles and protons are positively charged and, hence, electrically repulsive. Inside the nucleus the nuclear attraction is dominating, however, outside the nucleus the electrical repulsion is the only one present. The potential curve of the α-particle

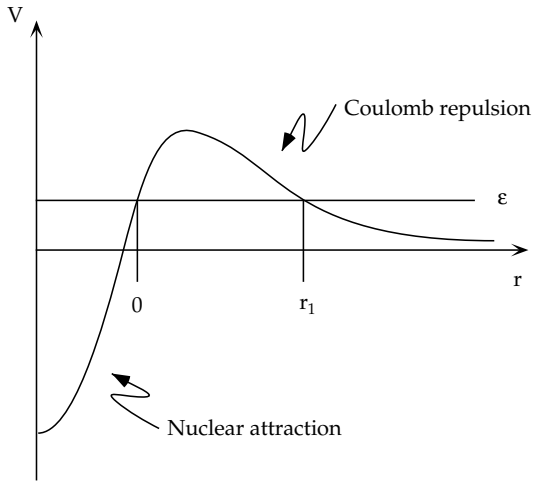

Figure 1.2: Potential curve of the α-particle as a function of the distance r from the center of the nucleus.

as a function of the distance r from the center of the nucleus typically looks like in Fig. 1.2 and is seen to have clear similarities with the potential barrier in Fig. 1.1. Supposing that the α-particle is inside the nucleus with the energy ε less than the repulsive Coulomb barrier. Then, classical physics tells that it would be trapped there forever. But because of the quantum mechanical properties of the α-particle, there is a small probability for the particle to leak out through the barrier. This is the origin of radioactivity.

1.2.2 Transmission resonances

In the case of a single barrier the tunneling probability is usually small. The situation becomes another if instead we look at two succeeding barriers forming a

potential well in between, see Fig. 1.3 a). Although the transmittance of each barrier is low there are wavelengths for which the double potential barrier structure is completely or almost completely transparent. Under such conditions the system is said to be in a state of *resonant tunneling*. For a discussion of the resonance phenomenon itself we will look at the simple system given by the potential

$$V(x) = \begin{cases} -v_0 & \text{if } x \in (0, x_0) \\ 0 & \text{otherwise,} \end{cases}$$

i.e. a potential well, see Fig. 1.3 b).[2] The wave vectors are $k_1 = \sqrt{2m\varepsilon/\hbar^2}$,

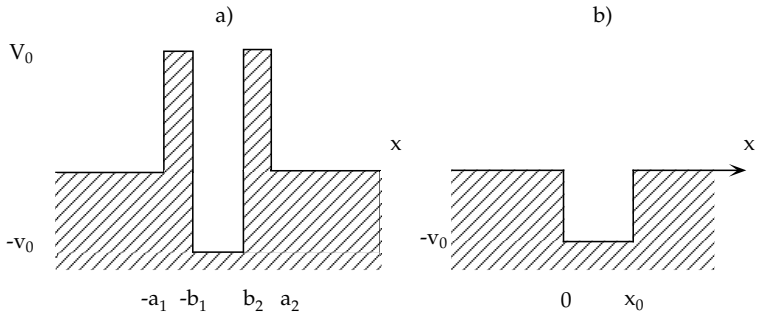

Figure 1.3: a) Double potential barrier structure forming a potential well between the barriers. Inside the well bound states may appear depending on the height of the barriers and distance between them. b) Potential well with bound states.

$x \in (-\infty, 0) \cup (x_0, \infty)$ and $k_2 = \sqrt{2m/\hbar^2(\varepsilon + v_0)}$, $x \in (0, x_0)$. By the same argument as in the single barrier case, we find the transmission probability for an electron incident from the left with energy $\varepsilon > 0$

$$T = \frac{1}{1 + \frac{1}{4}\left(\frac{k_1}{k_2} - \frac{k_2}{k_1}\right)^2 \sin^2 \frac{2k_2 x_0}{\hbar}}.$$

In this case we see that whenever $k_1 = k_2$ the transmission is unity, which is trivial since the potential is constant in this case. However, even for $k_1 \neq k_2$ the transmittance is unity if the equation

$$\sin \frac{2k_2 x_0}{\hbar} = 0 \;\Leftrightarrow\; k_2 = \frac{\hbar}{2x_0} n\pi$$

is satisfied. Here n is an integer. It is the rapid shift[3] in the potential at $x = 0$ and $x = x_0$ that makes this resonance possible. Electrons, reflected at $x = x_0$, that arrives back at $x = -x_0$ with a phase shift of $2n\pi$ interfere constructively

[2] Due to its complicated structure of the system in figure 1.3 a) the mathematical treatment becomes more opaque than what it does in the system in Fig. 1.3 b). However, since there are resonances in both systems, nothing is lost in principle by doing the analysis in the latter.

[3] By *rapid shift* in the potential we mean, for example, that the potential rises from the zero level to its maximum in a distance much shorter than the dimensions of the system.

with other electrons incident from the left at $x = -x_0$ and, as a result, the wave function is reinforced. Thus, for certain energies/wavelengths the transmittance is unity.

Chapter 2

Transport in mesoscopic systems

THE PURPOSE OF this thesis is not to give a general account of electric transport theory but rather to focus on what is going on in the mesoscopic regime. In addition, we will restrict the considerations to the case of a quantum dot (QD) weakly coupled to contacts. One of the main targets in our study is to investigate effects of electron correlations. Such effects are expected to be strong in small QD with a small number of electrons, the QD being weakly coupled to external contacts. In contrast, when the coupling is strong, the individual properties of the QD are lost leading to that the QD can be treated as an ordinary inhomogenity in metal. In order to straighten out the reason why we have to develop a new mathematical tool for the description of the transport through systems with small QD, we give a short account of other approaches.

2.1 Boltzmann equation

To any system that contains electrons, one can associate a distribution function f with the particles. In the present context we will assume the electrons to be satisfactory described by a classical distribution $f(\mathbf{r}, \mathbf{k}, t)$, where $\mathbf{r}$ is the spatial coordinate, $\mathbf{k}$ is the wave vector and t is time. The objective here, is to describe the transport and the electrical resistivity in the simplest possible fashion. Therefore we consider a homogeneous system except for randomly located impurities,

as the model of a solid. The electrons are free particles except for occasional scattering at isolated impurities. The impurities are very dilute, thus interference between successive scatterings can be neglected. A charge current is described by the motion of particles, and one can find that the time rate of change of the distribution function $f(\mathbf{r}, \mathbf{k}, t)$ is governed by the equation

$$\frac{df}{dt} = \frac{\partial f}{\partial t} + \mathbf{v} \cdot \nabla f + \frac{\partial \mathbf{k}}{\partial t} \cdot \nabla_k f = \left(\frac{df}{dt}\right)_{\text{collisions}}.$$

The collisions of electrons with impurities is described by the term on the right hand side of this equation. In a homogeneous system there is no spatial dependence in $f(\mathbf{r}, \mathbf{k}, t)$. If we restrict ourselves to steady state currents, there will neither be any time-dependence. This is done by assuming that the system is subject to a weak external electric field. Hence, the distribution function is only a function of the wave vector and obeys the equation

$$\frac{\partial \mathbf{k}}{\partial t} \cdot \nabla_k f(\mathbf{k}) = \left(\frac{df}{dt}\right)_{\text{collisions}}.$$

In a solid, the time-derivative of the wave vector is equivalent to an acceleration which equals the forces acting on the electron [49], that is,

$$\frac{\partial \mathbf{k}}{\partial t} = -e\mathbf{E} - \frac{e}{c}\mathbf{v} \times \mathbf{H}.$$

By assuming that only a electric field $\mathbf{E}$ and no magnetic field $\mathbf{H}$ is present, the transport equation becomes

$$-e\mathbf{E} \cdot \nabla_k f(\mathbf{k}) = \left(\frac{df}{dt}\right)_{\text{collisions}}. \tag{2.1}$$

In order to solve Eq. 2.1, it is necessary to find out what properties the collision term carries. The simplest approach then, is to calculate it in the *relaxation time* approximation. This assumes that collisions seek to return the system into equilibrium configuration $f_0(k)$, which is the configuration of the system when the external field is absent. Then, it is assumed that the rate of change of $f(\mathbf{k})$ due to collisions is proportional to the deviation of $f(\mathbf{k})$ from $f_0(k)$, or

$$\left(\frac{df}{dt}\right)_{\text{collisions}} = -\frac{f(\mathbf{k}) - f_0(k)}{\tau_1(k)}.$$

This is the definition of the relaxation time $\tau_1(k)$. More details of the derivation can be found, for instance, in Refs. [2, 61, 96]

We are looking for the conductivity[1] σ_{ij} which can be found if we know the relaxation time $\tau_1(k)$. However, we will not concern ourselves by finding an expression for $\tau_1(k)$. The interested reader may find more on this subject in Ref. [62]. Instead, we suppose that the relaxation time is known. For example, by considering the impurities as being static, fixed objects with a spherically symmetric

[1] If j_i is the i:th component of the current $\mathbf{j} = -e\sum_k \mathbf{k} f(\mathbf{k})$, then $j_i = \sigma_{ij} E_j$, since $\mathbf{j}_0 = -e\sum_k \mathbf{k} f_0(\mathbf{k}) = 0$.

potential and no internal excitations, so that the electrons scatters elastically, the relaxation time can be found as

$$\frac{1}{\tau_1(k)} = \frac{4\pi n_i}{mk} \sum_l l \sin^2[\delta_l(k) - \delta_{l-1}(k)], \tag{2.2}$$

where n_i is the concentration of impurities and l is the angular momentum quantum number. When the electric field is small, only a small current flows through the system - the system is only slightly out of equilibrium. Thus, we may write the distribution function $f(\mathbf{k}) = f_0(k) + f_1(\mathbf{k})$, where $f_1(\mathbf{k})$ is a small deviation from $f_0(k)$. In this case, the equation for the distribution function can be written as

$$f(\mathbf{k}) = f_0(k) + e\tau_1(k)\mathbf{E} \cdot \nabla_k f(\mathbf{k}). \tag{2.3}$$

Replacing f by f_0 on the right hand side of Eq. 2.3, the distribution function can be evaluated

$$f(\mathbf{k}) = f_0(k) + e\tau_1(k)\frac{\mathbf{E} \cdot \mathbf{k}}{m}\frac{\partial f_0(k)}{\varepsilon_k}. \tag{2.4}$$

The electric current density $\mathbf{j}$ is the product of the electron charge $-e$, the electron's density n_0 and the average velocity $\langle \mathbf{v} \rangle$. This is obtained by averaging over the electron distribution

$$\mathbf{j} = -en_0\langle \mathbf{v} \rangle = -\frac{en_0}{8\pi^3}\int f(\mathbf{k})\frac{\hbar \mathbf{k}}{m}\mathrm{d}\mathbf{k},$$

$$1 = \frac{1}{8\pi^3}\int f(\mathbf{k})\mathrm{d}\mathbf{k} = \frac{1}{8\pi^3}\int f_0 \mathrm{d}\mathbf{k}.$$

The distribution function is normalized to unity. By using Eq. 2.4, the term f_0 gives an average $\langle \mathbf{v} \rangle$ of zero, since there should be any current flow when there is no electric field. Therefore, the current is proportional to the second term, thus it is proportional to the electric field $\mathbf{E}$

$$\mathbf{j} = -\frac{e^2 n_0}{8\pi^3}\int \tau_1(k)\mathbf{v}_k(\mathbf{E} \cdot \mathbf{v}_k)\frac{\partial f_0(k)}{\partial \varepsilon_k}\mathrm{d}\mathbf{k}. \tag{2.5}$$

In a homogeneous isotropic system the current flows along the direction of the electric field. The equilibrium distribution function $f_0(k)$ is then independent of the k-direction. The only angular factors are $\mathbf{v}_k(\mathbf{E} \cdot \mathbf{v}_k)$ and the angular integrals average to $v_k^2\mathbf{E}/3$. The conductivity is the quotient of $\mathbf{j}$ to $\mathbf{E}$, which gives the final formula for the electric conductivity

$$\sigma = -\frac{e^2 n_0}{24\pi^3}\int v_k^2 \tau_1(k)\frac{\partial f_0(k)}{\partial \varepsilon_k}\mathrm{d}\mathbf{k}. \tag{2.6}$$

The conductivity $\sigma > 0$ since the derivative $\partial f_0(k)/\partial \varepsilon_k < 0$. It should be noted that the relaxation time $\tau_1(k)$ is not simply the time between the scattering events, which would be found if one considers the inverse time relaxation as the scattering cross section. Instead, it contains a combination of phase shifts which are different from that found in the formula for the cross section.

The Boltzmann equation considered here, applies for classically distributed electrons in the solid. It is certainly possible to use quantum mechanically distributed electrons by introducing the Wigner distribution function $f(\mathbf{k}, \omega; \mathbf{r}, t)$. However, because of the uncertainty principle, it is rather ambiguous to describe the electrons both by its position and momentum. In principle, such an approach applies for systems where the disturbances varies on macroscopic distances and, then, it is possible to specify the momentum of the particle with microscopic accuracy [47]. Another drawback of the Boltzmann equation approach (classical or quantum mechanical) is that, it is somewhat simple to use whenever the investigated systems are fairly homogeneous. If we, for example, are to consider a QD, with strong internal correlations, coupled to external contacts, then the Boltzmann equation provides a very complicated framework to handle. For more details on the quantum Boltzmann equation we refer to Refs. [31, 47, 62].

2.2 Kubo formula

Using a statistical mechanics approach to the transport problem one can very easily derive the Kubo formula [52], as a result of *linear* response approximation. The starting point is the application of an external electric field

$$E_\alpha^{ext}(\mathbf{r}, t) = \theta_\alpha^{ext} e^{i(\mathbf{q}\cdot\mathbf{r} - \omega t)}, \ \alpha = x, y, z,$$

to a system, see Fig. 2.1, where θ_α^{ext} is a constant, $\mathbf{q}$ the wave vector and ω the frequency of the field. The field induces a current $J_\alpha(\mathbf{r}, t)$ in the system and as a linear response theory one can write

$$J_\alpha(\mathbf{r}, t) = \sum_\beta \sigma'_{\alpha\beta}(\mathbf{q}, \omega) E_\beta^{ext}(\mathbf{r}, t).$$

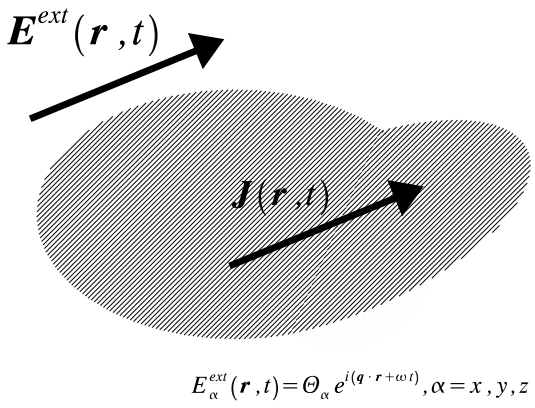

Figure 2.1: An external electric field $E^{ext}(\mathbf{r}, t)$ applied to a system induces a charge current $J(\mathbf{r}, t)$.

Now, the induced current gives rise to new electric fields and so forth. Therefore, it is more appropriate to write the current as a result of the total electric field $E_\alpha(\mathbf{r},t)$, as

$$\begin{aligned} J_\alpha(\mathbf{r},t) &= \sum_\beta \sigma_{\alpha\beta}(\mathbf{q},\omega)E_\beta(\mathbf{r},t), \\ E_\alpha(\mathbf{r},t) &= \theta_\alpha e^{i(\mathbf{q}\cdot\mathbf{r}-\omega t)}, \quad \sigma_{\alpha\beta}(\mathbf{q},\omega)\in\mathbb{C}, \end{aligned} \tag{2.7}$$

where $\mathbb{C}$ is the set of complex numbers. This certainly looks as a very simple task but the question that arises is how we find the conductance $\sigma_{\alpha\beta}$? This is where we make use of a result from statistical mechanics, namely, the **Fluctuation-Dissipation theorem**. The statement is that *there is a simple relationship between the time-dependent correlations among the fluctuating quantities and the response to changing a parameter in the Hamiltonian in a time-dependent way*. The fluctuations correspond to correlation functions which means that the conductance $\sigma_{\alpha\beta}$ (fluctuations) should be found in the form of a correlation function. Before we answer the question of what is fluctuating under the influence of the external field, let us think about what is actually measured in experiments. Consider a system with N charged particles, see Fig. 2.2, say electrons for convenience. Because of the external field the ith electron acquires the velocity $\mathbf{v}_i$ and the net current in the system is $J_\alpha(\mathbf{r},t) = (e/V)\sum_i\langle v_{i\alpha}\rangle$, where V is the volume of the system. The

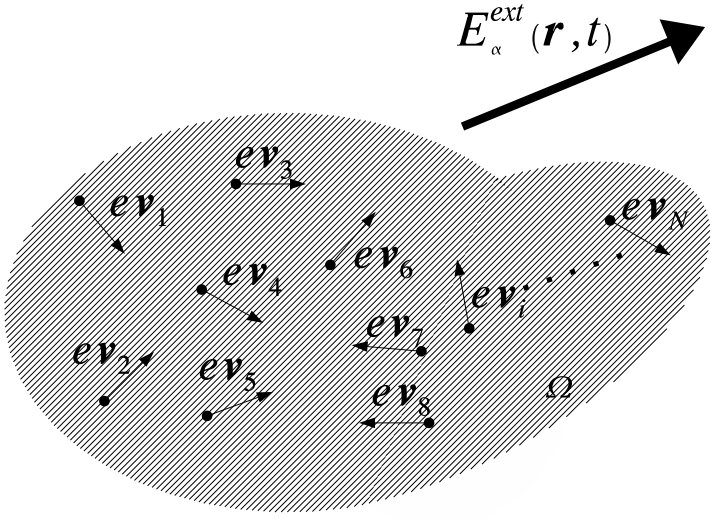

Figure 2.2: A system of volume Ω with N charged particles. The external field induces a motion to each particle $n_i,\ i=1,\ldots,N$, acquiring the velocity $\mathbf{v}_i$ which gives the current $e\mathbf{v}_i$.

electron velocity $v_{i\alpha} = [p_i - (e/c)A_\alpha(\mathbf{r}_i)]/m$ and, thus,

$$J_\alpha(\mathbf{r},t) = \frac{e}{mV}\sum_i \langle p_i\rangle - \frac{e^2}{mcV}\sum_i \langle A_\alpha(\mathbf{r}_i)\rangle.$$

By the substitutions $j(\mathbf{r},t) = (e/m)p_i$ and $A_\alpha(\mathbf{r},t)/c = -(i/\omega)E_\alpha(\mathbf{r},t)$ we can rewrite the previous expression as

$$J_\alpha(\mathbf{r},t) = \langle j_\alpha(\mathbf{r},t)\rangle + i\frac{n_0e^2}{m\omega}E_\alpha(\mathbf{r},t),$$

where n_0 is the equilibrium density of electrons. The last term is of the desired form and does not need any further consideration. The first term, on the other hand, needs some extra care for which we find the answer in quantum mechanics. In equilibrium the system is described by the Hamiltonian H_0 and the wave functions $|\phi\rangle$ whereas in non-equilibrium the system is disturbed by $H'(t)$ which results in the wave function $|\phi'\rangle$. Under influence of $H'(t)$, then,

$$\langle j_\alpha(\mathbf{r},t)\rangle \equiv \langle\phi'|\, j_\alpha(\mathbf{r},t)\,|\phi'\rangle = \langle\phi|\, S^\dagger(t,-\infty)j_\alpha(\mathbf{r},t)S(t,-\infty)\,|\phi\rangle\,,$$

where $S(t,-\infty) = 1 - i\int_{-\infty}^{t} H'(t')\mathrm{d}t'$ in linear response. Substituting this expression for S into the correlation function results in a term $\langle\phi|\, j_\alpha(\mathbf{r},t)\,|\phi\rangle = 0$ since there cannot be any current in equilibrium. Therefore, the correlation function of the current operator equals

$$\langle j_\alpha(\mathbf{r},t)\rangle = -i\int_{-\infty}^{t}\langle\phi|\,[j_\alpha(\mathbf{r},t), H'(t')]\,|\phi\rangle\,\mathrm{d}t'.$$

By writing the disturbance as $H'(t) = (i/\omega)j_\beta(\mathbf{q},t)E_\beta(\mathbf{r},t)\exp i[\mathbf{q}\cdot\mathbf{r} + \omega(t-t')]$, then

$$\langle j_\alpha(\mathbf{r},t)\rangle = \frac{1}{\omega}E_\beta(\mathbf{r},t)e^{i\mathbf{q}\cdot\mathbf{r}}\int_{-\infty}^{t}\langle\phi|\,[j_\alpha(\mathbf{r},t), j_\beta(\mathbf{r},t)]\,|\phi\rangle\, e^{i\omega(t-t')}\mathrm{d}t',$$

which is precisely what we want, since then we have obtained the form given in Eq. (2.7). The Kubo formula for the conductance is then given by, with some extra polishing of the formula,

$$\sigma_{\alpha\beta}(\mathbf{q},\omega) = \frac{1}{\omega V}\int_{-\infty}^{t}\langle\phi|\,[j_\alpha^\dagger(\mathbf{q},t), j_\beta(\mathbf{q},t')]\,|\phi\rangle\,\mathrm{d}t' + i\frac{n_0e^2}{m\omega}\delta_{\alpha\beta}. \tag{2.8}$$

Now we can see that it is actually the current density operator $\mathbf{j}(\mathbf{r},t)$ that fluctuates due to the external field $E(\mathbf{r},t)$. The current density operator is a local quantity in the sense that it varies in time and space. Moreover, the current density operator describes a creation and annihilation of a particle which is something that actually cannot be measured. In general one can only measure transitions from one state to another, which is described by the products $j_\alpha^\dagger j_\beta$ and $j_\beta j_\alpha^\dagger$.

The Kubo formula given in Eq. (2.8) is correct for both ac and dc currents even though it was derived for a time-dependent external field. The dc case is given by first letting $\mathbf{q}\to 0$ and then $\omega\to 0$. Also temperature can be taken into account

for in Eq. (2.8), simply by interpreting the $|\rangle$ and $\langle|$ as thermal averages. However, it should be noted that the Kubo formula only holds true in the linear response regime and the predicted current-voltage characteristics is Ohmic. Thus, this formalism cannot provide any non-linear features in the way we may encounter in a careful investigation of the response in the system to an applied external field. A thorough analysis of the results along with rigorous derivations of the Kubo formulas can be found, for example, in [62].

2.3 Landauer formula

By taking a statistical mechanical approach we saw in the previous section how the Kubo formalism was developed. Another point of view was given by regarding the transport as a scattering problem, by means of the Boltzmann equation, cf. 2.1. Yet another way of looking at the transport phenomenon, as a scattering problem, is given by the Landauer formula.

For instance, in semi-conductors the charge fluctuations near the interfaces between the contacts and the device can substantially affect the potential near the interfaces. In addition, the current flow may significantly perturb the distribution of the particles from equilibrium. The spatial inhomogeneities that results from the current flow around the scattering centers was early recognized by Landauer [56], who formulated the problem by considering a one-dimensional system in which a constant current was forced to flow through the structure containing scatterers. The question he posed was inhomogeneities influence the current through the system, in the case of coherent electron motion. The result in one dimension is now called the Landauer formula, which is briefly derived below taken from Ref. [24].

Consider a general barrier connected to ideal one-dimensional conductors, see Fig. 2.3. By ideal conductor we mean that the particles flow without scattering in the extreme quantum limit with only one subband (channel) occupied. The leads connect the sample to reservoirs to the right and left characterized by the quasi-chemical potentials μ_1 and μ_2, respectively. Moreover, the reservoirs randomize the phase of the injected and absorbed electrons through inelastic processes, hence there is no phase relation between the particles. The current injected from the left and the right can be written as the sum of the flux, that is

$$J = \frac{2e}{2\pi}\left(\int_0^\infty v(k) f_1(k) T(E) \mathrm{d}k - \int_0^\infty v(k') f_2(k') T(E') \mathrm{d}k'\right),$$

where $2e/(2\pi)$ is the one-dimensional density of states (DOS) in k-space, $v(k)$ is the particles velocity, $T(E)$ is the transmission coefficient and $f_1,\ f_2$ are the reservoir distribution functions at the quasi-chemical potentials $\mu_1,\ \mu_2$, respectively. The integrations over positive k and k' correspond to the direction of the injected charge. At low temperature the electrons are injected up to the energy μ_1 into the left reservoir and up to μ_2 into the right. Converting the k-space integrations into energy integration, the current becomes

$$J = \frac{2e}{2\pi}\left(\int_0^{\mu_1} T(E) v(k) \frac{dk}{dE} \mathrm{d}E - \int_0^{\mu_2} T(E) v(k') \frac{dk'}{dE} \mathrm{d}E\right) = \frac{2e}{2\pi\hbar}\int_{\mu_2}^{\mu_1} T(E) \mathrm{d}E,$$

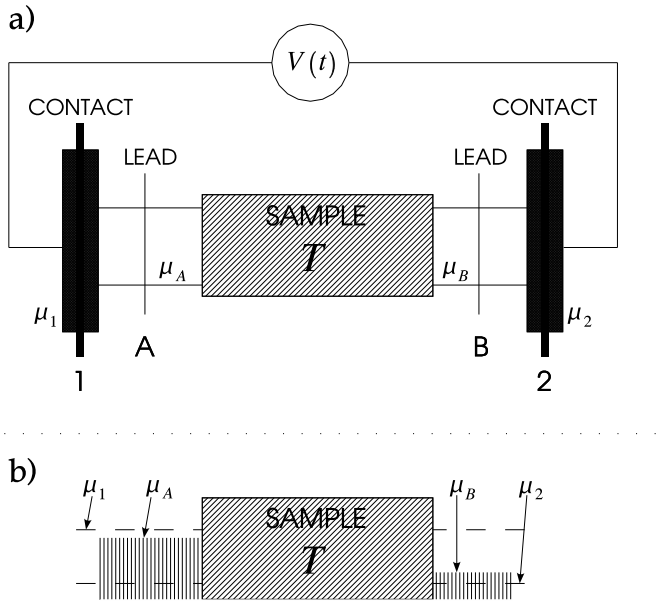

Figure 2.3: A model of a quantum barrier. The barrier, which has transmission probability T is connected to two reservoirs through ideal leads.

since $v(k)dk/dE = 1/\hbar$ in one dimension. Further simplification is obtained by assuming that the applied voltage is small (i.e. in the linear response regime). Then, the energy dependence of $T(E)$ is negligible and the current becomes simply

$$J = \frac{2e}{2\pi\hbar} T(\mu_1 - \mu_2). \tag{2.9}$$

Supposes that the current is measured between the reservoirs. Then, the voltage drop is $eV = \mu_1 - \mu_2$, hence the conductance for the sample and leads, regarded as one unity, is

$$\sigma_{res} = \frac{J}{V} = \frac{2e^2}{2\pi\hbar} T. \tag{2.10}$$

However, in real applications one is more interested in the conductance of the sample itself. As a result of the charge flow there will be a reduction of the charge density to the left of the sample and a charge pile up to the right. Assuming that we are still in the linear response regime we can approximate the charge rearrangement by an average density in the ideal leads in either side of the sample characterized by the quasi-chemical potentials μ_A and μ_B, see Fig. 2.3 b). The voltage drop over the sample is thus $eV_{sample} = \mu_A - \mu_B < \mu_1 - \mu_2$. The difference between the two voltage drops represents the potential drop in the leads. However, the voltage eV_{sample} has to be found in terms of the current flowing through the sample. Thus, we look at the one-dimensional density in the ideal

lead to the left

$$n_A = \frac{2}{2\pi}\int_{-\infty}^{\infty} f_A(E)\mathrm{d}k = \frac{2}{2\pi}\int_0^{\infty}\Big([2-T]f_1(E) + Tf_2(E)\Big)\mathrm{d}E, \tag{2.11}$$

where f_A is the near equilibrium distribution function on the left lead at the quasi-chemical potential μ_A. The first term in the last integral includes both the transmitted and reflected charge injected from the left reservoir ($2-T = 1+R$) whereas the second only contains the transmitted charge from the right. The expression in Eq. (2.11) is an asymptotic form of the charge density in the left lead for which it is assumed that Friedell oscillations of the charge density around the barrier damp out sufficiently rapidly. Similarly, the density in the right lead is given by

$$n_B = \frac{2}{2\pi}\int_{-\infty}^{\infty} f_B(E)\mathrm{d}k = \frac{2}{2\pi}\int_0^{\infty}\Big([2-T]f_2(E) + Tf_1(E)\Big)\mathrm{d}k. \tag{2.12}$$

For low temperatures Eq. (2.12) can be subtracted from Eq. (2.11), giving

$$n_A - n_B = 2\int_{\mu_B}^{\mu_A}\frac{dk}{dE}\mathrm{d}E = \int_{\mu_B}^{\mu_A}\Big([2-T]-T\Big)\frac{dk}{dE}\mathrm{d}E. \tag{2.13}$$

Assuming V_{sample} to be sufficiently small the energy dependence of T and the velocity $v(k) \sim dE/dk$ can be neglected. Thus, Eq. (2.13) becomes simply

$$\mu_A - \mu_B = (1-T)(\mu_1 - \mu_2). \tag{2.14}$$

In the leads, the charge is not Fermi-Dirac distributed, especially not for non-zero bias voltages. The charge do not populate all the states between μ_1 and μ_2. However, if we use the quasi-chemical potential μ_B only as a counting scheme for the density of charge in the right lead, it can be defined as the number of occupied states above this level equal to the number of unoccupied states below [12]. The number of states above μ_B transmitted from the left is $TD(E)(\mu_1 - \mu_B)$, where $D(E)$ is the density of states in energy corresponding to positive k, and the number of unoccupied state below μ_B is $2D(E)(\mu_B - \mu_2) - TD(E)(\mu_B - \mu_2)$. The states below μ_2 are completely filled. Equating the two expressions gives

$$T(\mu_1 - \mu_B) = (2-T)(\mu_B - \mu_2).$$

Analogously, μ_A is defined from

$$(2-T)(\mu_1 - \mu_A) = T(\mu_A - \mu_2),$$

where the left expression is the number of occupied states above μ_A whereas the right is the number of unoccupied below. Combining these two equations gives Eq. (2.14). Finally, substituting Eq. (2.14) into Eq. (2.9) yields the current

$$J = \frac{2e}{2\pi\hbar}\frac{T}{1-T}(\mu_A - \mu_B), \tag{2.15}$$

or in terms of the conductance

$$\sigma = \frac{J}{V} = \frac{2e^2}{2\pi\hbar}\frac{T}{1-T} = \frac{2e^2}{2\pi\hbar}\frac{T}{R}. \tag{2.16}$$

This is the celebrated single-channel Landauer formula [56, 57].

First thing to notice is the difference between the Eq. (2.16) and Eq. (2.10), for instance $\sigma > \sigma_{res}$. This difference is actually a matter of how the voltage is measured. As already stated above, the conductance σ_{res} is measured from the reservoir whereas σ is measured by attaching ideal probes directly to the sample, where the leads are connected. In the latter case one has a four-terminal measurement whereas in the former one has a two-terminal in which the resistance of the leads, created by the potential drop and pile up, is taken into account. In general, the transmission coefficient T is very small and provides the dominating part of the series resistance. Thus, the two- and four-terminal measurement give the same results.

We also notice that the conductances are given as a product of the transmission and reflection quotient at the quasi-chemical potential and the fundamental conductance $2e^2/(2\pi\hbar) = 7.748 \cdot 10^{-5}$ A/V corresponding to a resistance of 12.907 $k\Omega$. This conductance quanta plays an important role in the physics of mesoscopic systems, being the conductance associated with a single one-dimensional channel. The reason is that the conductance properties of mesoscopic systems can be governed by transport through a few such channels, giving rise to characteristic changes of precisely $2e^2/(2\pi\hbar)$.

Although the results in this section were given in the linear response regime and for low temperatures, the Landauer formula can be extended to a wider voltage range and higher temperatures. Thus, one can avoid the problems of linear response. However, in scattering theory it is hard to handle two-particle processes (e.g. inelastic scattering) leading to that the Landauer formalism can only give a reliable interpretation of experiments where strong electron correlations in the sample are not important. Hence, in order to go beyond the single-particle picture we need to consider other techniques which offer the desired opportunities.

Chapter 3

Transfer Hamiltonian formalism

As was pointed out in the previous chapter, the Landauer approach runs into problems whenever inelastic scattering processes are present in the system. In the Kubo formalism inelastic scattering processes can be treated, however, the formalism is based upon linear response argument and is therefore not considered as sufficient. These problems can be avoided by employing the transfer Hamiltonian formalism [10, 15] which was developed in the 1960s as a phenomenological model explanation of the current through tunnel junctions, for example metal-insulator-metal (MIM) and metal-insulator-superconductor junctions. In this formalism the current and the differential conductance are given explicit dependences of the densities of electron states in both sides of the tunnel junction. With this model, then, information about the materials electronic properties can be obtained from experiments, by measuring the current through the junction.

In the end of the 1980s, when it had become technically possible to construct electronics devices on a length scale of 10-1000 of nanometres, the transfer Hamiltonian formalism became an interesting and useful tool again. Among many reasons for this, one notes that the formalism provides an intuitive and transparent picture of the physics in the system. Another reason is that both elastic and inelastic scattering processes along with phase randomizing processes can be handled within the same approach. Also, time-dependent currents can be treated rather easily.

The basic idea, for an MIM junction, is to treat the metal on each side of the insulator as separate systems which interact weakly through the insulating layer.

Mathematically, this can be expressed as

$$\mathcal{H} = \sum_{p\sigma\in L} \varepsilon_{p\sigma}(t) c^\dagger_{p\sigma} c_{p\sigma} + \sum_{q\sigma\in R} \varepsilon_{q\sigma}(t) c^\dagger_{q\sigma} c_{q\sigma} + \sum_{pq\sigma} (v_{pq\sigma}(t) c^\dagger_{p\sigma} c_{q\sigma} + H.c.), \quad (3.1)$$

where the first and second terms give the energy of the quasi-particles in the left (L) and right (R) metal, respectively, and the last term describes the transfer of electrons from one metal into the other.[1] In this notation $c^\dagger_{k\sigma}$ ($c_{k\sigma}$) creates (annihilates) a quasi-particle, $\varepsilon_{k\sigma}(t) = \varepsilon^0_{k\sigma} + \Phi_\alpha(t)$ is the quasi-particle energy in the metals and $v_{pq\sigma}(t)$ is the mixing of the metallic states through the insulator. The time-dependences of the quasi-particle energies and the mixing is imposed by the time-varying bias voltage $\Phi_{sd}(t)$ through the quasi-chemical potentials $\mu_\alpha(t) = \mu + \Phi_\alpha(t),\ \alpha = L, R$, where μ is the equilibrium chemical potential and $\Phi_L(t) + \Phi_R(t) = \Phi_{sd}(t)$. Suppose that the population number operator in the left metal can be written as $N_L(t) = \sum_{p\in L} \langle c^\dagger_{p\sigma}(t) c_{p\sigma}(t)\rangle$. By studying the time-derivative of the left population numbers, the expression

$$\begin{aligned} J(t) &= -2\mathrm{Re} \sum_\sigma \int v^*_{LR\sigma}(t) \rho^L_\sigma(\omega) \rho^R_\sigma(\omega') \\ &\quad \times \int_{-\infty}^{t} v_{LR\sigma}(t') [f(\omega') - f(\omega)] e^{-i\int_{t'}^{t} [V(s)+\omega-\omega]\mathrm{d}s} \mathrm{d}t' \mathrm{d}\omega' \mathrm{d}\omega, \end{aligned} \quad (3.2)$$

for the time-dependent tunnel current from the left to the right lead can be derived. Here $f(\omega)$ is the Fermi-Dirac distribution function and $\rho^\alpha_\sigma(\omega)$ is the conduction electron density of states (DOS) in the lead α. The general assumption underlying the derivation of the tunnel current is that the bias voltage $\Phi_{sd}(t)$ drops entirely over the scattering region between the leads. This is a common approach for theoretical studies of the tunnel current between two, or more, leads and is by no means restricted to the case of tunnel junctions. Physically, this relies upon a free electron like approximation of the conduction electrons in the leads, which corresponds well to many realistic situations.

3.1 Generalization of the formalism

The transfer Hamiltonian formalism has shown successful as a description of transport phenomena. Nevertheless, there are some inconsistencies which are non-desirable. For example, the transfer (tunneling) of an electron from the left to the right side of the junction arises due to an overlap of the wave functions in the two metals. In turn, since a wave function in the left metal extends into the right, the electron operators cannot be anti-commuting, i.e. $\{c_{p\sigma}, c^\dagger_{q\sigma}\} \neq 0$. However, for simplicity it is often assumed that the operators do anti-commute. This assumption can be avoided by making the following consideration. Suppose that ψ is the exact particle-field operator of the real system $H = p^2/2 + V$ and let $H_{L,R}$ be two auxiliary Hamiltonians for single particles in the potentials $V_{L,R}$. The left potential may be thought of as a semi-infinite metal to the left of a semi-infinite

[1] From now, except for a couple of places in the beginning of Chap. 4, on we work with atomic units (a.u.) in which $e = 1$, $\hbar = 1$, $m = 1$, et.c.

insulator, and analogously for the right potential. To each of these Hamiltonians corresponds an orthonormal eigensystem $\{\varepsilon_{k\sigma}, \phi_k\}_{k\in L,R}$, where ϕ_k is a wave function. Define the quasi-particle operators [25, 27, 77]

$$c_{k\sigma}(t) = \sum_{k'\in L\cup R} \mathcal{O}^{-1}_{kk'} \int \phi^*_{k'}(x)\psi(x,t)\mathrm{d}x, \tag{3.3}$$

where $\mathcal{O}^{-1}_{kk'}$ is an element of the inverse of the overlap matrix $\mathcal{O}$ defined by $\mathcal{O}_{kk'} \equiv \langle\phi_k|\phi_{k'}\rangle = \mathcal{O}^*_{k'k}$. It is a simple task to show that $\{c_{k\sigma}, c^\dagger_{k'\sigma}\} = \mathcal{O}^{-1}_{kk'}$ and thereby the assumption of anti-commuting quasi-particles is not only avoided, the value of the anti-commutator is also well-defined. In terms of the operators defined in Eq. (3.3) the field operator $\psi_{L,R}(x,t) = \sum_{k\in L,R} c_{k\sigma}(t)\phi_k(x)$ is introduced, where $x = (\mathbf{r},\sigma)$. Putting $\psi(x,t) = \psi_L(x,t) + \psi_R(x,t) + [\psi(x,t) - \psi_L(x,t) - \psi_R(x,t)]$ and assuming that the term in brackets is negligible in the energy interval under consideration, it is possible to derive a second quantized Hamiltonian which formally equals Eq. (3.1) [27], starting from $\mathcal{H} = \int \psi^\dagger H\psi \mathrm{d}x$. The result is only formally true since the quasi-particle operators have to be interpreted differently. Under these, somewhat altered, circumstances the dynamics of the operators have to be found. From the Heisenberg equation of motion, say for the operator $c_{p\sigma},\ p\sigma \in L$, in a Hamiltonian system formally given by Eq. (3.1), one finds that

$$i\frac{\partial}{\partial t}c_{p\sigma} = [c_{p\sigma},\mathcal{H}] = \sum_{p'} \mathcal{O}^{-1}_{pp'}\varepsilon_{p'\sigma}(t)c_{p'\sigma} + \sum_q V_{pq\sigma}(t)c_{q\sigma} + \sum_{p'q} \mathcal{O}^{-1}_{pp'}v^*_{p'q\sigma}(t)c_{p'\sigma}, \tag{3.4}$$

where $V_{pq\sigma}(t) = \mathcal{O}^{-1}_{pq}\varepsilon_{q\sigma}(t) + \sum_{p'} \mathcal{O}^{-1}_{pp'}v_{p'q\sigma}(t)$. Assuming that scattering between states in the same lead is negligible, that is putting $\mathcal{O}^{-1}_{pp'} = \delta_{pp'}$, simplifies Eq. (3.4) to

$$\left(i\frac{\partial}{\partial t} - \varepsilon_{p\sigma}(t)\right)c_{p\sigma} = \sum_q V_{pq\sigma}(t)c_{q\sigma}. \tag{3.5}$$

The tunnel current from the left to the right lead is then derived to [25]

$$\begin{aligned} J(t) \quad &= \quad -2\mathrm{Re}\sum_\sigma \int V^*_{LR\sigma}(t)\rho^L_\sigma(\omega)\rho^R_\sigma(\omega') \\ &\quad \times \int_{-\infty}^t V_{LR\sigma}(t')[f(\omega') - f(\omega)]e^{-i\int_{t'}^t [V(s)+\omega-\omega]\mathrm{d}s}\mathrm{d}t'\mathrm{d}\omega'\mathrm{d}\omega, \end{aligned} \tag{3.6}$$

thus, formally the same expression as given in Eq. (3.2), however, the tunneling coefficient is altered $v_{LR\sigma}(t) \to V_{LR\sigma}(t) = v_{LR\sigma}(t) + \mathcal{O}^{-1}_{LR}\varepsilon_R(t)$. In principle, taking the non-orthogonality into account decreases the tunneling rate since $\mathcal{O}^{-1}_{pq} \sim -\mathcal{O}_{pq}/\det\mathcal{O}$ implying that $|V_{pq\sigma}(t)|^2 \leq |v_{pq\sigma}(t)|^2$, in general. It then follows that for a given value of the tunneling rate in the two formulations, with and without the non-orthogonality, the corresponding tunnel barrier is thicker and/or higher when the non-orthogonality is neglected than when it is not. Further details can be found in Papers I and II.

The thus developed extension of the transfer Hamiltonian formalism looks very well in order from a principle point of view. Nevertheless one may wonder

Table 3.1: Energy levels $\varepsilon \leq V_0$ in μeV for barrier of width 2 nm and height 0.3 meV. The left and right leads are 100 nm and 48 nm, respectively. The panels, from the left to right, show the four energy levels below the barrier height calculated exactly, without the overlap (OR), and with the overlap (NOR).

Exact	OR	**NOR**
21.5	1.55	**21.7**
73.3	53.7	**72.2**
150	142	**153**
273	229	**303**

whether the inclusion of the overlap has some implications of the physics in the system, apart from that the magnitude of the calculated current becomes smaller. Therefore, let us first look at an equilibrium situation. Suppose that the system is constituted by a hard walled box of length $L_1 + L_2$ with an $a+b$ thick and V_0 high scattering potential, see Fig. 3.1. In this system there is no net current but since it is exactly solvable we can investigate its electronic properties, that is, where the energy levels are located and what are the corresponding values determined from the transfer Hamiltonian approach with and without the inclusion of the overlap $\mathcal{O}_{pq}^{-1}$. For the particular values of the system given in Table 3.1 the system has four energy levels below the barrier height. We see from Table 3.1 that the three lowest energy levels are reproduced with very good agreement when the overlap is taken into account (NOR), while the fourth is in much better agreement with the exact than that where the overlap is neglected (OR). Thus, these values give a hint of the achieved quantitative improvement when the overlap is included.

Going further and looking at the charge distributions of the state corresponding to these energy levels, one can draw the same conclusion from Fig. 3.2. The figure displays the spatial charge distributions for the four levels below the barrier height calculated exactly (solid), with the overlap (dotted) and without the overlap (dashed). The figure also shows the corresponding positions of the energy levels (straight lines). What is noticeable is the extremely bad agreement of

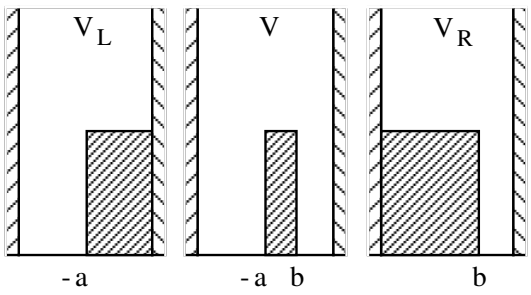

Figure 3.1: The $L_1 + L_2$ wide hard walled box with the $a + b$ wide and V_0 high scattering barrier is displayed in the middle panel, the potential V. The left and right panels correspond to the potentials V_L and V_R, respectively.

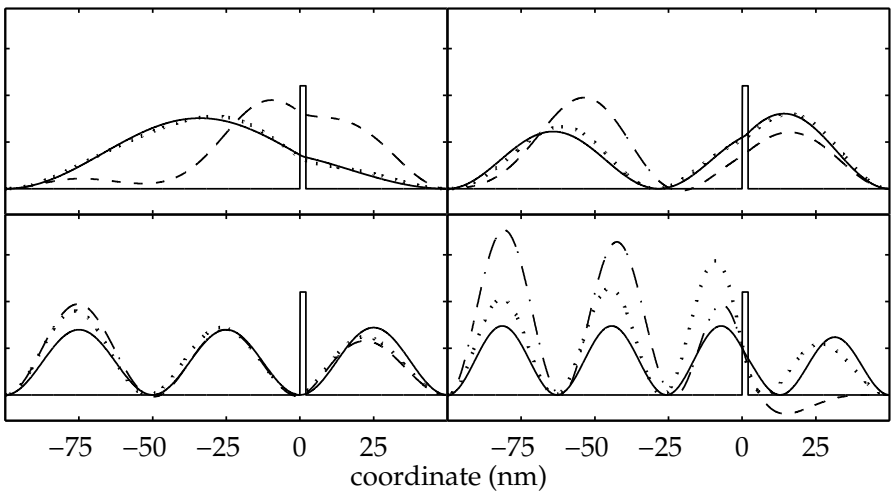

Figure 3.2: The charge distributions of the energy levels in Table 3.1 calculated exactly (solid lines), with the overlap (dotted lines) and without the overlap (dashed lines). The horizontal axes show the spatial coordinates whereas the vertical show the charge distribution probability amplitude (arb. units).

the charge distribution for the lowest level calculated without the overlap compared to the exact. As the energy increases the agreement is slightly better, however, never really convincing as a description of the exact distribution.

Having established an improved description in equilibrium the natural question that arises is how well this is transferred to the non-equilibrium case. For in non-equilibrium the wave functions of the electrons are not confined to a finite space but rather to an infinite one. Therefore we will neither look at the energy levels nor the charge distributions, but instead look directly at the resulting current through the single barrier system. For this reason we make a comparison with an experimental result where the tunnel current through an MIM junction is shown in Fig. 3.3 (solid-dotted). In this particular case the barrier height and width were extracted from a theory developed by Simmons [83, 84], briefly discussed below. By taking the values thus obtained, the tunnel current is then computed with (solid) and without (dashed) the overlap. The conclusion then, is that the qualitative behaviour is improved by including the overlap into the picture. Actually, the higher degree of non-linearity seen in Fig. 3.3 for the case with the overlap taken into account, can be explained from the fact that the tunneling coefficient $V_{pq} = v_{pq} + \mathcal{O}_{pq}^{-1}\varepsilon_{q\sigma}$ is the sum of two quantities of the same order of magnitude. For low voltages, though, they are of opposite signs.[2] As the voltage increases and passes a threshold value, the mixing v_{pq} becomes the dominating quantity in this sum and therefore the current grows very rapidly. Increasing the barrier width by 6% (dash-dotted), the agreement with the experimental curve

[2]Actually, they are of opposite signs for all voltages but the importance of this fact lies mainly within the low voltage regime.

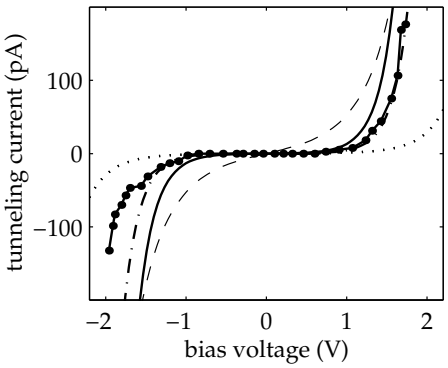

Figure 3.3: The $J - V$ characteristics of a 1.46 nm wide and 1.85 eV high MIM junction (the height measured from the equilibrium chemical potential). The experimental results by Haraichi *et al.*(Ref. [30]) (solid-dotted line) are compared with the computations within the NOR (solid line), NOR with a 6% increase of the width (dash-dotted line), OR (dashed line), and the Simmons formula (dotted line) (Ref. [83, 84]). The equilibrium chemical potential is 1.75 eV and the conduction band width is $2W = 40$ eV.

for positive voltages becomes striking. The asymmetry of the experimental curve is believed to arise from lattice defects in the experimental system, thus responsible for an offset to the left. The dotted line is computed by using the Simmons formula [83, 84] with the values given in Ref. [30].

The theory developed by Simmons [83, 84] is based on a semi-classical approach by calculating the transmission probability in the WKB (Wentzel-Kramers-Brillouin) approximation. The resulting formula for the tunnel current through a single barrier system is given by

$$J \sim \varphi e^{-A\sqrt{\varphi}} - (\varphi + eV)e^{-A\sqrt{\varphi+eV}},$$

where φ is the barrier mean height and A is a constant depending on the barrier width. For low voltages it is shown that this formula reduces to a linear, or Ohmic, $J-V$ dependence whereas for slightly larger voltages such that eV is less than the barrier height the current depends on the voltage roughly as $V + \gamma V^3$, thus explaining the non-linearity of the current.

The results obtained for the single barrier case is motivation enough to proceed in the same spirit when we turn our attention to quantum dot systems. In the systems to be considered then, the charge tunnels from the leads into the quantum dot and vice versa. Since we now know how the conduction electrons in the leads and how the tunneling through insulating barriers can be treated, we can turn our focus on the properties of the quantum dot.

Chapter 4

Current through quantum dots

DURING THE LAST years of the 1980s the first attempts to understand transport through a QD coupled to external leads, based on the concept of the transfer Hamiltonian, were made. Thereafter an enormous amount of reports have been published on the subject. One of the first reported formulas was derived by Larkin and Matveev [59] for low impurity concentrations in the channel and short contacts. Just as in the case of single barrier tunneling, one basic assumption is that the bias voltage drops entirely over the scattering region, e.g. over the QD and the tunnel barriers. Then, the current is proportional to the conductance of the scattering region summed up over the interval between the quasi-chemical potentials in the leads. Mathematically, this is expressed as

$$J = \frac{4e}{\pi\hbar} \sum_i \int \frac{\Gamma_L \Gamma_R}{(\varepsilon - \varepsilon_i)^2 + (\Gamma_L + \Gamma_R)^2} \Big(f(\varepsilon - eV/2) - f(\varepsilon + eV/2) \Big) \mathrm{d}\varepsilon, \quad (4.1)$$

where the sum over the fraction gives the energy dependent conductance of the scattering region and $f(\varepsilon)$ is the Fermi-Dirac distribution function for the electrons in the leads. The scattering region has an impurity resonance at the energy ε_i and is coupled to the left and right leads by the strengths Γ_L and Γ_R, respectively, cf. Fig. 4.1. If we consider the limit with a single impurity, at the energy ε_0, the sum reduces to a single term and if the couplings to the left and right leads are equal, then at zero temperature, $T = 0$, the current is simply

$$J = \frac{4e}{\pi\hbar} \int_{-eV/2}^{eV/2} \frac{\Gamma_L \Gamma_R}{(\varepsilon - \varepsilon_0)^2 + (\Gamma_L + \Gamma_R)^2} \mathrm{d}\varepsilon = \frac{2e^2}{\pi\hbar} V.$$

Thus, the fundamental conductance $\sigma = e^2/(\pi\hbar)$ is retained. It should be noticed that Eq. (4.1) only accounts for time-independent, or stationary, currents.

For the derivation of Eq. (4.1) it was assumed that the impurity resonance energies were known. A formulation of the current that enables further analysis of the impurity resonances in a systematic way and also taking into account time-dependent phenomena, requires a more sophisticated mathematical technique.

4.1 Non-equilibrium Green function approach

Consider an interacting region, e.g. a QD, which is tunnel coupled to the external leads characterized by the quasi-chemical potentials μ_L and μ_R for the left (L) and the right (R) lead, respectively. A typical model of such a system is illustrated schematically in Fig. 4.1. Denote the energy levels of the isolated QD by $\{\varepsilon_n\}_{n\in \text{QD}}$ and the transfer rate (mixing) of an electron between the leads and the QD by $v_{kn\sigma}(t)$, where σ is the spin-projection of the transferred electron. Furthermore, the single-electron energies of the conduction electrons in the leads are denoted by $\varepsilon_{k\sigma}(t) = \varepsilon_{k\sigma} + \Phi_\alpha(t),\ k\sigma \in \alpha = L, R$, where $\Phi_\alpha(t)$ imposes a time-dependent shift to the equilibrium energies through the source-drain (bias) voltage $\Phi_{sd}(t) = \Phi_L(t) + \Phi_R(t)$. A second quantized formulation of the system

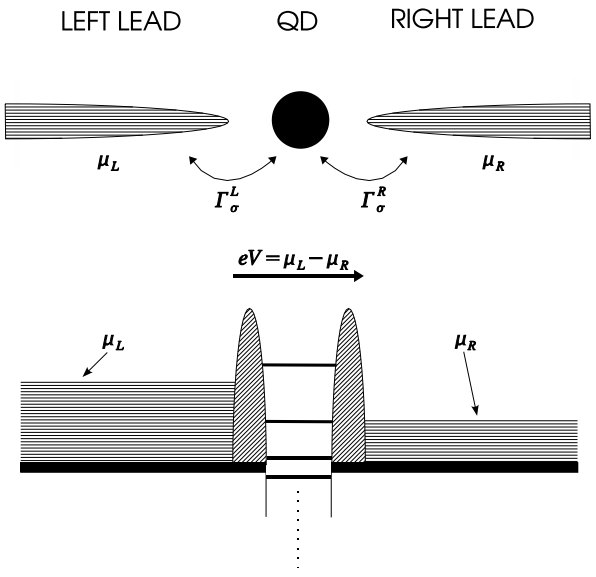

Figure 4.1: A model sketch of a single electron QD system. The QD is located between the leads and due to its size a distinct level quantization is realized, see lower panel. The bias voltage drops entirely over the tunnel barriers and the QD.

can be written as

$$\mathcal{H} = \sum_{k\sigma\in L,R} \varepsilon_{k\sigma}(t) c^\dagger_{k\sigma} c_{k\sigma} + \sum_n \varepsilon_n(t) d^\dagger_n d_n + \mathcal{H}_{int}(t) + \sum_{kn\sigma} (v_{kn\sigma}(t) c^\dagger_{k\sigma} d_n + H.c.), \tag{4.2}$$

where $c^\dagger_{k\sigma}$ ($c_{k\sigma}$), $d^\dagger_n$ (d_n) creates (annihilates) an electron in the lead α and and the QD, respectively. The third term accounts for possible interactions between the states in the QD and knowledge about its specific character is not necessary here. Thus, the analysis of $\mathcal{H}_{int}(t)$ will be postponed to the succeeding chapter. The electron operators in the leads and the QD are assumed to anti-commute, i.e. $\{c_{k\sigma}, d^\dagger_n\} = 0$. Later on in this chapter we will also include the overlap, between the states in the leads and the QD, in the electron operators.

We want to express the current flowing through the system in Eq. (4.2), hence we first have to sort out which quantities we are actually looking for. In Chap. 1 we saw that the current is conserved, the continuity equation Eq. (1.6) is satisfied. If we consider divergence free currents, $\nabla \cdot \mathbf{j}(\mathbf{r}, t) = 0$, it then follows that the total current through the system equals the charge rate of change, or equivalently,

$$J(t) = -\frac{\partial \langle N(t) \rangle}{\partial t} = 0, \tag{4.3}$$

where $\langle N(t) \rangle$ is the total population number of the system. Here and in the following we use atomic units (m, e and $\hbar = 1$). Working within the transfer Hamiltonian formalism this population number can be separated into the quasi-population numbers in the leads and the QD in the sense

$$\langle N(t) \rangle = \langle N_L(t) \rangle + \langle N_R(t) \rangle + \langle N_D(t) \rangle, \tag{4.4}$$

where $\langle N_D(t) \rangle$ is the population number in the QD. The total population number in each part of the system is a sum of the occupied states therein, thus we can write $\langle N_\alpha(t) \rangle = \sum_{k\sigma\in\alpha} \langle n_{k\sigma}(t) \rangle$, $\alpha = L, R$ and $\langle N_D(t) \rangle = \sum_n \langle n_n(t) \rangle$, where $n_{k\sigma} = c^\dagger_{k\sigma} c_{k\sigma}$ and $n_n = d^\dagger_n d_n$. From now on it is clear how to proceed, in principle, since the dynamics of an operator is governed by the Heisenberg equation of motion. Let us first look at the dynamics of the population number in the left lead

$$\frac{\partial \langle N_L(t) \rangle}{\partial t} = i \langle [N_L(t), \mathcal{H}] \rangle = 2\mathrm{Re} \sum_{kn\sigma} v^*_{kn\sigma}(t) \langle d^\dagger_n(t) c_{k\sigma}(t) \rangle. \tag{4.5}$$

Thus, it is proportional to the correlators (correlation functions) between the particles in the lead and the QD. These correlators are given by

$$\langle d^\dagger_n(t) c_{k\sigma}(t) \rangle = -i \int_{-\infty}^{\infty} v_{kn\sigma}(t) \Big(g^<_{k\sigma}(t,t') G^a_{n'n}(t',t) + g^r_{k\sigma}(t,t') G^<_{n'n}(t',t) \Big) \mathrm{d}t', \tag{4.6}$$

where $g^<_{k\sigma}$ and $g^r_{k\sigma}$ are the lesser and retarded forms of the conduction band Green function $g_{k\sigma}(t,t') = (-i)\langle \mathrm{T} c_{k\sigma}(t) c^\dagger_{k\sigma}(t')\rangle$ and are given by

$$g^<_{k\sigma}(t,t') = if(\varepsilon_{k\sigma}-\mu_L)e^{-i\int_{t'}^t \varepsilon_{k\sigma}(s)\mathrm{d}s}, \tag{4.7}$$

$$g^r_{k\sigma}(t,t') = -i\theta(t-t')e^{-i\int_{t'}^t \varepsilon_{k\sigma}(s)\mathrm{d}s}. \tag{4.8}$$

Here $\theta(t)$ is the Heaviside step function. The other quantities, $G^a_{n'n}$ and $G^<_{n'n}$, are the advanced and lesser counterparts of the QD GF to be considered in the succeeding chapter. By defining the couplings between the leads and the QD as

$$\Gamma^\alpha_{nn'}(\varepsilon,t',t) = 2\pi\sum_\sigma \rho^\alpha_\sigma(\varepsilon)v_{n\sigma}(\varepsilon,t)v^*_{n'\sigma}(\varepsilon,t')e^{i\int_{t'}^t \Phi_\alpha(s)\mathrm{d}s}, \tag{4.9}$$

where $\rho^\alpha_\sigma(\varepsilon)$ is the conduction band DOS for the spin projection σ, the tunnel current flowing through the left barrier into the QD is given by the expression [43, 92]

$$\begin{aligned} J_L(t) &= -\frac{1}{\pi}\mathrm{Im}\int_{-\infty}^t \int \mathrm{tr}\ \mathbf{\Gamma}^L(\varepsilon,t',t) \\ &\quad\times\Big(\mathbf{G}^<(t,t') + f(\varepsilon-\mu_L)\mathbf{G}^r(t,t')\Big)e^{i\varepsilon(t-t')}\mathrm{d}\varepsilon\mathrm{d}t'. \end{aligned} \tag{4.10}$$

The bold face notation indicates that the coupling $\mathbf{\Gamma}^L$ and the QD GF $\mathbf{G}^{<,r}$ are matrices in the level indices n, n'. An analogous expression is found for the tunnel current flowing into the QD through the right barrier. However, because of the present time-dependence, the left and the right tunnel currents are not equal, in general.

The tunnel current as expressed in Eq. (4.10) contains the desired target, namely that it includes the time-dependence and is formulated in terms of local properties of the QD. In fact, the current is proportional to the local density of population $N_D(t) = \mathrm{Im}\mathbf{G}^<(t,t)$ and the local DOS $\rho(t) = -\mathrm{Im}\mathbf{G}^r(t,t)/\pi$. Thus, the tunnel current can be interpreted as the sum of the in- and out-tunneling rates. One should bear in mind, though, that both $\mathbf{G}^<$ and $\mathbf{G}^r$ must be calculated in the presence of the tunneling which implies that $\mathbf{G}^<$ depends on the population in the leads and $\mathbf{G}^r$ on the QD occupation.

From the previous discussion we see rather immediately how the dynamics of the QD population can be extracted from the lesser QD GF, since $N_D(t) = \mathrm{Im}\mathbf{G}^<(t)$. Actually, this gives the displacement current in the QD as a response to the tunnel current from the left and right leads. We have

$$J_D(t) = -\frac{\partial\langle N_D(t)\rangle}{\partial t} = -\mathrm{Im}\frac{\partial}{\partial t}\mathrm{tr}\ \mathbf{G}^<(t,t), \tag{4.11}$$

showing that all information about the current through the system can be calculated in terms of the local properties of the QD. In the next chapter we will show that the lesser QD GF can be naturally partitioned into a left and a right contribution, i.e. $\mathbf{G}^<(t) = \mathbf{G}^<_L(t) + \mathbf{G}^R_R(t)$. The part of the displacement current flowing through the left barrier can be written

$$J^L_D(t) = -\mathrm{Im}\frac{\partial}{\partial t}\mathrm{tr}\ \mathbf{G}^<_L(t,t) \tag{4.12}$$

and similarly for the displacement current flowing through the right barrier. The importance of including fluctuating charge distribution in the time-dependent current was first recognized by Anantram and Datta [4] and further emphasized by Hettler and Schoeller [33] and Jauho [42]. Starting from forming the total current through the system, Wang *et al.* [90] derived the linear dynamic conductance for mesoscopic systems. Along these lines You *et al.* [94] made an analysis of the different contributions to the current for a single level QD in non-linear regimes. One important feature they found was that the displacement current tends to retard the tunnel current, thus canceling oscillations in the transient behaviour of the current. The resulting output current then becomes an exponentially growing/ decaying function of the external field. Such a behaviour, which in a sense is expected in a double barrier system, resembles the current growth/decay in a macroscopic capacitor.

From Eqs. (4.10) and (4.11), we obtain the current conservation formula

$$J_L(t) + J_D^L(t) = -\Big(J_R(t) + J_D^R(t)\Big).$$

Thus, we easily see that for time-independent, or stationary, external fields, the displacement current $J_D(t) = 0$ giving that the current flowing through the left barrier equals the current flowing through the right. Then, the net current can be written [64]

$$\begin{aligned} J &= \frac{i}{4\pi}\int \mathrm{tr}\left\{\Big(\mathbf{\Gamma}^L(\varepsilon) - \mathbf{\Gamma}^R(\varepsilon)\Big)\mathbf{G}^<(\varepsilon)\right. \\ &\quad \left. + \Big(f(\varepsilon-\mu_L)\mathbf{\Gamma}^L(\varepsilon) - f(\varepsilon-\mu_R)\mathbf{\Gamma}^R(\varepsilon)\Big)\Big(\mathbf{G}^r(\varepsilon) - \mathbf{G}^a(\varepsilon)\Big)\right\}\mathrm{d}\varepsilon. \end{aligned} \tag{4.13}$$

The stationary current becomes particularly simple if couplings between the QD and the leads are proportionate, that is, suppose that $\mathbf{\Gamma}^R(\varepsilon) = \lambda\mathbf{\Gamma}^L(\varepsilon)$, $\lambda \in [0,1]$.[1] Then, the net current $J = xJ_L + (1-x)J_L = xJ_L - (1-x)J_R$, where $x \in \mathbb{R}$ is arbitrary, and by choosing $x = \lambda/(1+\lambda) = \mathbf{\Gamma}^R(\varepsilon)[\mathbf{\Gamma}^L(\varepsilon) + \mathbf{\Gamma}^R(\varepsilon)]^{-1}$ the stationary current can be written [31, 43, 64]

$$\begin{aligned} J &= \frac{i}{2\pi}\int \Big(f(\varepsilon-\mu_L) - f(\varepsilon-\mu_R)\Big)\mathcal{T}(\varepsilon)\mathrm{d}\varepsilon, \\ \mathcal{T}(\varepsilon) &= \mathrm{tr}\left\{\mathbf{\Gamma}^L(\varepsilon)\mathbf{\Gamma}^R(\varepsilon)\Big(\mathbf{\Gamma}^L(\varepsilon) + \mathbf{\Gamma}^R(\varepsilon)\Big)^{-1}\Big(\mathbf{G}^r(\varepsilon) - \mathbf{G}^a(\varepsilon)\Big)\right\}. \end{aligned} \tag{4.14}$$

Although this formula appears similar to the Landauer formula , the expression preceding Eq. (2.16), it is important to bear in mind that there is no immediate connection between these two formulations. Especially, if inelastic scattering is present in the interacting region there is no such connection.

Within the formulation presented in this section one may very well introduce the non-orthogonality, which is straight forward with the technique defined in Sec. 3.1, and many-body effects into the treatment. However, although the existing diagram techniques for single-electron GF are well-established and have

[1] We can assume that $\mathbf{\Gamma}^L(\varepsilon) \geq \mathbf{\Gamma}^R(\varepsilon)$ and let $\lambda \in [0,1]$, for if not, we can instead put $\mathbf{\Gamma}^L(\varepsilon) = \lambda\mathbf{\Gamma}^R(\varepsilon)$ and retain the requirement that $\lambda \in [0,1]$.

proven successful for the explanation of lots of effects, it is motivated to express the physics of the QD in terms of many-body states. For instance, the full mean-field approximation (MFA) of the QD GF within a many-body approach turns out to go beyond the standard MFA as obtained within any single-electron theory. Therefore, in the succeeding section, we will do both, that is, introduce the non-orthogonality between the states in the leads and the QD and, in addition, express the QD fermion operators in terms of many-body operators.

4.2 Non-orthogonality and many-body states

Including the non-orthogonality into the formalism is straight forward by the technique discussed in Chap. 3. For clarity, though, we introduce the annihilation operators for the electrons in the leads and the QD by

$$c_{k\sigma}(t) = \sum_{m\in L\cup D\cup R} \mathcal{O}^{-1}_{km\sigma} \int \phi^*_m(x)\psi(x,t)\mathrm{d}x, \quad k \in L, R, \tag{4.15}$$

$$d_n(t) = \sum_{m\in L\cup D\cup R} \mathcal{O}^{-1}_{nm\sigma} \int \phi^*_m(x)\psi(x,t)\mathrm{d}x, \quad m \in D, \tag{4.16}$$

where $\psi(x,t)$ is the field operator of the exact model system and $\phi_k(x)$, $\phi_D(x)$ are wave functions in the auxiliary systems $\alpha = L, R$ and D, cf. Fig. 4.2. Here, we

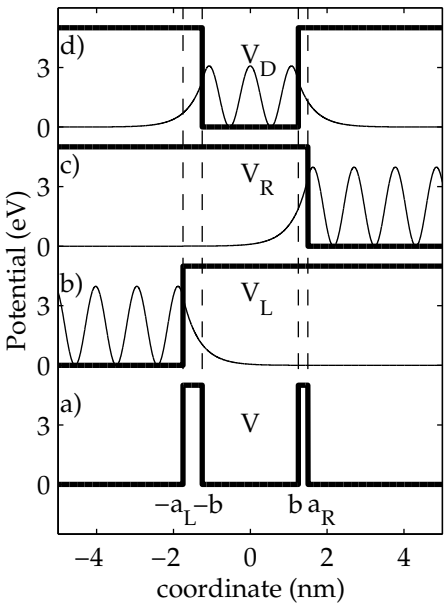

Figure 4.2: The potential V in the real system (bottom panel) is divided into the auxiliary left V_L, right V_R and middle V_D potentials. For the auxiliary potentials the squared modulus of examples of wave functions in each system are plotted.

put the spin index σ on the overlap matrix element in order to keep track of the spin projections of the electrons. The creation operators are defined analogously. Just as in the single barrier case the anti-commutation relations between the electrons on the leads and the QD become $\{c_{k\sigma}, d_n\} = \mathcal{O}^{-1}_{kn\sigma}$ and $\{c_{p\sigma}, c^\dagger_{q\sigma}\} = \mathcal{O}^{-1}_{pq\sigma}$, $p \in L$ and $q \in R$. Now, since the overlap between states in the left and right leads are exponentially small we replace the latter anti-commutator by zero, thus neglecting possible direct tunneling between the leads. The model Hamiltonian remains formally the same as in Eq. (4.2), however, with the new interpretation and anti-commutation relations of the electron operators.

Consider the system in Fig. 4.1 and Eq. (4.2) and suppose that we want to include the Coulomb repulsion between the QD states into the picture. For simplicity, we assume that there is only a single QD level taking part in the conduction. Then, the interaction Hamiltonian $\mathcal{H}_{int}$ contains the Hubbard U term $Un_\uparrow n_\downarrow$ for the electron-electron repulsion between the states $|\uparrow\rangle$ and $|\downarrow\rangle$. In the QD, the kinetic energy and the Hubbard U term can be written $\mathcal{H}_D = \sum_\sigma \varepsilon_\sigma d^\dagger_\sigma d_\sigma + Un_\uparrow n_\downarrow$. In the 1960s, Hubbard [36, 37] introduced the many-body operator $X^{pp'} \equiv |p\rangle\langle p'|$, describing the transition from the state $|p'\rangle$ to $|p\rangle$. By doing this, a diagonalization of $\mathcal{H}_D$ is possible since the operator

$$\begin{aligned} d_\sigma &= \sum_{pp'} |p\rangle\langle p|\, d_\sigma\, |p'\rangle\langle p'| = \sum_{pp'} \langle p|\, d_\sigma\, |p'\rangle\, X^{pp'} \\ &= \langle 0|\, d_\sigma\, |\sigma\rangle\, X^{0\sigma} + \eta_\sigma \langle \bar\sigma|\, d_\sigma\, |2\rangle\, X^{\bar\sigma 2} = X^{0\sigma} + \eta_\sigma X^{\bar\sigma 2}, \end{aligned} \tag{4.17}$$

where $\eta_\sigma = \pm 1$, for $\sigma = \uparrow, \downarrow$, and where $|2\rangle$ denotes the doubly occupied state $|\uparrow\downarrow\rangle$. Then, the products $d^\dagger_\sigma d_\sigma = (X^{\sigma 0} + \eta_\sigma X^{2\bar\sigma})(X^{0\sigma} + \eta_\sigma X^{\bar\sigma 2}) = h^\sigma + h^2$ and $n_\uparrow n_\downarrow = h^2$, where we have put the diagonal transition $h^p \equiv X^{pp}$. The equalities are simple to derive by recalling that $\langle p|p'\rangle = \delta_{pp'}$. Thus, the diagonal form of $\mathcal{H}_D$ becomes

$$\mathcal{H}_D = E_0 h^0 + E_\uparrow h^\uparrow + E_\downarrow h^\downarrow + E_2 h^2 = \sum_{p=0,\sigma,2} E_p h^p, \tag{4.18}$$

where $E_0 = 0$ is the energy of the unoccupied state, $E_\sigma = \varepsilon_\sigma$ and $E_2 = \varepsilon_\uparrow + \varepsilon_\downarrow + U$. Later on we will consider a large Coulomb repulsion between the intra QD states. Therefore, we let $U \to \infty$ already at this stage, so that the doubly occupied QD state is excluded in the sequel.

If we let $\mathcal{H}'_{int}$ contain all other interactions than the Coulomb repulsion, the model Hamiltonian can be written

$$\begin{aligned} \mathcal{H} = \sum_{k\sigma\in L,R} \varepsilon_{k\sigma}(t) c^\dagger_{k\sigma} c_{k\sigma} + \sum_{p=0,\sigma} E_p(t) h^p + \mathcal{H}'_{int}(t) \\ + \sum_{k\sigma} \Big(v_{k\sigma}(t) c^\dagger_{k\sigma} X^{0\sigma} + H.c. \Big). \end{aligned} \tag{4.19}$$

This model has certain formal similarities with the model given in Eq. (4.2). However, in the present case the Coulomb repulsion between the QD state is already included into the second term. This actually simplifies the treatment of the physics in the QD, as we will see in the Chap. 5. The prize we have to pay, though, is that the anti-commutator of the Hubbard operators are not as simple as between single-particle operators. We have $\{X^{pp'}, X^{qq'}\} = \delta_{p'q} X^{pq'} + \delta_{pq'} X^{qp'}$. The

physical interpretation of the non-zero anti-commutator are known as *kinematic interactions*, to be distinguished from *dynamic interactions* that occur in a Dyson equation representation of a given quantity. The terminology was introduced by Dyson [18] in a study of spin-wave interactions by means of the spin-operators $\mathbf{S}^i$, $i = x,y,z$. These operators satisfy the commutation relations $[\mathbf{S}^i, \mathbf{S}^j] = i\epsilon_k^{ij}\mathbf{S}^k$, where ϵ_k^{ij} is the Levi-Cevita density tensor. Further details can be found in, for instance, Refs. [17, 45, 62, 68].

4.2.1 Commutation relations

By the introduction of the many-body operators we need to know the commutation relations between a conduction electron in the leads and the different Hubbard operator. From the commutation relations between the c- and d-operators together with the expansion of the d-operators in terms of Hubbard operators we find that [26, 75, 76]

$$\{c_{k\sigma}, X^{\sigma' 0}\} = \mathcal{O}_{k\sigma}^{-1}\{X^{0\sigma}, X^{\sigma' 0}\} = \mathcal{O}_{k\sigma}^{-1}(\delta_{\sigma\sigma'}h^0 + Z^{\sigma'\sigma}), \tag{4.20}$$

where $Z^{\sigma'\sigma} \equiv X^{\sigma'\sigma}$ denotes a Bose-like transition (the total number of electrons is changed by an integer number). Similarly, we have

$$\{c_{k\sigma}, X^{0\sigma'}\} = 0, \tag{4.21}$$

since there cannot occur annihilation of a particle in the lead and the QD simultaneously. In the Heisenberg equation of motion combinations of the c- and h-operators will occur as commutators rather than anti-commutators. Thus, we calculate

$$[c_{k\sigma}, h^{\sigma'}] = \delta_{\sigma\sigma'}\mathcal{O}_{k\sigma}^{-1}X^{0\sigma}, \tag{4.22}$$

$$[c_{k\sigma}, h^0] = -\mathcal{O}_{k\sigma}^{-1}X^{0\sigma}. \tag{4.23}$$

4.2.2 Dynamics of the conduction electrons

Now, when the commutation relations between the introduced operators have been sorted out, we can approach the formulation of the current in the system. As mentioned in Sec. 4.1, the current can be expressed as the charge rate of change and therefore the Heisenberg equation of motion comes handy again. The dynamics of a conduction electron in the leads is given by [26]

$$\left(i\frac{\partial}{\partial t} - \varepsilon_{k\sigma}\right)c_{k\sigma} = V_{kD\sigma}(t)X^{0\sigma} + \left(\mathcal{O}_{kD\sigma}^{-1}v_{k\sigma}^*(t)(h^0 + h^\sigma)c_{k\sigma} + \mathcal{O}_{kD\bar{\sigma}}^{-1}v_{k\bar{\sigma}}^*(t)Z^{\bar{\sigma}\sigma}c_{k\bar{\sigma}}\right), \tag{4.24}$$

where $V_{kD\sigma}(t) = v_{k\sigma}(t) + \mathcal{O}_{kD\sigma}^{-1}\Delta_{\sigma 0}^0(t)$ is the new tunneling coefficient and $\Delta_{\sigma 0}^0(t) = E_\sigma(t) - E_0(t)$ is the bare energy for the transition $|0\rangle \rightarrow |\sigma\rangle$. The second term in $V_{kD\sigma}(t)$ is a direct consequence of taking the non-orthogonality into account and

just as for the single barrier case, its magnitude is in the order of $v_{k\sigma}$ but with opposite sign. Thus, the resulting current amplitude will become much smaller than when the non-orthogonality is neglected. In comparison with experiments then, the two pictures will provide different values for the widths and heights of the tunnel barriers, since they are directly linked to the strength of the couplings between the leads and the QD. Actually, the product of the barrier width and height is always interpreted as being smaller within the non-orthogonal picture than when the overlap is neglected.

4.3 Current in the non-orthogonal framework

Being interested in the total current in the system it is necessary to find out what the total population number $\langle N(t)\rangle$ is constituted of. By means of the electron operators introduced in Eqs. (4.15) and (4.16) we expand the field operators ψ_L, ψ_R and ψ_D for the leads and the QD, respectively, as

$$\psi_\alpha(x,t) = \sum_{k\sigma\alpha} c_{k\sigma}(t)\phi_k(x), \tag{4.25}$$

$$\psi_D(x,t) = \sum_{\sigma} d_\sigma(t)\phi_D(x). \tag{4.26}$$

Here, $\phi_k(x)$, $k \in L, R$ is a wave function in the lead subsystem $\alpha = L, R$, whereas ϕ_D is a wave function in the QD subsystem. By the trivial expansion $\psi(x,t) = \psi_A(x,t) + [\psi(x,t) - \psi_A(x,t)]$, where $\psi_A(x,t) = \psi_L(x,t) + \psi_R(x,t) + \psi_D(x,t)$, the exact field operator is approximated by $\psi_A(x,t)$. The term in brackets can be made arbitrarily small by including sufficiently many states in the field operators of the auxiliary system.[2] We assume that this is already done and therefore we can neglect the remainder term in brackets. The total population number in the system now becomes

$$\langle N(t)\rangle = \int \langle \psi^\dagger(x,t)\psi(x,t)\rangle \mathrm{d}x = \sum_\alpha [\langle N_{\alpha\alpha}(t)\rangle + \langle N_{\alpha D}(t)\rangle] + \langle N_{DD}(t)\rangle, \tag{4.27}$$

where $N_{\alpha\alpha}(t) = \int \psi^\dagger_\alpha(x,t)\psi_\alpha(x,t)\mathrm{d}x$, $N_{\alpha D}(t) = 2\mathrm{Re}\int \psi^\dagger_D(x,t)\psi_\alpha(x,t)\mathrm{d}x$ and $N_{DD}(t) = \int \psi^\dagger_D(x,t)\psi_D(x,t)\mathrm{d}x$ are the quasi-population numbers in the leads, the barriers and in the QD, respectively. The quasi-population numbers $N_{\alpha D}(t)$, being products of creation and annihilation operators of the leads and the QD, describe electrons in the mixed state. This quasi-population gives a refinement of the transport theory directly due to the non-orthogonality and is always absent in the usual transfer Hamiltonian approach. The conclusion is that when the non-orthogonality is neglected, quantities that may be significant in some situations are completely lost. The significance of the different contributions, which appear in our theory and are absent in orthodox theories, is analyzed in Papers III and IV and further discussed in Secs. 5.3 and 5.4.

[2] The idea behind this method [75] is similar to the method of linear combinations of atomic (molecular) orbitals LCAO (LCMO), which is well known in quantum chemistry and *ab initio* electronic structure calculations.

The expression for the tunnel current $J_{LL}(t)$ through the left barrier, which is derived in detail Paper III, reads

$$J_{LL}(t) = -\frac{1}{\pi}\mathrm{Im}\sum_{\sigma}\int_{-\infty}^{t}\int \Gamma_{\sigma}^{L}(\varepsilon,t,t') \Big(G_{\sigma}^{<}(t,t') + f(\varepsilon-\mu_L)G_{\sigma}^{r}(t,t')\Big)e^{i\varepsilon_(t-t')}\mathrm{d}t'. \quad (4.28)$$

Formally, this expression is exactly the one shown in Eq. (4.10), apart from that the coupling and the QD GF are not given as matrices. However, in the present case the coupling between the leads and the QD is given by

$$\Gamma_{\sigma}^{L}(\varepsilon,t,t') = 2\pi V_{LD\sigma}(t)V_{LD\sigma}^{*}(t')\rho_{\sigma}^{L}(\varepsilon)e^{i\int_{t'}^{t}\Phi_L(s)\mathrm{d}s}, \quad (4.29)$$

where $V_{LD\sigma}(t) = v_{L\sigma}(t)+\mathcal{O}_{LD\sigma}^{-1}\Delta_{\sigma 0}^{0}$. Similarly as in Sec. 4.1, the QD displacement current $J_{DD}(t) = -\partial/\partial t\langle N_{DD}(t)\rangle$ is given by

$$J_{DD}(t) = -\mathrm{Im}\frac{\partial}{\partial t}\sum_{\sigma}G_{\sigma}^{<}(t,t), \quad (4.30)$$

since $\langle N_{DD}(t)\rangle = \sum_{\sigma}\langle N_{\sigma}(t)\rangle = \mathrm{Im}G_{\sigma}^{<}(t,t)$. Just as in the case where the overlap is neglected, the lesser counterpart of the QD GF can be partitioned into a left and a right term according to $G_{\sigma}^{<}(t,t) = G_{L\sigma}^{<}(t,t) + G_{R\sigma}^{<}(t,t)$. Thus, we can write the part of the QD displacement current that flows through the left barrier as

$$J_{DD}^{L}(t) = -\mathrm{Im}\frac{\partial}{\partial t}\sum_{\sigma}G_{L\sigma}^{<}(t,t) \quad (4.31)$$

and similarly for the flow through the right barrier.

In order to completely determine the current through the left barrier, the last quantity to take care of is the current coming from $\langle N_{LD}(t)\rangle$. We note that

$$\langle N_{LD}(t)\rangle = 2\mathrm{Re}\sum_{\sigma}\sum_{p\in L}\mathcal{O}_{p\sigma}\langle X^{\sigma 0}(t)c_{p\sigma\sigma}(t)\rangle, \quad (4.32)$$

that is, the quasi-population number describes the correlations between the conduction electrons and the localized states in the QD. Hence, the resulting current will be rate of change of this quantity. The correlation function $\mathrm{Re}\langle X^{\sigma 0}(t)c_{p\sigma}(t)\rangle = i\partial/\partial t\langle N_{LL}(t)\rangle$ and is already known from the derivation of the tunnel current $J_{LL}(t)$, cf. Paper III. The displacement current $J_{LD}(t)$ is given by

$$J_{LD}(t) = -\frac{1}{\pi}\mathrm{Re}\frac{\partial}{\partial t}\sum_{\sigma}\int\Bigg(\mathcal{O}_{DL\sigma}\mathcal{O}_{LD\sigma}^{-1}\rho_{\sigma}^{L}(\varepsilon)P_{\sigma}(t)f(\varepsilon-\mu_L) - \int_{-\infty}^{t}\gamma_{\sigma}^{L}(\varepsilon,t,t')\Big[G_{\sigma}^{<}(t,t') + f(\varepsilon-\mu_L)G_{\sigma}^{r}(t,t')\Big]e^{i\varepsilon(t-t')}, \quad (4.33)$$

where the overlap $\mathcal{O}_{DL\sigma} = \mathcal{O}_{LD\sigma}^{*}$ and the end-factor $P_{\sigma}(t) \equiv \langle\{X^{0\sigma}, X^{\sigma 0}\}(t)\rangle = \langle N_0(t)\rangle + \langle N_{\sigma}(t)\rangle$ is the sum of the time-dependent populations of the states $|0\rangle$ and $|\sigma\rangle$ in the QD. The coupling

$$\gamma_{\sigma}^{L}(\varepsilon,t,t') = 2\pi\mathcal{O}_{DL\sigma}V_{LD\sigma}(t')\rho_{\sigma}^{L}(\varepsilon)e^{i\int_{t'}^{t}\Phi_L(s)\mathrm{d}s}. \quad (4.34)$$

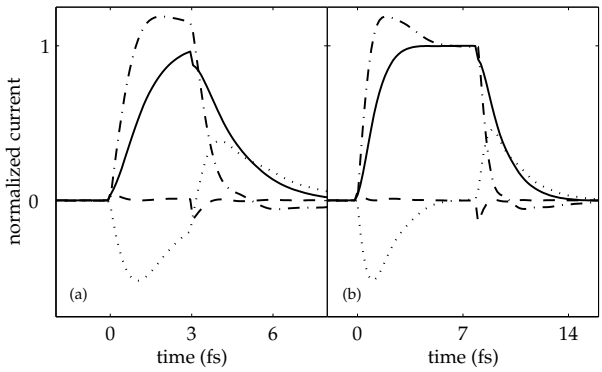

Figure 4.3: The time-dependent current $J_L(t)$ (solid line), the tunnel current $J_{LL}(t)$ (dash-dotted line) and the displacement currents $J^L_{DD}(t)$ (dotted line) and $J_{LD}(t)$ (dashed line) flowing through the left barrier, cf. Fig. 4.1. The QD is 4 nm wide and is connected to the leads via 0.5 nm tunnel barriers. The bare many-body level $\Delta^0_{\sigma 0} = 325$ meV relative to the equilibrium chemical potential ($\mu = 0$). The coupling $\Gamma^L_\sigma + \Gamma^R_\sigma \sim 350$ meV giving the relaxation time $\tau_\sigma \sim 2$ fs. The conduction band width is 2 eV, the end-factor $P_\sigma \sim 0.785$ and the bias voltage $\Phi_{sd}(t) = \theta(t) - \theta(t - t_1)$ V, $t_1 = 3$ fs (a) and 8 fs (b).

Physically, the displacement currents are responsible for a redistribution of the charge in the system as an effect of the charge rate of change (current flow). The QD displacement current $J^L_{DD}(t)$ is a response of the charge accumulation in the QD and tends to retard the tunnel current flowing into the QD through the left barrier. In contrast, the displacement current $J_{LD}(t)$ is directly connected to the rate of change of the tunnel current $J_{LL}(t)$ and can either function as to retard or accelerate the tunnel current, depending on the phase of the input voltage.

Now, we know all the formal details about the current through the QD system, as given within the non-orthogonal approach to the transfer Hamiltonian formalism. We summarize it by concluding that the current conservation law in the present formulation has the form

$$J_{LL}(t) + J^L_{DD}(t) + J_{LD}(t) = -\Big[J_{RR}(t) + J^R_{DD}(t) + J_{RD}(t)\Big]. \tag{4.35}$$

All terms in this equation are, via the couplings Γ^α_σ and γ^α_σ, influenced by the inclusion of the overlap. Moreover, the terms $J_{LD}(t)$ and $J_{RD}(t)$ serve as a direct consequence of taking the non-orthogonality into account. In Fig. 4.3, an example that also can be found in Paper IV, the net current (solid) flowing through the left barrier, c.f. Fig. 4.1, is given as a function of time, for two different rectangular bias voltage pulses $\Phi_{sd}(t) = \Phi[\theta(t) - \theta(t - t_1)]$. The previously mentioned exponential growth/decay of the net current is readily seen in the plots. The figure also illustrates the tunnel current $J_{LL}(t)$ (dash-dotted) and the displacement currents $J^L_{DD}(t)$ (dotted) and $J_{LD}(t)$ (dashed). It is noticeable that the tunnel current grows, at the onset of the bias voltage pulse ($t = 0$), to a value that exceeds its steady state value, cf. Fig. 4.3 (b). For some parameters tunnel current shows an apparent oscillatory behaviour decaying to the steady state amplitude, as we

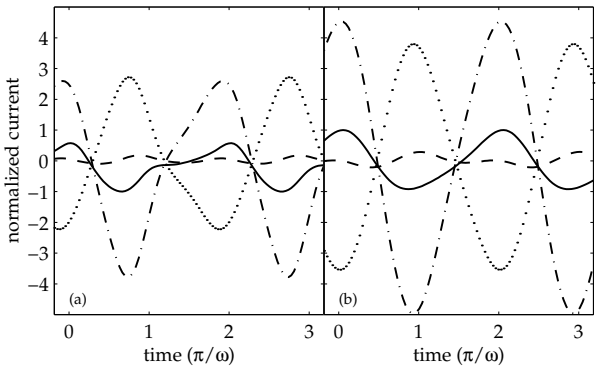

Figure 4.4: The time-dependent current $J_L(t)$ (solid line), the tunnel current $J_{LL}(t)$ (dash-dotted line) and the displacement currents $J^L_{DD}(t)$ (dotted line) and $J_{LD}(t)$ (dashed line) flowing through the left barrier, c.f. Fig. 4.1. The system is the same as in Fig. 4.3, now with the bias voltage $\Phi_{sd}(t) = \cos(\omega t)$ V for the frequencies $\omega = 500$ THz a) and 1000 THz b).

will see in Chap. 5. These oscillations, ringing, is an effect of the very rapid onset of the bias voltage, due to charge pile up at the barrier interfaces. Also at the termination of the voltage pulse the tunnel current shows a weak ringing. The displacement current $J^L_{DD}(t)$ has the opposite sign of the tunnel current which, thus, displays that it tends to retard the tunnel current, as a response to the charge accumulation between the tunnel barriers. As expected, its steady state value is zero, since then the current rate of change vanishes. The displacement current $J_{LD}(t)$ has the same sign as the tunnel current which corresponds to the intuitive picture, since when the current grows/decays its rate of change is positive/negative. However, for a harmonic bias voltage $\Phi_{sd}(t) = \Phi\cos(\omega t)$, as is illustrated in Fig. 4.4, c.f. Paper IV, it is readily seen that $J_{LD}(t)$ tends to retard the tunnel current for some times t whereas at other times the tunnel current is accelerated. We believe this to be an effect of that the tunnel current is constituted by a superposition of currents with different phases which rate of change become dominating at different times in the period. With this interpretation, the intuitive picture holds even though the observed behaviour of the tunnel current seems to follow the input bias voltage, although with an altered phase. Actually, in Fig. 4.4 the total current displays some ringing (distortions). It is expected that the tunnel current shows a higher degree of non-linearity for lower frequencies and we will see a mathematical explanation of this fact in the next chapter.

In the time-independent case the displacement currents J^α_{DD} and $J_{\alpha D}$, $\alpha = L, R$ vanish and the current through the left barrier equals the current through the right, as expected. Hence, the net current through the system can be written

$$\begin{aligned} J &= \frac{i}{4\pi}\sum_\sigma \int \Big\{ \Big(\Gamma^L_\sigma(\varepsilon) - \Gamma^R_\sigma(\varepsilon)\Big) G^<_\sigma(\varepsilon) \\ &\quad + \Big(f(\varepsilon-\mu_L)\Gamma^L_\sigma(\varepsilon) - f(\varepsilon-\mu_R)\Gamma^R_\sigma(\varepsilon)\Big)\Big(G^r_\sigma(\varepsilon) - G^a_\sigma(\varepsilon)\Big)\Big\} \mathrm{d}\varepsilon. \end{aligned} \quad (4.36)$$

Also, this formula can be extensively simplified by considering the case of proportionate couplings $\Gamma^R_\sigma(\varepsilon) = \lambda\Gamma^L_\sigma(\varepsilon)$, cf. Sec. 4.1. By the same procedure leading to Eq. (4.14), we obtain

$$\begin{aligned} J &= \frac{i}{2\pi}\sum_\sigma \int \Big(f(\varepsilon-\mu_L) - f(\varepsilon-\mu_R)\Big)\widetilde{\mathcal{T}}_\sigma \mathrm{d}\varepsilon \\ \widetilde{\mathcal{T}}_\sigma &= \frac{\Gamma^L_\sigma(\varepsilon)\Gamma^R_\sigma(\varepsilon)}{\Gamma^L_\sigma(\varepsilon)+\Gamma^R_\sigma(\varepsilon)}\Big(G^r_\sigma(\varepsilon) - G^a_\sigma(\varepsilon)\Big). \end{aligned} \tag{4.37}$$

If we consider the trace in the definition of $\mathcal{T}$ in Eq. (4.14) to only generate the sum over the spin degrees of freedom, then Eq. (4.14) is directly generalized by Eq. (4.37) with respect to the included non-orthogonality in the latter. Thus, the same observation holds also in this case, that despite the apparent similarity of Eq. (4.37) to the Landauer formula there is no immediate connection between them.

An example of both experimental [71] and calculated stationary currents in a small QD proportionate coupled to external contacts is provided in Fig. 4.5 for two different temperatures. The QD is constructed by a ~ 4 nm diameter large gold cluster and the contacts are put a distance ~ 3 nm from the QD. Thus, the tunnel barriers are given by the vacuum between the contacts and the QD. It is

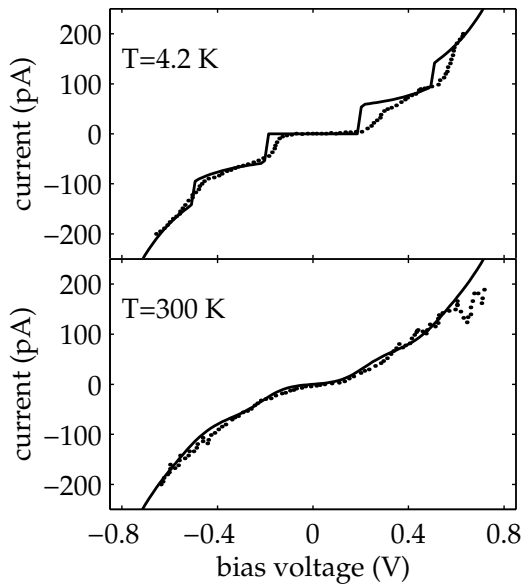

Figure 4.5: The experimental (dotted lines) and calculated (solid lines) stationary current through a 4 nm QD (gold cluster) attached to external contacts via 3 nm wide and ~ 1 eV high (vacuum) tunnel barriers. For the calculations the conduction band density of states is assumed to be $\rho^\alpha = 1/(2W)$, where $2W \sim 2$ eV is the conduction electrons band width.

expected that the two levels with the lowest energy are found at roughly 10 meV and 50 meV. The experimental data (dotted) in the upper panel in Fig. 4.5 displays this fact by the staircase structure. The steps are found at 20 mV and 100 mV, respectively, which correspond to the expected values since the device is biased by $\pm\Phi/2$. Taking the experimental information about the QD and the tunnel barriers (estimating the barrier height to ~ 1 eV), the current calculated by Eq. (4.37). The result shown in the upper panel in Fig. 4.5 (solid) displays the qualitative behaviour of the current in good agreement. Also, for the higher temperature (lower panel) the agreement is satisfactory. Actually, for high temperatures electron-phonon interactions in the QD should be important. In the present case, though, contributions from such interactions do not seem to be essential.

We conclude this chapter by noting that the transfer Hamiltonian formalism can be generalized in a straight forward way to include the non-orthogonality between the leads and the interacting region. The non-orthogonality leads to altered (anti-) commutation relations between the electron operators in the leads and the QD. As an effect, the tunneling coefficient is replaced $v_{k\sigma}(t) \to V_{kD\sigma}(t) = v_{k\sigma}(t)+\mathcal{O}^{-1}_{kD\sigma}\Delta^0_{\sigma 0}$. The new tunneling coefficient consists of two terms of the same order of magnitudes but with opposite signs. The resulting current has one to two orders of magnitudes smaller amplitude, for certain ranges of the bias voltage, than the corresponding current given without including the overlap. This fact is important for an adequate development of the theory and a sound interpretation of the mathematical formulation.

Chapter 5

Focusing on the quantum dot

FROM NOW ON we will put our efforts in understanding the properties of the QD. For simplicity, we will remain with a single level QD with a large Coulomb repulsion between the states and thereby excluding the double occupancy of the level. We will disregard all other types of interactions that may occur in the QD. A sketch of such a system in some different configurations is illustrated in Fig. 5.1. When the QD is unoccupied, Fig. 5.1 a), an electron, say of spin $\uparrow$, from the lead with the higher potential can tunnel into the QD. Actually, tunneling of an electron from the lead with the lower potential is physically possible, however, unlikely. As the QD has an occupied state, Fig. 5.1 b), no second electron from the leads can tunnel into the QD. The spin $\uparrow$ state is already populated and, hence, by the Pauli principle a second spin $\uparrow$ electron is forbidden. Spin $\downarrow$ electrons, which are allowed, have a very high energy barrier to overcome, due to the large intra-dot Coulomb repulsion. On the other hand, if the electron that populates the QD is pushed out at the same time as an electron from the leads enters, a net charge flow between the leads is created, from the higher to the lower potential, see Fig. 5.1 c). In this case the entering electron may have any spin since the occupying spin $\uparrow$ electron leaves the QD at the same time.

The system constituted by a QD attached to contacts is roughly characterized by the ratio of the effective Coulomb repulsion U between electrons in the QD and the coupling $\Gamma \sim 2\pi \sum_\alpha |v_\alpha|^2 \rho^\alpha$ between the QD and the leads. Here, v_α is the mixing between states in the lead α and the QD whereas ρ^α is the DOS in the lead. If the ratio $U/\Gamma \ll 1$, then one uses the weak-coupling perturbation theory, where U is treated as the perturbation to the single-particle picture. In the oppo-

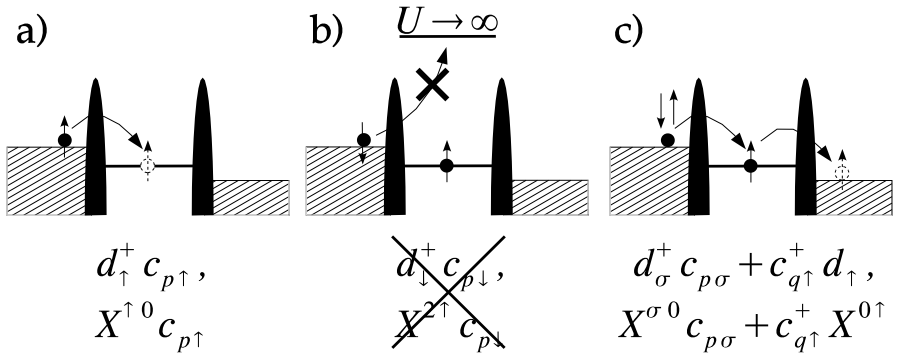

Figure 5.1: A mechanism for tunneling. a) An electron in the lead with the higher potential enters the empty QD. b) A second electron cannot enter already occupied QD. c) An electron enters the QD combined with a simultaneous exit of the QD electron.

site case, that is $U/\Gamma \gg 1$, a more appropriate approach would be strong-coupling perturbation theory. In practice, though, both cases are met. When the contact is good, usually the coherent current picture works well whereas when the contact is not very good, the individual features of the QD are preserved. Then, it is better to consider the diagonal representation of the corresponding isolated QD, thus treating the couplings Γ through the contacts as a perturbation. Here we are focusing on the latter case.

First, though, we will discuss the properties as given with a single-particle operator formulation and thereafter we move on to the many-body picture. As we will see, the two formulations give rise to different descriptions and, for instance, already the MFA of the system actually give rather different behaviour of the electronic properties in the QD. In order not to make the discussion too involved we start up in the formulation where the non-orthogonality is neglected and include it at the very end, in combination with the many-body states in the QD.

5.1 Single-particle picture

The mathematical formulation of the QD system in terms of single-particle operators reads

$$\begin{aligned} \mathcal{H} &= \sum_{k\sigma \in L,R} \varepsilon_{k\sigma}(t) c_{k\sigma}^\dagger c_{k\sigma} + \sum_\sigma \varepsilon_\sigma(t) d_\sigma^\dagger d_\sigma + U n_\uparrow n_\downarrow \\ &\quad + \sum_{k\sigma} (v_{k\sigma}(t) c_{k\sigma}^\dagger d_k + H.c.). \end{aligned} \tag{5.1}$$

This model is known as the extended Anderson model.[1] In the 1960s Anderson [5] introduced this model for the investigation of magnetic impurities in alloys.

[1] the word extended calls on the presence of the two conduction bands

Then, the *single* conduction band, corresponding to the first term in Eq. (5.1), represents s-electron orbitals whereas the second and and third terms describes the localized d-orbitals. The Anderson model has also been used for an understanding of rare earth alloys, magnetic impurities in non-magnetic metals, investigations of the Kondo effect etc. For a review of the Anderson model in the theory of magnetic alloys we refer to [88]. Introductory descriptions can also be found in [34, 93].

The behaviour of a localized QD electron with spin σ can be found by solving the equation of motion

$$\left(i\frac{\partial}{\partial t}-\varepsilon_\sigma(t)\right)G_\sigma(t,t')=\delta(t-t')+\sum_k v^*_{k\sigma}(t)G_{k\sigma}(t,t')+UG_{\bar\sigma\sigma}(t,t'), \tag{5.2}$$

where $G_\sigma(t,t')=(-i)\langle \mathrm{T}d_\sigma(t)d^\dagger_\sigma(t')\rangle$ is the single-particle QD GF and $G_{k\sigma}(t,t')=(-i)\langle \mathrm{T}c_{k\sigma}(t)d^\dagger_\sigma(t')\rangle$ describes the transfer of an electron through the tunnel barriers. The transfer GF is given by

$$\left(i\frac{\partial}{\partial t}-\varepsilon_{k\sigma}(t)\right)G_{k\sigma}(t,t')=v_{k\sigma}(t)G_\sigma(t,t'). \tag{5.3}$$

The GF $G_{\bar\sigma\sigma}(t,t')=(-i)\langle \mathrm{T}n_{\bar\sigma}(t)d_\sigma(t)d^\dagger_\sigma(t')\rangle$ accounts for the double occupancy in the QD. Although this state will be excluded in the end, we have to include it in order not to be within a non-interacting description.

5.1.1 Non-interacting resonant level

Suppose that the doubly populated state is excluded already in the Hamiltonian, Eq. (5.1). Then, the solution of the QD GF can be written exactly as

$$G_\sigma(t,t')=g_\sigma(t,t')+\int_{t_0}^{t_0-i\beta} g_\sigma(t,s)\Sigma_\sigma(s,s')G_\sigma(s',t')\mathrm{d}s\mathrm{d}s', \tag{5.4}$$

where the self-energy

$$\Sigma_\sigma(t,t')=\sum_k v^*_{k\sigma}(t)v_{k\sigma}(t')g_{k\sigma}(t,t'). \tag{5.5}$$

Here, $g_{k\sigma}(t,t')=(-i)\langle \mathrm{T}c_{k\sigma}(t)c^\dagger_{k\sigma}(t')\rangle$ is the conduction electron GF satisfying $(i\partial/\partial t-\varepsilon_{k\sigma}(t))g_{k\sigma}(t,t')=\delta(t-t')$, leading to the retarded and lesser forms given in Eqs. (4.8) and (4.7), respectively. In the time-independent regime Eq. (5.4) can be Fourier transformed and its retarded version reads

$$G^r_\sigma(\omega)=\frac{1}{\omega-\varepsilon_\sigma-\Lambda_\sigma(\omega)+i\Gamma_\sigma(\omega)/2}, \tag{5.6}$$

where $\Gamma_\sigma(\omega)=\Gamma^L_\sigma(\omega)+\Gamma^R_\sigma(\omega)$ and $\Gamma^\alpha_\sigma(\omega)\equiv 2\pi\sum_k|v_{k\sigma}|^2\delta(\omega-\varepsilon_{k\sigma})$ gives the level width due to the tunneling. The level shift $\Lambda_\sigma(\omega)=\mathrm{Re}\Sigma^r_\sigma(\omega)$ is usually very small. It should be noticed that the solution in Eq. (5.6) exactly equals the one given in Eq. (4.1) and is commonly referred to as a single non-interacting

resonant level system. Indeed, by starting from the expression for the stationary current, Eq. (4.13), one can easily derive the formula [31, 43, 92]

$$J = \frac{1}{2\pi}\sum_{\sigma}\int \frac{\Gamma^L_\sigma(\omega)\Gamma^R_\sigma(\omega)}{[\omega-\varepsilon_\sigma-\Lambda_\sigma(\omega)]^2+[\Gamma_\sigma(\omega)/2]^2} \times\Big(f(\omega-\mu_L)-f(\omega-\mu_R)\Big)\mathrm{d}\omega, \quad (5.7)$$

which exactly equals Eq. (4.1), apart from the coefficients.

5.1.2 Weak-coupling mean-field approximation

Now, let the intra-dot interactions be present, i.e. include the Hubbard U term in the Hamiltonian, Eq. (5.1). Then, the equation of motion for the QD GF G_σ cannot be solved exactly and we have to employ an approximation scheme in order to extract any physics. The simplest approximation that includes the electron-electron interactions in the QD is the MFA. The localized state $|\sigma\rangle$ is treated in the mean field $U\langle n_{\bar\sigma}\rangle$ of the opposite spin state $|\bar\sigma\rangle$, thus giving the Hamiltonian

$$\mathcal{H}=\sum_{k\sigma}\varepsilon_{k\sigma}(t)c^\dagger_{k\sigma}c_{k\sigma}+\sum_\sigma(\varepsilon(t)+U\langle n_{\bar\sigma}\rangle)d^\dagger_\sigma d_\sigma+\sum_{k\sigma}(v_{k\sigma}(t)c^\dagger_{k\sigma}d_\sigma+H.c.), \quad (5.8)$$

which structurally resembles the model of the non-interacting resonant level. The time-independent solution for this problem is thus given by

$$G^r_\sigma(\omega)=\frac{1}{\omega-(\varepsilon_\sigma+U\langle n_{\bar\sigma}\rangle)+i\Gamma_\sigma(\omega)/2}. \quad (5.9)$$

The mean field experienced by the spin σ state from the opposite spin state, furnishes the state with a non-negligible shift of its energy. The population number $\langle n_\sigma\rangle=-\mathrm{Im}\int f(\omega)G^r_\sigma(\omega)\mathrm{d}\omega/\pi$ has to be calculated self-consistently in the MFA, for a full account of the interaction.

5.1.3 Further perturbation expansion

Further information about the interactions in the QD can be obtained by investigating the two-particle GF $G_{\bar\sigma\sigma}$ in more detail. For instance, Meir *et al.*[65, 66] found that, for a QD in the Kondo regime and letting $U\to\infty$ in the solution,

$$G^r_\sigma(\omega)=\frac{1-\langle n_{\bar\sigma}\rangle}{\omega-\varepsilon_\sigma-\Sigma^r_{0\sigma}(\omega)-\Sigma^r_{1\sigma}(\omega)}, \quad (5.10)$$

with $\Sigma^r_{0\sigma}(\omega)=\sum_k|v_{k\sigma}|^2/(\omega-\varepsilon_{k\sigma}+i\delta)$ and

$$\Sigma_{1\sigma}(\omega)=\sum_k\frac{|v_{k\sigma}|^2}{\omega-\varepsilon_\sigma+\varepsilon_{\bar\sigma}-\varepsilon_{k\bar\sigma}+i/2\tau_{\bar\sigma}}f(\varepsilon_{k\bar\sigma}-\mu_\alpha), \quad (5.11)$$

where $\tau_{\bar\sigma}$ is the intermediate state life-time. A similar result was reported by Lacroix [54] in an investigation of the DOS for the Anderson model. In this picture an electron in the QD can experience the transition $|\sigma\rangle\to|\bar\sigma\rangle$, a spin-flip,

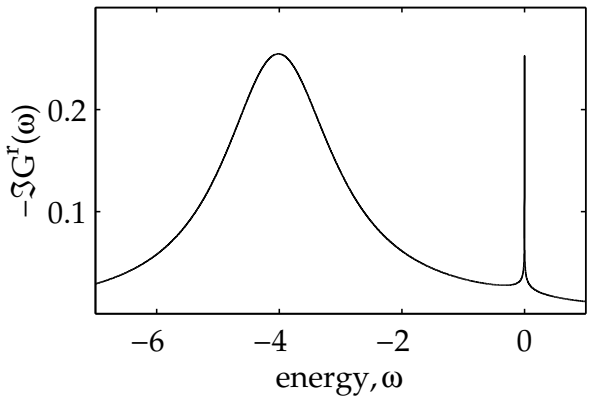

Figure 5.2: A qualitative plot of the equilibrium QD DOS in which the Kondo contribution to the self-energy, Eq. (5.11), is included. The QD has a level lying deep in the QD with a large width and a spin-flip resonance at the chemical potential ($\mu = 0$).

with the resonant energy $\varepsilon_\sigma - \varepsilon_{\bar{\sigma}}$ which provides a peak, Kondo [51] peak or Abrikosov-Suhl [1, 86] resonance, in the local DOS at the quasi-chemical potentials of the leads. In Fig. 5.2 this behaviour is qualitatively illustrated by the QD DOS $-\mathrm{Im}\sum_\sigma G^r_\sigma(\omega)/\pi$, where $G^r_\sigma(\omega)$ is given by Eq. (5.10). Although we will not discuss the Kondo physics in QD and therefore leave this subject here, we remark that the behaviour of the QD DOS given in Fig. 5.2 can actually be obtained, let be with reversed order of the peaks, within the many-body approach (presented in Sec. 5.2 and forward) in an approximation that does not include any spin-flip scattering. Thus, even though the Kondo contributions are completely neglected, the system shows a QD DOS that indeed resembles the one given in Fig. 5.2.

5.1.4 Simple model of a Coulomb island

Another approach to the problem of solving the QD GF is to first consider an isolated QD, that is, not being connected to the conduction bands in the leads. The Hamiltonian for the QD can be written

$$\mathcal{H}_D = \sum_\sigma \varepsilon_\sigma(t) d^\dagger_\sigma d_\sigma + U n_\uparrow n_\downarrow, \tag{5.12}$$

as was discussed in Sec. 4.2. This system is exactly solvable since, for instance in the time-independent regime,

$$g_\sigma(i\omega) = \frac{1 + U G_{\bar{\sigma}\sigma}(i\omega)}{i\omega - \varepsilon_\sigma}, \tag{5.13}$$

$$g_{\bar{\sigma}\sigma}(i\omega) = \frac{\langle n_{\bar{\sigma}} \rangle}{i\omega - \varepsilon_\sigma - U}. \tag{5.14}$$

By inserting Eq. (5.14) into Eq. (5.13) we obtain the retarded QD GF

$$g^r_\sigma(\omega) = \frac{\omega - \varepsilon_\sigma - (1 - \langle n_{\bar\sigma}\rangle)U}{(\omega - \varepsilon_\sigma - U)(\omega - \varepsilon_\sigma)} = \frac{1 - \langle n_{\bar\sigma}\rangle}{\omega - \varepsilon_\sigma + i\delta} + \frac{\langle n_{\bar\sigma}\rangle}{\omega - \varepsilon_\sigma - U + i\delta}. \tag{5.15}$$

Obviously the GF has the two resonances $\omega = \varepsilon_\sigma$ and $\omega = \varepsilon_\sigma + U$ with the spectral weights $1 - \langle n_{\bar\sigma}\rangle$ and $\langle n_{\bar\sigma}\rangle$, respectively.

However, Eq. (5.15) only provides information about the QD being decoupled from the leads in equilibrium. Phenomenologically, by replacing the infinitesimal δ by the level width $\Gamma_\sigma(\omega)$, previously obtained from the case of a non-interacting resonant level, one can model the couplings to the leads [13, 29], thereby obtaining an expression which can be used in calculations of the current. The retarded QD GF thus becomes

$$\begin{aligned} G^r_\sigma(\omega) &= \frac{g^r_\sigma(\omega)}{1 + i g^r_\sigma(\omega)\Gamma_\sigma(\omega)/2} \\ &= \frac{\omega - \varepsilon_\sigma - (1 - \langle n_{\bar\sigma}\rangle)U}{(\omega - \varepsilon_\sigma - U)(\omega - \varepsilon_\sigma) + i\Gamma_\sigma[\omega - \varepsilon_\sigma - (1 - \langle n_{\bar\sigma}\rangle)U]}. \end{aligned} \tag{5.16}$$

In the limit of a very large Coulomb repulsion U the resulting QD GF becomes

$$G^r_\sigma(\omega) = \frac{1 - \langle n_{\bar\sigma}\rangle}{\omega - \varepsilon_\sigma + i\Gamma_\sigma(\omega)/2} + \frac{\langle n_{\bar\sigma}\rangle}{\omega - \varepsilon_\sigma - U + i\Gamma_\sigma(\omega)/2}. \tag{5.17}$$

The second term in this expression becomes very small for a large Hubbard U. Nevertheless, structurally Eq. (5.17) resembles Eq. (5.15) but now the tunneling broadens the resonances ε_σ and $\varepsilon_\sigma + U$.

The result in Eq. (5.17) was also reported by Pals *et al.* [69] by neglecting simultaneous tunneling of the electron of the opposite spin projection $\bar\sigma$ and decoupling the higher order GF similarly as in the previous discussion. As the tunneling of the opposite spin electron is not taken into account, its creation and annihilation operators are always paired together in the higher order GF. The operators for both spins do not truly intermingle, which results in the probabilistic expression for the QD GF.

5.1.5 The retarded and lesser quantum dot Green functions

In this section we have derived the QD GF in the single-particle picture and in some case provided the complex time-ordered contour integral equation for the GF. However, in the expressions for the current we need the GF expressed in real times and thereto, we need the retarded and lesser counterparts of the GF. For simplicity, consider the expression given in Eq. (5.4), which indeed displays the general structure of the QD GF in the single-particle picture. The conversion into the retarded real-time integral equation is simply

$$G^r_\sigma(t,t') = g^r_\sigma(t,t') + \int_{-\infty}^{\infty} g^r_\sigma(t,s)\Sigma^r_\sigma(s,s')G^r_\sigma(s',t')\mathrm{d}s\mathrm{d}s'. \tag{5.18}$$

This equation can in some cases be solved analytically but, in general, it has to be solved numerically. However, we still have to obtain an expression for the lesser

GF $G^<_\sigma(t,t')$. For this, we apply the analytical continuation rules [31, 58], or the Keldysh technique [48], giving the algebraic equation

$$G^<_\sigma = g^<_\sigma + g^r_\sigma \Sigma^r_\sigma G^<_\sigma + g^r_\sigma \Sigma^<_\sigma G^a_\sigma + g^<_\sigma \Sigma^a_\sigma G^a_\sigma.$$

Collecting the lesser GF $G^<_\sigma$ to the left in this equation, we obtain

$$g^r_\sigma \Big[(g^r_\sigma)^{-1} - \Sigma^r_\sigma \Big] G^<_\sigma = g^<_\sigma (1 + \Sigma^a_\sigma G^a_\sigma) + g^r_\sigma \Sigma^<_\sigma G^a_\sigma.$$

Noting that $[(g^r_\sigma)^{-1} - \Sigma^r_\sigma]^{-1} = G^r_\sigma$ and recalling that $(g^r_\sigma)^{-1} g^<_\sigma = 0$ identically and $(g^r_\sigma)^{-1} g^r_\sigma = 1$, the lesser QD GF can be written

$$G^<_\sigma(t,t') = \int_{-\infty}^{\infty} G^r_\sigma(t,s) \Sigma^<_\sigma(s,s') G^a_\sigma(s',t') \mathrm{d}s \mathrm{d}s'. \tag{5.19}$$

Hence, the lesser QD GF is written solely in terms of the retarded and advanced QD GF and lesser self-energy. It is usually easier to find an analytical expression for the lesser self-energy $\Sigma^<_\sigma$ than it is for the lesser QD GF. Therefore, we will be satisfied with Eq. (5.19). In particular, for the non-interacting case the lesser self-energy is given by

$$\Sigma^<_\sigma(t,t') = i \sum_k v^*_{k\sigma}(t) v_{k\sigma}(t') f(\varepsilon_{k\sigma} - \mu_\alpha) e^{-i \int_{t'}^t \varepsilon_{k\sigma}(s) \mathrm{d}s} \tag{5.20}$$

and since $[G^a_\sigma(t',t)]^* = G^r_\sigma(t,t')$ we have the lesser QD GF

$$G^<_\sigma(t,t') = i \sum_k f(\varepsilon_{k\sigma} - \mu_\alpha) \int_{-\infty}^{\infty} \Big| v^*_{k\sigma}(s) G^r_\sigma(t,s) \Big|^2 \mathrm{d}s. \tag{5.21}$$

Knowing the retarded QD GF one thus can obtain the time-dependent tunnel current through the QD system by inserting Eqs. (5.18) and (5.19) into Eq. (4.10). As we have seen, also the stationary current can be obtained by Eq. (4.13) when all the details of the QD GF are at hand.

The methods of finding the non-equilibrium GF techniques tacitly used in this section can be found in Refs. [47, 48, 58]. The mathematical techniques of finding the perturbation expansions of the QD GF in this section can be found, for instance, in Refs. [3, 31, 62, 63].

5.2 Many-body picture

The treatment of strongly correlated states in the QD is a complicated and, in addition, unsolvable story to tell about. We saw in the previous section that the single-electron picture leads to problems of finding the two-electron GF when the QD is coupled to the leads. However, we can actually get rid of this problem by expressing the QD states in terms of many-body operators, e.g. the Hubbard operators introduced in Sec. 4.2. The problem still remains, however, the matter is that we are using that $U/\Gamma \gg 1$. Then, by only considering the (large) Coulomb repulsion between the QD states, the model Hamiltonian can be written

$$\mathcal{H} = \sum_{k\sigma \in L,R} \varepsilon_{k\sigma}(t) c^\dagger_{k\sigma} c_{k\sigma} + \sum_{p=0,\sigma} E_\sigma(t) h^\sigma + \sum_{k\sigma} \Big(v_{k\sigma}(t) c^\dagger_{k\sigma} X^{0\sigma} + H.c. \Big). \tag{5.22}$$

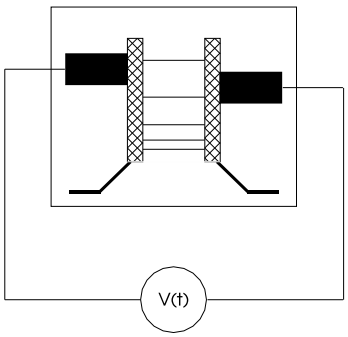

Figure 5.3: A typical model sketch of a QD connected to contacts. In the QD, the region between the barriers, the energy spectrum is discrete whereas the spectrum in the leads is continuous.

In this model, the dynamics of the Hubbard operator $X^{0\sigma}$ is given by

$$\left(i\frac{\partial}{\partial t} - \Delta^0_{\sigma 0}(t)\right)X^{0\sigma} = \sum_k \left(v^*_{k\sigma}(t)(h^0 + h^\sigma)c_{k\sigma} + v^*_{k\bar{\sigma}}(t)Z^{\bar{\sigma}\sigma}c_{k\bar{\sigma}}\right). \tag{5.23}$$

The first term on the right hand side of this equation, containing the product $\langle(h^0 + h^\sigma)c_{k\sigma}\rangle$, would allow for a separation of the *mean-field* term $\langle h^0 + h^\sigma\rangle$. After this step we would obtain the term $v^*_{k\sigma}\langle h^0 + h^\sigma\rangle c_{k\sigma}$, which is similar to the term responsible for $v^*_{k\sigma}(t)G_{k\sigma}(t,t')$ in Eq. (5.2), and the two terms $(h^0 + h^\sigma + \langle h^0 + h^\sigma\rangle c_{k\sigma}$ and $Z^{\bar{\sigma}\sigma}c_{k\bar{\sigma}}$ for which such decoupling is not allowed. These terms give rise to the kinematic interactions. As we will see later in this chapter, the contribution from the former exactly vanishes, which is expected since this contribution describes effective interactions with the transition itself. Thus, only the term with the spin-flip gives a contribution. As will be shown later, the absence of the self-interaction leads to an explicit spin-dependence of the kinematic interactions which, in turn, can manifest itself in interesting physical effects. Actually, such contributions are characteristic for systems with complexes of two or more bounded particles, e.g. between spins or atoms with open shells, interacting with conduction electrons [75, 76].

In reality, a QD contains several levels, see Fig. 5.3, but for sufficiently small devices the level separation is large compared to the relevant energy interval between the quasi-chemical potentials imposed by the bias voltage. If, in addition, the band widths of the conduction electrons or filling of the bands in the leads are small enough, then there will only be one or possibly two levels taking part in the charge transfer. Therefore, as a first approximation, it is relevant to discuss the properties of a single-level device.

The Hubbard operator $X^{0\sigma}$ describes the transition $|0\rangle \rightarrow |\sigma\rangle$ while in order to understand the physics of the QD we need to look at the QD GF defined by

$$G_{\sigma\sigma'}(t,t') = (-i)\langle \mathrm{T}X^{0\sigma}(t)X^{\sigma'0}(t')\rangle_U \equiv (-i)\frac{\langle \mathrm{T}SX^{0\sigma}(t)X^{\sigma'0}(t')\rangle}{\langle \mathrm{T}S\rangle}. \tag{5.24}$$

The subscript U denotes that the QD GF have to be considered with respect to the time-dependent disturbance

$$\mathcal{H}'(t) = U_0(t)h^0 + \sum_\sigma \Big(U_\sigma(t)h^\sigma + U_{\sigma\bar{\sigma}}(t)Z^{\sigma\bar{\sigma}} \Big), \tag{5.25}$$

giving the action $S = \exp\left(-i\int_{t_0}^{t_0-i\beta}\mathcal{H}'(t)\mathrm{d}t\right)$. The source fields $U_\xi(t)$ are used for the generation of a perturbation expansion of the QD GF in terms of the functional derivatives $\delta G_{\sigma\sigma'}/\delta U_\xi$. Such a method was first introduced by Schwinger [78] and further developed for quantum statistical mechanics by Kadanoff and Baym [47]. Recently, Sandalov *et al.* [75, 76] introduced a similar method for the study of f-electron systems in terms of Hubbard operators. The very same mathematical technique provides a pleasant framework for fruitful investigations of strongly correlated states in a QD.

5.2.1 Diagram technique in brief

In this subsection we briefly explore some details on the diagrammatic expansion of the QD GF and may be somewhat technical. An extended version of this subsection can be found in Appendix A. In the equation of motion for the QD GF the quantities

$$(-i)\langle \mathrm{T}(h^0 + h^\sigma)(t)c_{k\sigma}(t)X^{\sigma'0}(t')\rangle_U$$

$$(-i)\langle \mathrm{T}Z^{\bar{\sigma}\sigma}(t)c_{k\bar{\sigma}}(t)X^{\sigma'0}(t')\rangle_U$$

will appear, where there is no summation over the spin-indices. These can be rewritten in terms of $G_{\sigma\sigma'}(t,t')$ and functional derivatives thereof. By considering the variation $\delta F_{k\sigma\sigma'}$ of the mixed GF $F_{k\sigma\sigma'}(t,t') = (-i)\langle \mathrm{T}c_{k\sigma}(t)X^{\sigma'0}(t)\rangle_U$ with respect to the source field $U_\xi(t'')$, one finds that [75, 76]

$$(-i)\langle \mathrm{T}Z^\xi(t'')c_{k\sigma}X^{\sigma'0}(t')\rangle_U = \left(\langle \mathrm{T}Z^\xi(t'')\rangle_U + i\frac{\delta}{\delta U_\xi(t'')}\right)F_{k\sigma\sigma'}(t,t'). \tag{5.26}$$

The mixed GF is given by

$$F_{k\sigma\sigma'}(t,t') = \int_{t_0}^{t_0-i\beta} v_{k\sigma}(t)g_{k\sigma}(t,s)G_{\sigma\sigma'}(s,t')\mathrm{d}s. \tag{5.27}$$

For a shorter notation we introduce $V_\sigma(t,t') = \sum_k v^*_{k\sigma}(t)v_{k\sigma}(t')g_{k\sigma}(t,t')$ and put $R_{\sigma\sigma'}(t) = i[\delta_{\sigma\sigma'}\delta/\delta U_{00}(t) + \delta/\delta U_{\sigma'\sigma}(t)]$ (pay attention to the order of the spin-indices). We also define $P_\sigma(t) \equiv P_{\sigma\sigma}(t)$ and $R_\sigma(t) \equiv R_{\sigma\sigma}(t)$.

The end-factor [41, 39] $P_{\sigma\sigma'}(t) = \langle \mathrm{T}\{X^{0\sigma}, X^{\sigma'0}\}(t)\rangle_U$, already introduced in Sec. 4.3, is the sum of the population numbers $\langle N_0(t)\rangle_U$ and $\langle N_{\sigma'\sigma}(t)\rangle_U$. For time-dependent source fields $U_\xi(t)$, though, the QD populations are not well-defined. The reason is that the off-diagonal expectation values $\langle \mathrm{T}X^{\sigma\sigma'}(t)\rangle_U$ are non-zero, as well. Nevertheless, terminologically we disregard this complication

of the problem and refer to $\langle N_0(t)\rangle_U \equiv \langle \mathrm{T}h^0(t)\rangle_U$ and $\langle N_{\sigma\sigma'}(t)\rangle_U \equiv \langle \mathrm{T}X^{\sigma\sigma'}(t)\rangle_U$ as the *population numbers* of the transitions $|0\rangle \to |0\rangle$ and $|\sigma'\rangle \to |\sigma\rangle$, respectively.

The exact equation of motion for the QD GF can now be written

$$\begin{aligned}\left(i\frac{\partial}{\partial t} - \Delta^0_{\sigma 0}(t) - \Delta U_{\sigma 0}(t)\right)G_{\sigma\sigma'}(t,t') - U_{\sigma\bar{\sigma}}(t)G_{\bar{\sigma}\sigma'}(t,t') &= \delta(t-t')P_{\sigma\sigma'}(t) \\ &+[P_\sigma(t) + R_\sigma(t)]\int_{t_0}^{t_0-i\beta} V_\sigma(t,s)G_{\sigma\sigma'}(s,t')\mathrm{d}s \\ &+[P_{\sigma\bar{\sigma}}(t) + R_{\sigma\bar{\sigma}}(t)]\int_{t_0}^{t_0-i\beta} V_{\bar{\sigma}}(t,s)G_{\bar{\sigma}\sigma'}(s,t')\mathrm{d}s, \qquad (5.28)\end{aligned}$$

completely expressed in terms of the QD GF and functional derivatives thereof. The source fields $\Delta U_{\sigma 0}(t)$ and $U_{\sigma\bar{\sigma}}(t)$ on the left hand side of Eq. (5.28) appears due to the differentiation $i\partial \mathrm{T}SX^{0\sigma}(t) = \mathrm{T}S[X^{0\sigma}(t), \mathcal{H} + \mathcal{H}'(t)]$ in the QD GF. Physical information about the QD is obtained from Eq. (5.28) by applying the functional derivatives up to the desired order in the interactions V_σ and thereafter letting the source fields, that are not actually applied to the system, $U_\xi(t) \to 0$. In this limit, due to conservation of the total spin S^z by the Hamiltonian, all quantities that do not conserve the longitudinal component of the total spin vanish, although their functional derivatives may not. Thus, in the final expression of the QD GF, i.e. when then limit $U_\xi(t) \to 0$ has been taken, one can just discard terms containing locators and cumulants of the transitions $|\sigma\rangle \to |\bar{\sigma}\rangle$ and $|\bar{\sigma}\rangle \to |\sigma\rangle$. Also, in this limit $\langle N_0(t)\rangle$ and $\langle N_\sigma(t)\rangle$ become appropriate time-dependent population numbers of the states $|0\rangle$ and $|\sigma\rangle$, respectively.

When applying the functional derivatives on the QD GF it should be noticed that it is composed by the product of its locator $D_{\sigma\sigma}(t,t')$ and the end-factor $P_{\sigma\sigma}(t)$, that is, $G_{\sigma\sigma'}(t,t') = D_{\sigma\sigma''}(t,t')P_{\sigma''\sigma'}(t')$. In addition, not only the locator is subject to the functional derivative but also the end-factor. Hence, varying the QD GF yields $\delta G_{\sigma\sigma'} = (\delta D_{\sigma\sigma''})P_{\sigma''\sigma'} + D_{\sigma\sigma''}(\delta P_{\sigma''\sigma'})$. The locator matrix D should satisfy the relation $DD^{-1} = I = D^{-1}D$ which implies that $\delta(DD^{-1}) = (\delta D)D^{-1} + D(\delta D^{-1}) = 0$. This results in

$$\begin{aligned}R_{ss'}(t'')D_{\sigma\sigma'}(t,t') &= -i\int_{t_0}^{t_0-i\beta} D_{\sigma\sigma_1}(t,t_1)\Gamma_{\sigma_1\sigma_2}(t_1,t_2;R_{ss'}(t'')) \\ &\quad \times D_{\sigma_2\sigma'}(t_2,t')\mathrm{d}t_1\mathrm{d}t_2, \qquad (5.29)\end{aligned}$$

with the vertex function, cf. Appendix A,

$$\Gamma_{\sigma_1\sigma_2}(t_1,t_2;R_{ss'}(t'')) = \Gamma^0_{\sigma_1\sigma_2}(t_1,t_2;R_{ss'}(t'')) - iR_{ss'}(t'')S_{\sigma_1\sigma_2}(t_1,t_2), \qquad (5.30)$$

where the zero vertex

$$\Gamma^0_{\sigma_1\sigma_2}(t_1,t_2;R_{ss'}(t'')) = (\delta_{\sigma_1\sigma_2}\delta_{ss'} - \delta_{\sigma_1 s'}\delta_{\sigma_2 s})\delta(t_1-t_2)\delta(t_2-t''). \qquad (5.31)$$

and the self-operator

$$S_{\sigma_1\sigma_2}(t_1,t_2) \equiv P_{\sigma_1\sigma_2}(t_1)V_{\sigma_2}(t_1,t_2) - i\int_{t_0}^{t_0-i\beta} V_{\sigma_3}(t_1,t_3)D_{\sigma_3\sigma_4}(t_3,t_4)\Gamma_{\sigma_4\sigma_2}(t_4,t_2;R_{\sigma_1\sigma_3}(t_1))\mathrm{d}t_3\mathrm{d}t_4. \quad (5.32)$$

In Eqs. (5.29) and (5.32) summation over the spin-indices σ_1, σ_2 and σ_3, σ_4, respectively, is understood. Resolving the vertex in the self-operator, one comes to a perturbation series in terms of the interaction $V_\sigma(t)$, by successively applying the functional derivatives to the locators and cumulants. However, here we will not concern ourselves with any perturbation expansion of the QD GF further than to the first order in the interaction $V_\sigma(t)$. For the locator, this is actually obtained by only resolving the zero vertex in the expansion.

The functional derivative of the end-factor $R_{ss'}(t'')P_{\sigma\sigma'}(t)$ generates the cumulant

$$R_{ss'}(t'')P_{\sigma\sigma'}(t) = \langle \mathrm{T}[\delta_{ss'}h^0 + Z^{s's}](t'')[\delta_{\sigma\sigma'}h^0 + Z^{\sigma'\sigma}](t)\rangle_U - P_{ss'}(t'')P_{\sigma\sigma'}(t) \quad (5.33)$$

If the two involved quantities would be independent at different times the functional derivative $R_{ss'}(t'')P_{\sigma\sigma'}(t) \equiv 0$. Indeed, as is seen from Eq. (5.33), the *mean-field* decoupling of the first term cancels the whole expression. Therefore, the cumulant $R_{ss'}(t'')P_{\sigma\sigma'}(t)$ describes fluctuations of the population numbers. However, at coinciding times ($t'' \to t^+$) and vanishing source fields $U_\xi(t)$ we obtain $(N_0+N_\sigma)-(N_0+N_\sigma)^2$ for equal spins and $\langle Z^{\bar\sigma\sigma}Z^{\sigma\bar\sigma}\rangle = N_{\bar\sigma}$ from the spin-flip correlation function. Note that in pure states, when either the QD does not have an electron ($N_0 = 1$, $N_\sigma = 0$) or has one electron ($N_\sigma = 1$, $N_0 = N_{\bar\sigma} = 0$) the cumulant vanishes.[2] In contrast, the transverse functional derivative $R_{\sigma\bar\sigma}(t^+)P_{\bar\sigma\sigma}(t') = iK_{\bar\sigma\sigma}(t^+,t') - P_{\sigma\bar\sigma}(t^+)P_{\bar\sigma\sigma}(t')$, where

$$K_{\bar\sigma\sigma}(t^+,t') = (-i)\langle \mathrm{T}Z^{\bar\sigma\sigma}(t^+)Z^{\sigma\bar\sigma}(t')\rangle_U \equiv (-i)\frac{\langle \mathrm{T}SZ^{\bar\sigma\sigma}(t^+)Z^{\sigma\bar\sigma}(t')\rangle}{\langle \mathrm{T}S\rangle}.$$

The bare Bose-like GF $K_{\bar\sigma\sigma}(t^+,t')$ satisfies the equation

$$\left(i\frac{\partial}{\partial t} - \Delta^0_{\sigma\bar\sigma}(t^+) - \Delta U_{\sigma\bar\sigma}(t^+)\right)K_{\bar\sigma\sigma}(t^+,t') = \delta(t^+-t')[P_{\bar\sigma}(t^+) - P_\sigma(t^+)], \quad (5.34)$$

where $\Delta^0_{\sigma\bar\sigma}(t) = \Delta^0_{\sigma 0}(t) - \Delta^0_{\bar\sigma 0}(t)$. In Eq. (5.34), we have discarded propagators like $(-i)\langle \mathrm{T}h^\sigma(t^+)Z^{\sigma\bar\sigma}(t')\rangle_U$ since they only give contributions for functional derivatives that are irrelevant for $K_{\bar\sigma\sigma}(t^+,t')$, in our approximation.

[2] In mathematical terms Eq. (5.33) provides a dependence measure, the covariance, between the quantities $\delta_{ss'}h^0 + Z^{s's}$ and $\delta_{\sigma\sigma'}h^0 + Z^{\sigma'\sigma}$. It is readily seen that $R_\sigma(t^+)P_\sigma(t') = \langle \mathrm{T}(h^0+h^\sigma)(t^+)(h^0+h^\sigma)(t')\rangle_U - P_\sigma(t^+)P_\sigma(t')$. In this terminology, then, the two quantities are said to be uncorrelated whenever $R_{ss'}(t'')P_{\sigma\sigma'}(t) = 0$.

Before we continue with the discussion of the QD system we are urged to make some comments on the diagram technique thus introduced and henceforth employed. The choice of using many-body states for the description of the QD is motivated by the discussion in the introduction of this chapter. However, there are alternative approaches in a treatise of many-body states. For instance, Ruckenstein and Schmitt-Rink [73] introduced a similar method for strongly correlated electron systems via functional differentiations with respect to time-dependent source fields. In their approach the local GF of the isolated QD is not used as the zero GF. Rather the zero GF includes the mixing with the conduction electrons in the contacts. One reason for such an approach is that it is then possible to separate out a zero Hamiltonian $\mathcal{H}_0$ which commutes with the remainder part. We want to include the non-orthogonality between the localized states and the conduction electrons and, therefore, a separation into a zero Hamiltonian commuting with the interaction Hamiltonian is not possible. Another technique for Hubbard operator GF was developed by Izyumov *et al.* [41, 39]. In this technique a hierarchy is introduced between the operators which then is used in a decoupling scheme. However, having to choose the hierarchy among the operators for each new problem gives rise to non-desired complications and is avoided within the technique employed in the present context. Also, the non-orthogonality introduces separate problems with the perturbation expansion suggested in Ref. [41, 39].

5.2.2 Hubbard I approximation

The simplest approximation of Eq. (5.28) is given by neglecting all functional derivatives $R_{ss'}(t^+)$. From the above discussion it is realized that we here neglect the fluctuations of the population numbers and the processes with spin-flips. The resulting expression for the QD GF then becomes, letting the source fields $U_\xi(t) \to 0$,

$$G_\sigma(t,t') = g_\sigma(t,t') + \int_{t_0}^{t_0-i\beta} g_\sigma(t,s)V_\sigma(s,s')G_\sigma(s',t')\mathrm{d}s\mathrm{d}s', \qquad (5.35)$$

where $g_\sigma(t,t')$ is the GF for the isolated QD satisfying $(i\partial/\partial t - \Delta^0_{\sigma 0}(t))g_\sigma(t,t') = \delta(t-t')P_\sigma(t)$, in the same limit of the source fields. Here, we have defined $G_\sigma(t,t') \equiv G_{\sigma\sigma}(t,t')$ and $g_\sigma(t,t') \equiv g_{\sigma\sigma}(t,t')$. The interaction $V_\sigma(t,t')$ provides a width of the QD level $\Delta^0_{\sigma 0}(t)$. It should be noticed that, since the Coulomb repulsion is already included in the formulation of the QD in terms of many-body states, this approximation is somewhat similar to the standard MFA within the single-particle picture. This approximation is the so-called Hubbard I approximation (HIA) [36, 37, 75, 76]. Graphically, it reads

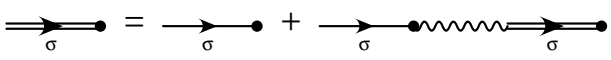

where the single and double solid lines terminated with a dot refers to the bare and dressed QD GF, respectively, whereas the wiggles signifies the interaction $V_\sigma(t,t')$. The dots terminating the solid lines denote the end-factor P_σ. This is the reason for calling P_σ the *end-factor*. The labels σ denote the spin projection of the transition. Actually, this approximation does not provide any new information about the physics in the system and, therefore, we proceed to the next section.

5.2.3 Loop correction

Now, let us take into account the first functional derivative in the locators, i.e. the zero vertex. The only non-vanishing term, after taking the limit $U_\xi(t) \to 0$, is the so-called loop correction

$$\begin{aligned} R_{\sigma\bar{\sigma}}(t^+)D_{\bar{\sigma}\sigma}(s,t') &= -i\int_{t_0}^{t_0-i\beta} D_{\bar{\sigma}}(s,t_1)\Gamma^0_{\bar{\sigma}\sigma}(t_1,t_2;R_{\sigma\bar{\sigma}}(t^+)) \\ &\quad \times D_\sigma(t_2,t')\mathrm{d}t_1\mathrm{d}t_2 = \\ &= iD_{\bar{\sigma}}(s,t^+)D_\sigma(t^+,t'), \end{aligned} \tag{5.36}$$

where $D_\sigma(t,t') \equiv D_{\sigma\sigma}(t,t')$. As explained earlier, this is the first correction from the kinematic interactions.

Constant population numbers

For a moment, assume that the cumulants are unaffected by the functional differentiations and the population numbers given by $N_\sigma = -\mathrm{Im}\int f(\omega)G^r_\sigma(\omega)\mathrm{d}\omega/\pi$ subject to the constraint $N_0 + N_\uparrow + N_\downarrow = 1$. Then, the resulting equation of motion for the QD GF can be written, in the limit $U_\xi(t) \to 0$,

$$\left(i\frac{\partial}{\partial t} - \Delta_{\sigma 0}(t)\right)G_\sigma(t,t') = \delta(t-t')P_\sigma(t) + \int_{t_0}^{t_0-i\beta} P_\sigma(t^+)V_\sigma(t,s)G_\sigma(s,t')\mathrm{d}s, \tag{5.37}$$

where $\Delta_{\sigma 0}(t)$ is the dressed many-body level given by the solution of the self-consistent equation

$$\Delta_{\sigma 0}(t) - \Delta^0_{\sigma 0}(t) = i\int_{t_0}^{t_0-i\beta} V_{\bar{\sigma}}(t,s)D_{\bar{\sigma}}(s,t^+)\mathrm{d}s. \tag{5.38}$$

The quantity on the right hand side of this equation is real and therefore provides a shift of the bare level. Being a second order correction, it pushes the dressed level below the bare one. The graphical equation corresponding to Eq. (5.37) reads

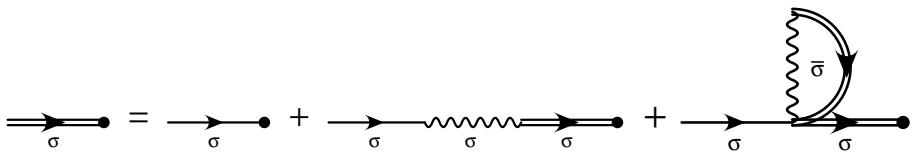

Note that the loop correction (in the last diagram) depends on the opposite spin projection $\bar{\sigma}$. The kinematic shift of the level is caused by the coupling of this transition with the continuum of the conduction electrons of spin projections. However, the contributions for the same spin projection are canceled.

The effect from this mechanism gives the possibility of inducing a spin-splitting of the localized levels in the QD by spin-polarizing the conduction bands in the

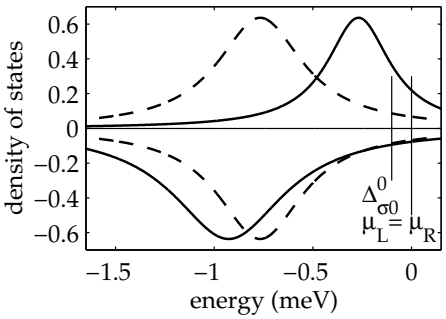

Figure 5.4: The equilibrium DOS of the interacting region for non-polarized (dashed lines) and spin-polarized (solid lines) leads. In the spin-polarized case, there is an amount of 3.5 % of the minority spin in the leads.

leads. The induced spin-splitting can result in a spin-polarization in the output current which is larger than that suggested by the polarization of the conduction bands. In Paper V this opportunity was investigated for stationary external fields applied to a QD in the mixed valence regime $(-0.5 \leq \Delta_{\sigma 0}/\Gamma_\sigma \leq 0)$. Then, the dressing of the QD level can be written in the form [3]

$$\Delta_{\sigma 0} - \Delta^0_{\sigma 0} = \sum_k |v_{k\bar{\sigma}}|^2 \frac{f(\varepsilon_{k\bar{\sigma}}) - f(\Delta_{\bar{\sigma}0})}{\varepsilon_{k\bar{\sigma}} - \Delta_{\bar{\sigma}0}}. \tag{5.39}$$

Results similar to this equation were previously found by other methods for different models in equilibrium [6, 8, 7, 9, 23, 38, 40, 74, 89]. However, in none of these studies the explicit spin dependence on the conduction electrons of the opposite spin projection, which is present in Eq. (5.39), was found.

The equilibrium DOS of the QD can be seen in Fig. 5.4 for two different polarizations of the conduction bands in the leads, where the vertical positive/negative axis corresponds to the spin $\uparrow$ / $\downarrow$. When the leads are non-polarized (dashed) the level is degenerate in energy with equal probability. As the conduction bands are spin-polarized (solid), the leads being ferro-magnetically aligned, the level is spin-spit. One of the states tends to get closer to the bare level whereas the other is pushed further below, as expected from Eq. (5.39). If the majority spins in the contacts is $\uparrow$, then the spin $\uparrow$ transition becomes less likely $(P_\uparrow = 0.39)$ whereas the weight of the spin $\downarrow$ transition increases $(P_\downarrow = 0.69)$.

The resulting tunnel current through the system, being computed using a spin-dependent version of Eq. (4.13) for the situation in Fig. 5.4), is displayed in Fig. 5.5. The current in the non-polarized (dashed) and in the case of completely spin-polarized (dotted) leads are given as reference to the case when the leads are incompletely spin-polarized (solid). Thus, it is seen that the current first grows and after a maximum value has been reached, it decreases down to the current of completely spin-polarized leads. This feature occurs because the bottom of mi-

[3] Remark: The sign in front of the sum on the right hand side in Eq. (5.39) was given incorrectly as "$-$" in Paper V, Eq. (3). However, the correct result is given here and in an erratum to the article in Physical Review Letters, see Paper V.

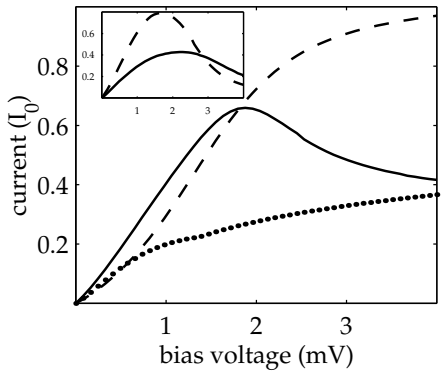

Figure 5.5: The tunnel current through the interacting region for non-polarized (dashed line) and spin-polarized leads. For the spin-polarized case, the minority spin percentage is 3.5 % (sold line) and 0 (dotted line). The inset shows a situation for very narrow conduction band widths.

nority spin sub-band in the lead with the higher potential eventually exceeds the corresponding QD level as the bias voltage is increased. One important feature to notice is the large change in the magneto resistance, up to 150%, as the configuration in the leads is shifted from being non-polarized to spin-polarized. Further details on the specific parameters used for these calculations can be found in Paper V.

Thinking of applications, we believe that this mechanism for inducing a spin-splitting of the localized level in the QD can be useful since it is extremely sensitive to changes in the surroundings. In the example, cf. Paper V, where it is shown how the electronic structure in the QD is changed simply by altering the spin-polarization in the leads. This very strong effect on the current seen in Fig. 5.5 as the conduction bands in the leads are shifted from a non-polarized to a strongly spin-polarized character, should be possible to use in magnetic sensor devices.

Another aspect of the approximation given in Eq. (5.37) is found in the stationary regime. Namely, it is possible to derive an analytical expression for the current without assuming proportionate coupled leads, similar to Eq. (4.1). In the stationary regime, the Fourier transform of the retarded QD GF becomes

$$G^e_\sigma(\omega) = \frac{P_\sigma}{\omega - \Delta_{\sigma 0} - \Lambda_\sigma(\omega)P_\sigma + i\Gamma_\sigma(\omega)P_\sigma/2}, \tag{5.40}$$

where $\Lambda_\sigma(\omega) = \mathrm{Re}\Sigma_k |v_{k\sigma}|^2/(\omega - \varepsilon_{k\sigma} + i\delta)$ and $\Gamma_\sigma(\omega) = \Gamma^L_\sigma(\omega) + \Gamma^R_\sigma(\omega)$. The level width is the sum of the couplings $\Gamma^\alpha_\sigma(\omega) = 2\pi \sum_{k\in\alpha} |v_{k\sigma}|^2 \delta(\omega - \varepsilon_{k\sigma})$. Using the methods of finding $G^<_\sigma(\omega)$, described in Sec. 5.2.4, and formally following the

derivation in Ref. [31, 43] leading to Eq. (5.7), one finds the expression

$$J = \frac{1}{2\pi}\sum_{\sigma}\int \frac{\Gamma^L_\sigma(\omega)\Gamma^R_\sigma(\omega)}{[\omega-\Delta_{\sigma 0}-\Lambda_\sigma(\omega)P_\sigma]^2+[\Gamma_\sigma(\omega)P_\sigma/2]^2}P^2_\sigma \times\Big(f(\omega-\mu_L)-f(\omega-\mu_R)\Big)\mathrm{d}\omega. \quad (5.41)$$

We notice that this expression very much resembles the one given for the non-interacting resonant model in Eq. (5.7). However, in the present case the strong intra-dot Coulomb repulsion between the states $|\uparrow\rangle$ and $|\downarrow\rangle$ is included in the renormalized many-body level $\Delta_{\sigma 0}$. Also, the end-factor P_σ indicates that a many-body approach has been used in obtaining Eq. (5.41).

Derivative of the end-factors

It was stated in Sec. 5.2.1 that also the cumulants are subject to the functional derivatives. The question that arises is if we really can draw any conclusions about the behaviour of the system, in the first order approximation in V_σ, without considering the perturbation expansion of the cumulants. This is a well-founded question since a drastical change in the spectral weights of the two transitions in the QD may provide a completely different behaviour of the tunnel current through the system. For example, suppose that the probability of the lower transition becomes very much larger. Then, also its width is increased since the cumulant of the corresponding transition occurs both in the spectral weight and in the width of the transition. This, in turn, implies that the current through this level can flow for higher voltages than in the case discussed in the example above. As a result, the drastic change of the magneto resistance will become smaller and the possibility of observing the effect experimentally may be substantially reduced. On the other hand, if the perturbation expansion of the cumulant provide the upper transition with a larger probability, and thus a large width, then the probability and width of the lower transition must be decreased by the constraint $N_0+N_\uparrow+N_\downarrow=1$. In this case the resulting change in the magneto resistance will be increased and, thus, the conclusion from the example in the previous paragraph becomes even more solid.

First, though, we derive the full equation of motion for the QD GF in the one-loop approximation and in the end we draw the correct conclusion from the provided picture. To this order, the equation of motion can be written

$$\Big(i\frac{\partial}{\partial t}-\Delta^0_{\sigma 0}(t)-\Delta U_{\sigma 0}(t)\Big)G_\sigma(t,t')-U_{\sigma\bar\sigma}(t)G_{\bar\sigma\sigma}(t,t') = = \delta(t-t')P_\sigma(t)+\delta P_\sigma(t,t')+\int_{t_0}^{t_0-i\beta}\Sigma_\sigma(t,s)G_\sigma(s,t')\mathrm{d}s, \quad (5.42)$$

with the correction to the cumulant

$$\begin{aligned}\delta P_\sigma(t,t') &= \langle \mathrm{T}(h^0+h^\sigma)(t^+)(h^0+h^\sigma)(t')\rangle_U \int_{t_0}^{t_0-i\beta} V_\sigma(t,s)D_\sigma(s,t')\mathrm{d}s \\ &\quad -P_\sigma(t^+)\int_{t_0}^{t_0-i\beta} V_\sigma(t,s)G_\sigma(s,t')\mathrm{d}s \\ &\quad +iK_{\bar\sigma\sigma}(t^+,t')\int_{t_0}^{t_0-i\beta} V_{\bar\sigma}(t,s)D_{\bar\sigma}(s,t')\mathrm{d}s \end{aligned} \tag{5.43}$$

and the self-energy

$$\Sigma_\sigma(t,s) = P_\sigma(t)V_\sigma(t,s) + i\delta(t-s)\int_{t_0}^{t_0-i\beta} V_{\bar\sigma}(t,s')D_{\bar\sigma}(s',t)\mathrm{d}s'. \tag{5.44}$$

It is clear that the second term of Eq. (5.43) and the first term of Eq. (5.44) cancel exactly when the two expressions above are inserted into Eq. (5.42). Thus, if the fluctuation in the first term of Eq. (5.43) is approximated by $P_\sigma(t^+)P_\sigma(t')$, the cumulants at different times are independent, then the width of the transition $|0\rangle \to |\sigma\rangle$ includes $P_\sigma V_\sigma$, exactly as in the preceding paragraph. In, contrast, if the fluctuation is approximated by $P_\sigma(t')$, then the level width includes V_σ which provides a larger width to the transition since the cumulant $P_\sigma \in [0,1]$.[4] The true value of the fluctuation lies somewhere between the two approximations. For simplicity, though, we will use the former in the sequel.

In the third term of Eq. (5.43), the kinematic interactions between the localized states in the QD due to the presence of the tunneling furnishes the spectral weight of the transition through the loop correction factor $i\int_{t_0}^{t_0-i\beta} V_{\bar\sigma}(t,s)D_{\bar\sigma}(s,t')\mathrm{d}s$. In addition, this integral is multiplied with the Bose-like GF $K_{\bar\sigma\sigma}(t^+,t')$ describing spin-flip processes in the QD. The graphical expression corresponding to Eq. (5.43) within the given approximations reads

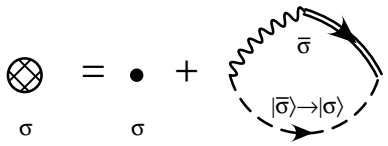

where the large cross-hatched circle denotes the dressed cumulant $\mathbb{P}_\sigma$, the dot signifies the bare cumulant P_σ and the dashed line in the loop corresponds to the Bose-like GF $K_{\bar\sigma\sigma}(i\omega) = (P_{\bar\sigma} - P_\sigma)/(i\omega - \Delta_{\sigma\bar\sigma})$. We have put the dressed spin-flip energy $\Delta_{\sigma\bar\sigma} \approx \Delta_{\sigma 0} - \Delta_{\bar\sigma 0}$ in order not to lose any information from the kinematic interactions. Actually, this energy should be calculated self-consistently along with the other quantities involved but for simplicity we have made the approximation which does not lie far from the real value. Here, one notices that the loop correction (the last diagram) gives a contribution to the cumulant whenever $P_\sigma \neq P_{\bar\sigma}$, that is, whenever the dressed transition $\Delta_{\sigma 0} \neq \Delta_{\bar\sigma 0}$. However, since there are no spin-flip processes taken into account in the self-energy of the QD

[4]Proof: Suppose that the cumulant $P_\uparrow > 1$. Then, the constraint $1 = N_0 + N_\uparrow + N_\downarrow = P_\uparrow + N_\downarrow$ requires that $N_\downarrow < 0$ which is a contradiction since N_0,$N_\uparrow$,$N_\downarrow \in [0,1]$

GF, the states in the QD will not redistribute because of the dressing of the cumulants. Only their spectral weights and widths will be affected by such processes. This can also be seen in the Fourier transform of the fully dressed QD GF

$$G_\sigma(i\omega) = \frac{\mathbb{P}_\sigma(i\omega)}{i\omega - \Delta_{\sigma 0} - \mathbb{P}_\sigma(i\omega)V_\sigma(i\omega)}, \tag{5.45}$$

where the dressed cumulant

$$\begin{aligned}\mathbb{P}_\sigma(i\omega) &= P_\sigma - \frac{P_{\bar\sigma} - P_\sigma}{i\omega - \Delta_{\sigma 0}} \sum_{k\in L,R} |v_{k\bar\sigma}|^2 \Bigg(\frac{f(\varepsilon_{k\bar\sigma}) - f(\Delta_{\bar\sigma 0})}{\varepsilon_{k\bar\sigma} - \Delta_{\bar\sigma 0}} \\ &\quad + \frac{f(\varepsilon_{k\bar\sigma}) - [1 + n_B(\Delta_{\sigma\bar\sigma})]}{i\omega - \Delta_{\sigma\bar\sigma} - \varepsilon_{k\bar\sigma}} \Bigg). \end{aligned} \tag{5.46}$$

Referring to the spin-dependent case discussed in the previous paragraph - constant population numbers - the probability of the spin $\uparrow$ state was $P_\uparrow = 0.39$ and for the spin $\downarrow$ state $P_\downarrow = 0.69$. Then, the dressed cumulant, Eq. 5.46, provides a larger probability of the spin $\downarrow$ state and a smaller for the spin $\uparrow$ state, because of the negative sign in front of the second term. Thus, the conclusion about the spin-polarized currents becomes slightly weaker when the derivative of the cumulant is included into the calculations. It is only slightly weaker, though, since the redistribution of the spectral weights is rather small, for the given set of parameters, cf. Paper V.

5.2.4 The retarded and lesser quantum dot Green functions

When the properties of the QD have been found up to the desired accuracy it is necessary to see what structure the retarded and lesser counterparts have. After all, we are not actually interested in the QD GF itself but rather its dynamic properties as a part of the whole system in which the current flows. Similarly as in the single-particle description, the retarded real-time integral equation for the QD GF is given by

$$G^r_\sigma(t,t') = \int_{-\infty}^{\infty} d^r_\sigma(t,s)\mathbb{P}^r_\sigma(s,t')\mathrm{d}s + \int_{-\infty}^{\infty} d^r_\sigma(t,s)\Sigma^r_\sigma(s,s')G^r_\sigma(s',t')\mathrm{d}s\mathrm{d}s', \tag{5.47}$$

where $\mathbb{P}_\sigma(t,t') = \delta(t-t')P_\sigma(t') + \delta P_\sigma(t,t')$. Note that the first term in this expression now is an integral, cf. Eq. (5.18), which is due to the double time-dependence of the correction $\delta P_\sigma(t,t')$ to the cumulant. Also note that the zero locator instead of the zero GF is multiplied from the left with the quantities on the right hand side of the equation. This is a consequence of the applied many-body technique in which the GF is expressed as the product of its locator and its cumulant.

An expression for the lesser QD GF is, just as in Sec. 5.1.5, easiest found by first regarding the algebraic structure

$$G^<_\sigma = d^r_\sigma\mathbb{P}^<_\sigma + d^<_\sigma\mathbb{P}^a_\sigma + d^r_\sigma\Sigma^r_\sigma G^<_\sigma + d^r_\sigma\Sigma^<_\sigma G^a_\sigma + d^<_\sigma\Sigma^a_\sigma G^a_\sigma.$$

Again, using the facts that $[(d^r_\sigma)^{-1} - \Sigma^r_\sigma]^{-1} = D^r_\sigma$, $(d^r_\sigma)^{-1}d^<_\sigma = 0$ and $(d^r_\sigma)^{-1}d^r_\sigma = 1$, we arrive at the simple expression

$$G^<_\sigma(t,t') = \int_{-\infty}^{\infty} D^r_\sigma(t,s)\Big(\mathbb{P}^<_\sigma(s,s')\delta(s-s') + \Sigma^<_\sigma(s,s')G^a_\sigma(s',t')\Big)\mathrm{d}s\mathrm{d}s'. \tag{5.48}$$

Hence, in this case the lesser QD GF is completely determined in terms of the retarded locator, the advanced QD GF, the advanced and lesser cumulants and the lesser self-energy. This is indeed the best form the lesser QD GF can be given and the quantities on the right hand side in Eq. (5.48) can be easily extracted either analytically or numerically.

We conclude the discussion of the non-orthogonal approaches showing the partitioning of the lesser QD GF which leads to a natural partitioning of the total current into a left and right contribution. As we saw in the previous chapter, it is the displacement current $J_{DD}(t) = -\mathrm{Im}\partial/\partial t G^<_\sigma(t,t)$ that has to be divided into two terms in order to achieve the desired property of the current. The following analysis also applies to the single-particle formulation with obvious modifications.

Both the cumulant $\mathbb{P}_\sigma(t,t')$ and the self-energy $\Sigma_\sigma(t,t')$ contain sums over the left and the right leads through the interaction $V_\sigma(t,t')$, for instance cf. Eqs. (5.43) and (5.44). By introducing the left interaction

$$V_{L\sigma}(t,t') = \sum_{P\in L} v^*_{p\sigma}(t) v_{p\sigma}(t') g_{p\sigma}(t,t')$$

and similarly for the right, we can define the left cumulant $\mathbb{P}_{L\sigma}(t,t')$ and self-energy $\Sigma_{L\sigma}(t,t')$ by the substitution $V_\sigma(t,t') \to V_{L\sigma}(t,t')$ in Eqs. (5.43) and (5.44). With these definitions then, we can extract the left lesser QD GF

$$G^<_{L\sigma}(t,t') = \int_{-\infty}^{\infty} D^r_\sigma(t,s)\Big(\mathbb{P}^<_{L\sigma}(s,s')\delta(s-s') + \Sigma^<_{L\sigma}(s,s')G^a_\sigma(s',t')\Big)\mathrm{d}s\mathrm{d}s'. \quad (5.49)$$

The right lesser QD GF is defined in a similar fashion, thus giving the partitioning

$$G^<_\sigma(t,t') = G^<_{L\sigma}(t,t') + G^<_{R\sigma}(t,t'). \quad (5.50)$$

It should be noticed that the partitioning does not depend on the used approximation scheme. It is simply an effect of the presence of two conduction bands entering the self-energy and, if needed, the cumulant, depending on whether the single-particle or many-body approach is employed. In contrast, their dependence of the two conduction bands is obvious.

Up to this point we have not included the overlap between the states in the QD and the leads. This means that the developed theory for the QD states under influence of the tunneling, that is the HIA [Eq. (5.35)] and the loop correction [Eq. (5.42)], should be applied to the formulation of the current in Sec. 4.1. However, the goal is to provide a complete picture of the charge transport through the system, both taking into account the many-body states in the QD and the non-orthogonality between the states in the QD and leads. This will be done in the succeeding section and in the final section of this chapter we make an analysis of the differences of the alternative descriptions.

5.3 Non-orthogonality in the many-body picture

Already in Sec. 4.2 we introduced the electron operators $c_{k\sigma}$ [Eq. (4.15)] and d_σ [Eq. (4.16)] for the conduction electrons in the leads and localized states in

the QD, respectively, in the non-orthogonal framework. We also rewrote the d-operators in terms of many-body states [Eq. (4.17)] and resolved the commutation relations between the c- and X-operators [Sec. 4.2.1]. The resulting Hamiltonian for the QD system was written [Eq. (4.19)] and by only considering the Coulomb repulsion between the localized states in the intra-dot interaction potential we arrived at the model

$$\mathcal{H} = \sum_{k\sigma\in L,R} \varepsilon_{k\sigma}(t) c^\dagger_{k\sigma} c_{k\sigma} + \sum_{p=0,\sigma} E_p(t) h^p + \sum_{k\sigma} \Big(v_{k\sigma}(t) c^\dagger_{k\sigma} X^{0\sigma} + H.c. \Big). \quad (5.22')$$

In order to derive an expression for the current we only had to consider the dynamics of the c-operators [Eq. (4.24)]. We observed that also in this formulation of the current, the unknown quantities was expressed solely in terms of the QD GF $G_\sigma(t,t')$ [cf. Eqs. (4.28), (4.31) and (4.33)]. It turns out that, the diagrammatic expansion of the QD GF looks very much similar in the case when the non-orthogonality is taken into account as without. Nevertheless, there appear some additional contributions, both to the self-energy and to the spectral weight of the QD GF, and therefore we have to work through the procedure given in Secs. 5.2.1, 5.2.2 and 5.2.3. This will be done, however, in a more compressed version.

Formally, the QD GF is defined exactly as in Sec. 5.2, i.e.

$$G_{\sigma\sigma'}(t,t') = (-i)\langle \mathrm{T} X^{0\sigma}(t) X^{\sigma' 0}(t')\rangle_U \equiv (-i) \frac{\langle \mathrm{T} S X^{0\sigma}(t) X^{\sigma' 0}(t')\rangle}{\langle \mathrm{T} S\rangle} \quad (5.24')$$

In the same notation as in the previous sections, the general equation of motion for $G_\sigma(t,t')$ now becomes

$$\begin{aligned} \Big(i\frac{\partial}{\partial t} - \Delta^0_{\sigma 0}(t) - \Delta U_{\sigma 0}(t) \Big) G_\sigma(t,t') - U_{\sigma\bar\sigma}(t) G_{\bar\sigma\sigma}(t,t') = \\ = \Big(\delta(t-t') + a_\sigma(t,t') P_\sigma(t') \Big) P_\sigma(t) + \delta P_\sigma(t,t') \\ + \int_{t_0}^{t_0 - i\beta} \Sigma_\sigma(t,t_1) G_\sigma(s,t') \mathrm{d}t_1, \end{aligned} \quad (5.51)$$

where

$$\delta P_\sigma(t,t') = \sum_s \Big(a_s(t,t') + \int_{t_0}^{t_0-i\beta} V_s(t,t_1) D_s(t_1,t') \mathrm{d}t_1 \Big) R_{\sigma s}(t^+) P_{s\sigma}(t') \quad (5.52)$$

is the correction to the cumulant $P_\sigma(t)$ whereas the self-energy

$$\begin{aligned} \Sigma_\sigma(t,t_1) &= \sum_{k\in L,R} \mathcal{O}^{-1}_{Dk\sigma} v^*_{k\sigma}(t) + P_\sigma(t^+) V_\sigma(t,t_1) \\ &\quad -i \sum_s \int_{t_0}^{t_0-i\beta} V_s(t,t_2) D_s(t_2,t_3) \Gamma_{s\sigma}(t_3,t_1; R_{\sigma s}(t^+)) \mathrm{d}t_2 \mathrm{d}t_3. \end{aligned} \quad (5.53)$$

Here, we have introduced the effective interactions

$$a_\sigma(t,t') = \sum_{k\in L,R} V_{Dk\sigma}(t) g_{k\sigma}(t,t') \mathcal{O}^{-1}_{kD\sigma} \tag{5.54}$$

$$V_\sigma(t,t') = \sum_{k\in L,R} V_{Dk\sigma}(t) g_{k\sigma}(t,t') V_{kD\sigma}(t'), \tag{5.55}$$

where the coefficients $V_{kD\sigma}(t) = v_{k\sigma}(t) + \mathcal{O}^{-1}_{kD\sigma}\Delta_{\sigma 0}(t)$ and $V_{Dk\sigma}(t) = v^*_{k\sigma}(t) + \mathcal{O}^{-1}_{Dk\sigma}\varepsilon_{k\sigma}(t)$. As seen, the coefficients $V_{kD\sigma}(t)$ and $V_{Dk\sigma}(t)$ are not simply the complex conjugates of one another, as one may expect. However, in the limit of zero overlap we have $V_{kD\sigma}(t) = v_{k\sigma}(t) = V^*_{Dk\sigma}(t)$ which is desired since the non-orthogonal approach should be a straight forward extension of the formulation where the overlap is neglected. Note that since we consider the interaction of fermion (linear) system with an atom-like (non-linear) one, the matrix of frequencies for the matrix GF is always non-Hermitian. It is also obvious that the interaction $v_\sigma(t,t') \to 0$ as the overlap $\mathcal{O}^{-1}_{kD\sigma} \to 0$. From these considerations it is clear that the difference between Eqs. (5.28) and (5.51) is the presence of the overlap in the latter.

The HIA is given by neglecting all functional derivatives and in the present description we have

$$\begin{aligned} G^{HIA}_\sigma(t,t') &= g_\sigma(t,t') + \int_{t_0}^{t_0-i\beta} g_\sigma(t,t_1) a_\sigma(t_1,t') P_\sigma(t') \mathrm{d}t_1 \\ &\quad + \sum_k \int_{t_0}^{t_0-i\beta} d_\sigma(t,t_1) \mathcal{O}^{-1}_{Dk\sigma} v^*_{k\sigma}(t_1) G^{HIA}_\sigma(t_1,t') \mathrm{d}t_1 \\ &\quad + \int_{t_0}^{t_0-i\beta} g_\sigma(t,t_1) V_\sigma(t_1,t_2) G^{HIA}_\sigma(t_2,t') \mathrm{d}t_1 \mathrm{d}t_2. \end{aligned} \tag{5.56}$$

Note, that already in this approximation the presence of the overlap introduces contributions both to the spectral weight and to the self-energy of the QD states, apart from altering the interpretation of the interaction V_σ. This is very well illustrated in the time-independent regime, where the Fourier transform of Eq. (5.56) can be performed and reads

$$G^{HIA}_\sigma(i\omega) = \frac{1 + a_\sigma(i\omega)P_\sigma}{i\omega - \Delta^0_{\sigma 0} - \sum_k \mathcal{O}^{-1}_{Dk\sigma} v^*_{k\sigma} - V_\sigma(i\omega)P_\sigma} P_\sigma. \tag{5.57}$$

The spectral weight acquires a frequency dependent redistribution through the interaction $a_\sigma(i\omega)$ whereas the many-body transition is additionally shifted by the quantity $\sum_k \mathcal{O}^{-1}_{Dk\sigma} v^*_{k\sigma}$. Usually, both these renormalizations are rather small compared to the other quantities involved and may be neglected but for some certain systems they are non-negligible. For example, in Fig. 5.6 a) and c) the total current for two different systems in the stationary regime are plotted. The currents have been calculated both by neglecting the renormalizations $a_\sigma(i\omega)$ and $\Sigma_{ov} = \sum_k \mathcal{O}^{-1}_{Dk\sigma} v^*_{k\sigma}$ (dashed) by including them (solid). In Fig. 5.6 a) the overlap is strong because of the narrow barrier width whereas in Fig. 5.6 b), where the

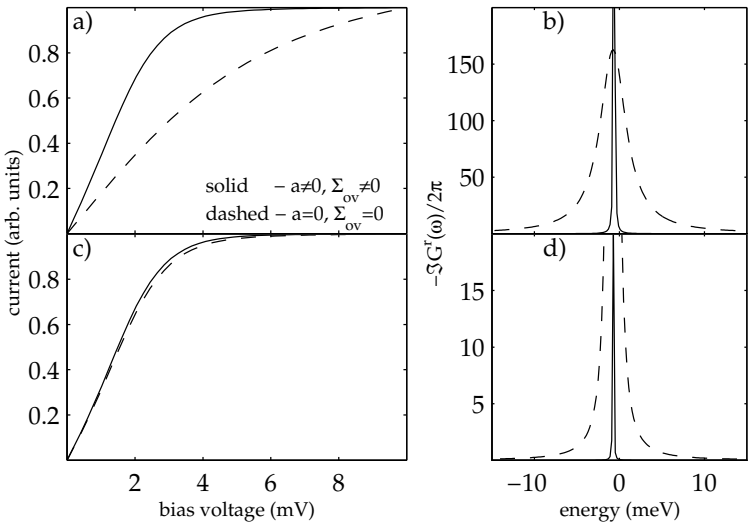

Figure 5.6: The stationary total current a) and c) and the QD DOS b) and d) with (solid lines) and without (dashed lines) the renormalizations $a_\sigma(i\omega)$ and $\Sigma_{ov} = \sum_k \mathcal{O}^{-1}_{Dk\sigma} v^*_{k\sigma}$. The system corresponding to the plots in the upper panel has 0.5 nm wide tunnel barriers whereas for the plots in the lower panel the tunnel barriers are 0.7 nm wide. Note the different scales on the vertical axes in b) and d).

barrier are somewhat wider, the overlap is weaker. Thus, when comparing the resulting currents the renormalizations $a_\sigma(i\omega)$ and Σ_{ov} seems to be negligible in the latter case, however, not in the former. The substantial difference in the currents given in Fig. 5.6 a) can be explained by looking at the corresponding QD DOS, c.f. Fig. 5.6 b). By neglecting the tow renormalizations the level is significantly smeared out providing a slower increase of the current as the bias voltage is increased, compared to the case when the renormalizations are included. A similar observation can be made for the current in Fig. 5.6 c). However, the small difference between the solid and the dashed lines is a result of the small level widths, both when the renormalizations are included and when they are not. Thus, in situations like this, we conclude that the shift Σ_{ov} and the additional spectral weight $a_\sigma P_\sigma$ become important when the overlap is large, i.e., when the tunnel barriers are narrow and/or low. We also observe in Eq. (5.56) that in this approximation, although the states in the QD are not independent, there is no renormalization of the spin σ state depending on the properties of the opposite spin $\bar{\sigma}$, exactly as in the case when the overlap is neglected.

By including the first functional derivative we arrive at the loop correction

$$G^{loop}_\sigma(t,t') = g_\sigma(t,t') + \int_{t_0}^{t_0-i\beta} g_\sigma(t,t_1)\Big(a_\sigma(t_1,t')P_\sigma(t') + \delta P^{loop}_\sigma(t_1,t')\Big)\mathrm{d}t_1 + \int_{t_0}^{t_0-i\beta} g_\sigma(t,t_1)\Sigma^{loop}_\sigma(t_1,t_2)G_\sigma(t_2,t')\mathrm{d}t_1\mathrm{d}t_2, \qquad (5.58)$$

where the correction to the cumulant reads

$$\begin{aligned}\delta P_\sigma(t_1,t') &= \left(a_\sigma(t_1,t') + \int_{t_0}^{t_0-i\beta} V_\sigma(t_1,t_2)D_\sigma(t_2,t')\mathrm{d}t_2\right) \\ &\quad\times\left(\langle \mathrm{T}(h^0+h^\sigma)(t_1^+)(h^0+h^\sigma)(t')\rangle_U - P_\sigma(t_1^+)P_\sigma(t')\right) \\ &\quad+i\left(a_{\bar\sigma}(t_1,t') + \int_{t_0}^{t_0-i\beta} V_{\bar\sigma}(t_1,t_2)D_{\bar\sigma}(t_2,t')\mathrm{d}t_2\right)K_{\bar\sigma\sigma}(t_1^+,t') \quad (5.59)\end{aligned}$$

and the self-energy

$$\begin{aligned}\Sigma_\sigma^{loop}(t_1,t_2) &= \sum_k \mathcal{O}^{-1}_{Dk\sigma}v^*_{k\sigma}(t_1) + \Big(P_\sigma(t_1^+) + \delta P_\sigma^{loop}(t_1^+,t_2)\Big)V_\sigma(t_1,t_2) \\ &\quad+i\delta(t_1-t_2)\int_{t_0}^{t_0-i\beta} V_{\bar\sigma}(t_1,t_3)D_{\bar\sigma}(t_3,t_1^+)\mathrm{d}t_3. \quad (5.60)\end{aligned}$$

Thus, in the loop correction there appear two additional contributions to the cumulant correction δP_σ due to the non-orthogonality, the interactions $a_s(t_1,t')$ times the functional derivatives $R_{\sigma s}(t_1^+)P_{s\sigma}(t')$. Denoting the total spectral weight $\mathbb{P}_\sigma = P_\sigma + v_\sigma P_\sigma + \delta P_\sigma$ by a cross-hatched circle, the graphical expansion of the loop correction reads

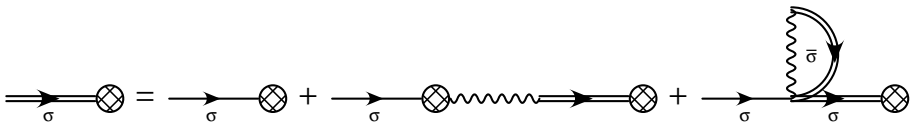

where the first term in Eq. (5.60) is absorbed in the single and double straight lines for simplicity. Then, although the non-orthogonality is taken into account in the present formulation, the final expression for the QD GF has a very similar structure as without the overlap, cf Eq. (5.42) and its corresponding graphical expression.

5.3.1 The retarded and lesser quantum dot Green functions

As mentioned earlier, when substituting the approximations of the QD GF given in Eqs. (5.56) and (5.58) into the expression for the current, we need the retarded and lesser counterparts of G_σ. The former is simply given by the real-time integral equation

$$G^r_\sigma(t,t') = \int_{-\infty}^{\infty} g^r_\sigma(t,s)\mathbb{P}^r_\sigma(s,t')\mathrm{d}s + \int_{-\infty}^{\infty} g^r_\sigma(t,s)\Sigma^r_\sigma(s,s')G^r_\sigma(s',t')\mathrm{d}s\mathrm{d}s', \quad (5.61)$$

where the dressed cumulant $\mathbb{P}_\sigma$ and the self-energy Σ_σ denote the corresponding expressions either in the HIA or in the loop correction.

The lesser QD GF is, once again, easiest found by considering the algebraic equation $G_\sigma = d_\sigma\mathbb{P}_\sigma + d_\sigma\Sigma_\sigma G_\sigma$. Then, an application of the analytical continuation rules [31, 58] yields the lesser QD GF, after tidying up the formulas,

$$G^<_\sigma(t,t') = \int_{-\infty}^{\infty} D^r_\sigma(t,s)\Big(\mathbb{P}^<_\sigma(s,s')\delta(s'-t') + \Sigma^<_\sigma(s,s')G^a_\sigma(s',t')\Big)\mathrm{d}s\mathrm{d}s' \quad (5.62)$$

The GF given in Eqs. (5.62) can be used in the formulas for the current, Eq. (4.28) and Eq. (4.33), expressing the current in terms of the retarded and advanced QD GF. Once, we have a suitable expression for the retarded/advanced QD GF, either analytically or numerically, the current through the system will be known. However, it was stated that also in the non-orthogonal formulation, the QD displacement current can be partitioned into a left and a right part. In particular Eq. (4.31) is written in terms of the lesser QD GF depending on the conduction electrons in the left lead. Below we show, somewhat detailed, how the lesser QD GF is naturally partitioned into a left and a right term.

We notice that the interactions a_σ and V_σ, cf. Eqs. (5.54) and (5.55), are actually sums over the left and the right conduction bands, i.e. $a_\sigma(t,t') = a_{L\sigma}(t,t') + a_{R\sigma}(t,t')$ and $V_\sigma(t,t') = V_{L\sigma}(t,t') + V_{R\sigma}(t,t')$, where

$$a_{L\sigma}(t,t') = \sum_{p\in L} V_{Dp\sigma}(t) g_{p\sigma}(t,t') \mathcal{O}^{-1}_{pD\sigma}, \tag{5.63}$$

$$V_{L\sigma}(t,t') = \sum_{p\in L} V_{Dp\sigma}(t) g_{p\sigma}(t,t') V_{pD\sigma}(t'), \tag{5.64}$$

and analogously for the right interactions. We introduce the left cumulant $\mathbb{P}_{L\sigma}(t,t')$ and self-energy $\Sigma_{L\sigma}(t,t')$, defined by making the replacements $a_\sigma(t,t') \to a_{L\sigma}(t,t')$, $V_\sigma(t,t') \to V_{L\sigma}(t,t')$ and $\sum_k \mathcal{O}^{-1}_{Dk\sigma} v^*_{k\sigma}(t) \to \sum_{p\in L} \mathcal{O}^{-1}_{Dp\sigma} v^*_{p\sigma}(t)$ in Eqs. (5.52) and (5.60). The right cumulant $\mathbb{P}_{R\sigma}(t,t')$ and self-energy $\Sigma_{R\sigma}(t,t')$ are defined analogously. Therefore, the right hand side of Eq. (5.62) can be naturally partitioned into a left and a right term according to $G^<_\sigma(t,t') = G^<_{L\sigma}(t,t') + G^<_{R\sigma}(t,t')$, where

$$G^<_{L\sigma}(t,t') = \int_{-\infty}^{\infty} D^r_\sigma(t,s) \Big(\mathbb{P}^<_{L\sigma}(s,s')\delta(s'-t') + \Sigma^<_{L\sigma}(s,s') G^a_\sigma(s',t') \Big) \mathrm{d}s\mathrm{d}s' \tag{5.65}$$

and similarly for the right. Hence, although the non-orthogonality has been included into the description, the formal appearance of the left/right lesser QD GF is exactly the same as without. One merely has to observe that the interactions between the QD states and the conduction electrons in the leads are given as sums over the number of probes involved. Actually, employing a similar scheme for the current and the analysis of the electronic structure of the QD as in Chap. 4 and the present chapter, this observation is true for any number of probes. The partitioning of the current into several terms may therefore be regarded as an universal property of the model, independent of the actual methods used for the considerations of the transport.

By this, we conclude the presentation of the different approaches in dealing with transport through mesoscopic interacting system, e.g. QD, coupled to external leads. Next, we compare the benefits and drawbacks of the techniques, using some numerical calculations for the resulting current through the QD system.

5.4 Comparison of the different approaches

One of the simplest ways to make numerical calculations for time-dependent transport is by employing the so-called wide-band limit (WBL). In this limit, it

Table 5.1: The approximations corresponding to the WBL for the case with (NOR) and without the overlap (OR). The last row displays the limit of the single-particle picture (SE), in which the end-factors equals unity.

OR	
level shift	$\mathrm{Re}\sum_k v^*_{k\sigma}(t)v_{k\sigma}(t')g^r_{k\sigma}(t,t') \to 0$
line width	$\mathrm{Im}V^r_\sigma(t,t') \to -i\delta(t-t')\Gamma_\sigma(t)$
NOR	
level shift	$\mathrm{Re}\sum_k V_{Dk\sigma}(t)V_{kD\sigma}(t')g_{k\sigma}(t,t') \to 0$ $\sum_k \mathcal{O}^{-1}_{Dk\sigma}v^*_{k\sigma}(t) \to 0$
line width	$\mathrm{Im}V^r_\sigma(t,t') \to -i\delta(t-t')\Gamma^D_\sigma(t)$ $\mathrm{Im}v^r_\sigma(t,t') \to -i\delta(t-t')\gamma^D_\sigma(t)$
SE	
end-factor	$P_\sigma(t) \to 1$

is assumed that the small shift of the QD level, caused by the coupling with the conduction electrons, is negligible. However, in the many-body approach, the loop correction due to the kinematic interactions should be included, since it may be large. If the time-dependence only comes from a small bias voltage it may be approximated by a time-independent constant. In order to be able to obtain some analytical results, we will make the following simplifications. In the non-orthogonal picture we also neglect the shift from $\sum_k \mathcal{O}^{-1}_{Dk\sigma}v^*_{k\sigma}(t)$. It is further assumed that the energy dependence of the line widths can be discarded because of its slow variation in the considered voltage regime. Thus, the conduction band widths can be regarded as infinite. We finally assume that the time-dependence for the energies in the two leads are the same. In this limit one rather easily can obtain analytical results for the QD GF which then are inserted into the current formulas. Furthermore, since the transport is often dominated by states close to the quasi-chemical potentials and the level shift and width are generally slowly varying functions of the energy, the WBL for this case is a fair approximation. The approximation also allows for asymmetric barriers ($\Gamma^L_\sigma \neq \Gamma^R_\sigma$).

Let us see what happens with the interactions $a_\sigma(t,t')$ and $V_\sigma(t,t')$ in the WBL. Neglecting the energy dependence in the mixing $v_{k\sigma}(t)$ and in the overlap

$\mathcal{O}^{-1}_{kD\sigma}$, the imaginary parts of the retarded interactions become

$$\begin{aligned}
\mathrm{Im}a^r_\sigma(t,t') &= -\frac{1}{2\pi}\theta(t-t')\sum_\alpha \gamma^{D\alpha}_\sigma(t,t')\int e^{i\varepsilon(t-t')}\mathrm{d}\varepsilon \\
&= -\delta(t-t')\gamma^D_\sigma(t), \qquad (5.66)\\
\mathrm{Im}V^r_\sigma(t,t') &= -\frac{1}{2\pi}\theta(t-t')\sum_\alpha \Gamma^{D\alpha}_\sigma(t,t')\int e^{i\varepsilon(t-t')}\mathrm{d}\varepsilon \\
&= -\delta(t-t')\Gamma^D_\sigma(t). \qquad (5.67)
\end{aligned}$$

Here, we have introduced the notations $\gamma^D_\sigma(t) = \gamma^{DL}_\sigma(t) + \gamma^{DR}_\sigma(t)$ and $\Gamma^D_\sigma(t) = \Gamma^{DL}_\sigma(t) + \Gamma^{DR}_\sigma(t)$, where

$$\gamma^{D\alpha}_\sigma(t) = \gamma^{D\alpha}_\sigma(t,t) \equiv \lim_{t'\to t} 2\pi V_{D\alpha\sigma}(t)\mathcal{O}^{-1}_{\alpha D\sigma}\rho^\alpha_\sigma e^{i\int_{t'}^t \Phi_\alpha(s)\mathrm{d}s}, \qquad (5.68)$$

$$\Gamma^{D\alpha}_\sigma(t) = \Gamma^{D\alpha}_\sigma(t,t) \equiv \lim_{t'\to t} 2\pi V_{D\alpha\sigma}(t)V_{\alpha D\sigma}(t')\rho^\alpha_\sigma e^{i\int_{t'}^t \Phi_\alpha(s)\mathrm{d}s}. \qquad (5.69)$$

The conduction band DOS for the left and right leads are denoted by ρ^α_σ, $\alpha = L, R$. When the overlaps between the states in the QD and in the leads are neglected, the interaction $a_\sigma(t,t')$ vanishes and the line width $\Gamma^D_\sigma(t) \to \Gamma_\sigma(t) = \Gamma^L_\sigma(t) + \Gamma^R_\sigma(t)$, that is, it equals the sum of the couplings with the left and the right leads defined in Eq. (4.29) with the overlap neglected. Therefore, the superscript D is dropped in this limit. For clarity, the approximations made are summarized in Table 5.1. The following analysis will be conducted with the non-orthogonality taken into account, recalling that all corresponding quantities when the non-orthogonality is neglected are given in the limit $\mathcal{O}^{-1}_{kD\sigma} \to 0$.

When the energy dependence of the interactions $a_\sigma(t,t')$ and $V_\sigma(t,t')$ are neglected, the retarded/advanced QD GF can be written in the simple form

$$G^{r,a}_\sigma(t,t') = \mp i\theta(\pm t \mp t')\Big(1 \mp i\gamma^D_\sigma(t)P_\sigma(t)\Big)P_\sigma(t)e^{-i\int_{t'}^t[\tilde{\Delta}_{\sigma 0}(s) \mp i\Gamma^D_\sigma(s)P_\sigma(s)]\mathrm{d}s}, \qquad (5.70)$$

where $\tilde{\Delta}_{\sigma 0}(s)$ equals $\Delta^0_{\sigma 0}(s)$ in the HIA and $\Delta_{\sigma 0}(s)$ within the loop correction. For numerical simplicity, we now also neglect the time-dependence in the many-body states in the QD and in the mixing, giving constant couplings, level widths and cumulants. Suppose that a step-like bias voltage $\Phi_{sd}(t) = \Phi_0 + \Phi_1(t)$, where Φ_0 provides a constant shift to the conduction electron energies and $\Phi_1(t) = \Phi_1[\theta(t-t_0) - \theta(t-t_1)]$ gives a superimposed time-dependence of the conduction electron energies is applied over the system. Then, the function

$$A^\alpha_\sigma(\omega,t) = \int_{-\infty}^{\infty} G^r_\sigma(t,t')e^{[i\omega(t-t') + i\int_{t'}^t \Phi_\alpha(s)\mathrm{d}s]}\mathrm{d}t', \qquad (5.71)$$

where $\Phi_\alpha(t) = \Phi_L(t)$, $\Phi_R(t)$ and $\Phi_L(t) + \Phi_R(t) = \Phi_1(t)$, becomes for $t < t_1$

$$A^\alpha_\sigma(\omega,t) = \frac{1-i\gamma^D_\sigma P_\sigma}{\omega-\tilde{\Delta}_{\sigma 0}+i\Gamma^D_\sigma P_\sigma}P_\sigma \times\left(1-\frac{1-e^{i(\omega+\Phi_\alpha-\tilde{\Delta}_{\sigma 0}+i\Gamma^D_\sigma P_\sigma)(t-t_0)}}{\omega+\Phi_\alpha-\tilde{\Delta}_{\sigma 0}+i\Gamma^D_\sigma P_\sigma}\theta(t-t_0)\right), \quad (5.72)$$

where $\omega = \varepsilon + \mu_\alpha$ and μ_α is the constant shift of the quasi-chemical potential in the lead α and Φ_α is the amplitude of $\Phi_\alpha(t)$. The analytical expression given in Eq. (5.72) is derived by neglecting the time-dependence in the couplings, that is $\gamma^D_\sigma(t) = \gamma^D_\sigma$ and $\Gamma^D_\sigma(t) = \Gamma^D_\sigma$. Letting $t \to \infty$ in Eq. (5.72) the limit expression is $A^\alpha_\sigma(\omega, t\to\infty) = (1-i\gamma^D_\sigma P_\sigma)P_\sigma/(\omega+\Phi_\alpha-\tilde{\Delta}_{\sigma 0}+i\Gamma^D_\sigma P_\sigma)$, that is, the system settles at its new steady state value as all the transients decay. For $t > t_1$ the formula in Eq. (5.72) is replaced by

$$A^\alpha_\sigma(\omega,t) = \frac{1-i\gamma^D_\sigma P_\sigma}{\omega-\tilde{\Delta}_{\sigma 0}+i\Gamma^D_\sigma P_\sigma}P_\sigma \times\left(1+\Phi_\alpha\frac{1-e^{i(\omega+\Phi_\alpha-\tilde{\Delta}_{\sigma 0}+i\Gamma^D_\sigma P_\sigma)(t_1-t_0)}}{\omega+\Phi_\alpha-\tilde{\Delta}_{\sigma 0}+i\Gamma^D_\sigma P_\sigma}e^{i(\omega-\tilde{\Delta}_{\sigma 0}+i\Gamma^D_\sigma P_\sigma)(t-t_1)}\right). \quad (5.73)$$

Similarly, the limit $t \to \infty$ gives $A^\alpha_\sigma(\omega, t\to\infty) = (1-i\gamma^D_\sigma P_\sigma)P_\sigma/(\omega-\tilde{\Delta}_{\sigma 0}+i\Gamma^D_\sigma P_\sigma)$, as expected.

The resulting time-dependent currents for the bias voltage step with and without the non-orthogonality taken into account are presented in Fig 5.7 a) and b),

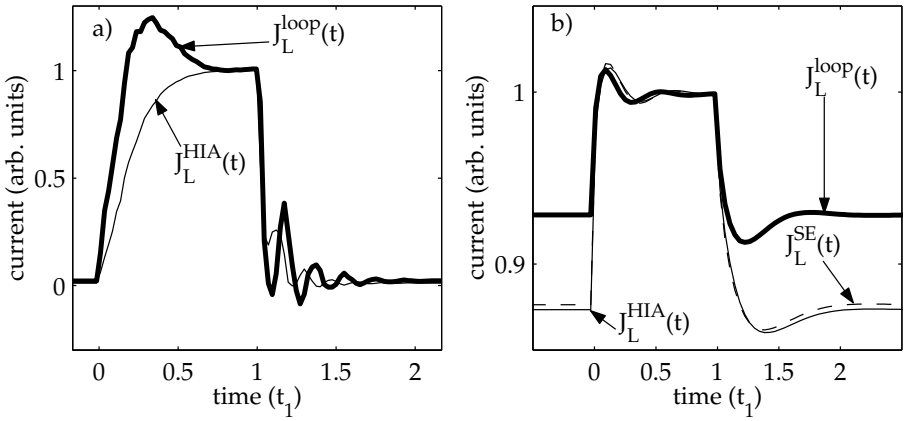

Figure 5.7: The time-dependent current for the bias voltage step $\Phi_{sd}(t) = 45 + 5[\theta(t-t_0) - \theta(t-t_1)]$ mV in the formulations with a) and without b) the overlap. In a) the currents are provided within the HIA (solid line) and with the loop correction (full line), taking the non-orthogonality into account. The time scale $t_1 = 600$ ps. In b) the currents are given within single electron theory (dashed line), within the HIA (solid line) and with the loop correction (full line), without the non-orthogonality. The time scale $t_1 = 1$ ps.

respectively. In the former the behaviour of the currents is seen to differ for the the HIA (solid) and the loop correction (full) around the onset of the voltage step. In the HIA the current grows exponentially to its saturation value whereas with the loop correction the current first goes to a peak value and thereafter decays to its new steady state value. Thus, the transient behaviour of the current is affected by many-body interactions in the QD. As the pulse terminates both the HIA and the loop correction provides an oscillating decay of the current, as expected from Eq. (5.73). Fig. 5.7 b) shows the currents provided in the single-particle picture (dashed), the HIA (solid) and with the loop correction (full) when the non-orthogonality is neglected. The three schemes display similar qualitative behaviour with rapidly decaying ringing at the onset and termination of the bias voltage pulse. As seen, the single-particle picture and the HIA gives essentially the same net currents whereas within the loop correction the current has a slightly larger amplitude before and after the voltage pulse, as expected from the stationary case (cf. Fig. 5.8).

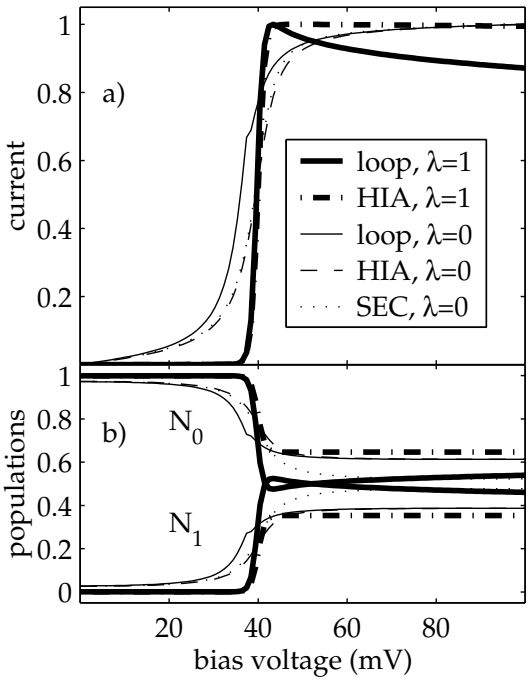

Figure 5.8: Characteristic features of the current $a)$ and the population numbers $b)$, for a 4 nm wide QD connected via 0.5 nm thick and 1 eV high tunnel barriers, as functions of the bias voltage. The bare level $\Delta^0_{\sigma 0} = 20$ meV and the conduction electron DOS $\rho^\alpha_\sigma = 1/(2W)$, where $W = 1$ eV is the conduction band width. The plots are made for the single-electron case (dotted lines), within the HIA with (dash-dotted lines) and without (dashed lines) the overlap and with the loop correction with (bold solid lines) and without (solid lines) the overlap. In order to analyze the effects of the overlap we have put $\mathcal{O}^{-1}_{kD\sigma} \to \lambda \mathcal{O}^{-1}_{kD\sigma}$, $\lambda \in [0, 1]$.

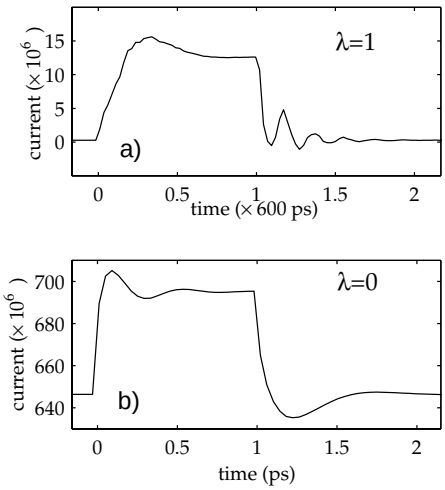

Figure 5.9: The time-dependent currents within the HIA with the loop correction with a) $(\lambda = 1)$ and without b) $(\lambda = 0)$ the non-orthogonality taken into account. Note the very different scales of the times and the amplitudes of the current.

One of largest differences between the currents shown in Figs. 5.9 a) and b) are the different time scales. As previously discussed, the non-orthogonality decreases the couplings $\Gamma_\sigma^{L,R}$ and the level width Γ_σ^D and, therefore, the relaxation time τ becomes longer, since $\tau \sim 1/(\Gamma_\sigma^D P_\sigma)$. As a result, the time scale of the tunneling process is longer within the non-orthogonal picture than in the orthodox one. A comparison of the net currents with and without the non-orthogonality within the loop correction is shown in Fig. 5.9 a) and b), respectively, from which the different time scales are directly seen. In this connection we also stress that the magnitudes of the two curves are actually very different, where the non-orthogonal picture results in a current which is approximately one to two orders of magnitudes less than that of the orthodox. Thus, the interpretation of experimental results give very different values of the couplings and the level width, and hence the barrier widths and heights, within the two pictures. In Fig. 5.10 the different contributions to the net current in Fig. 5.9 a) are shown and it is readily seen that the tunnel current gives the main contribution to the current while the displacement currents tend to retard the tunnel current. However, the displacement current do not cancel out the ringing of the tunnel current completely and therefore there remains a rapidly decaying ringing in the net current. The contribution from $J_{LD}(t)$ is seen to be small in this example but when the amplitude of $\Phi_1(t)$ is increased we have observed that this contribution plays an important role of the complete picture.

In summary, we have shown how the transfer Hamiltonian formalism can be generalized by including the non-orthogonality between the subsystems. It is formally shown that the tunnel current flowing through the left/right barrier into an interacting region, e.g. QD, can be expressed in a well-known formula-

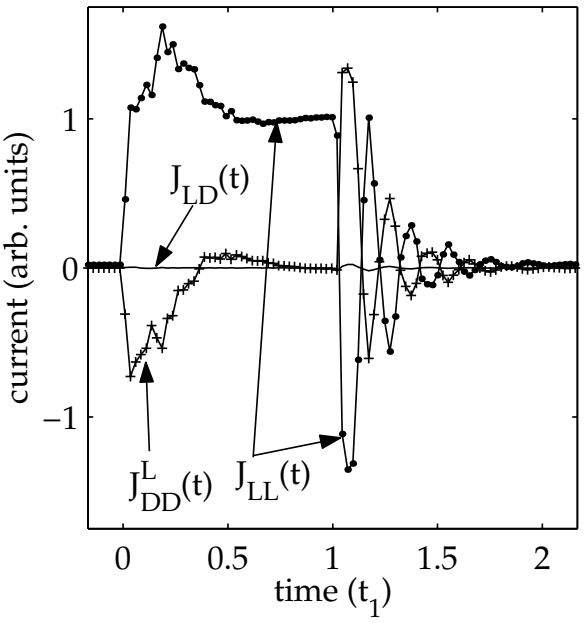

Figure 5.10: The different contributions to the net current shown in Fig. 5.9 a). The plot shows the tunnel current $J_{LL}(t)$ (solid-dotted line) and the displacement currents $J^L_{DD}(t)$ (solid line with pluses) and $J_{LD}(t)$ (solid line).

tion [Eq. (4.28)], however, with an interpretation of the tunneling coefficient that differs from orthodox theories $[v_{k\sigma}(t) \rightarrow V_{kD\sigma}(t) = v_{k\sigma}(t) + \mathcal{O}^{-1}_{kD\sigma}\Delta^*_{\sigma 0}(t)]$. Moreover, we derived expressions for the displacement currents [Eqs. 4.31, 4.33] and showed that the total current can be partitioned into two contributions, one for the flow through the left barrier and for the right. The QD was described in terms of Hubbard operator GF describing many-body interactions within the QD. The QD GF was given within the HIA [Eq. 5.35] and with the loop correction [Eq. 5.42], thus giving us the opportunity to analyze the significance of the non-Fermi statistics of the population numbers compared to Fermi statistics on the resulting current. The conclusion is that, although the behaviour of the population numbers of the QD level differ considerably, the behaviour of the current is only slightly affected. A comparison of the two approximate schemes for the QD GF gives that the many-body effects given by the loop correction, kinematic interactions, qualitatively alters the output current. Actually, it provides a range of voltages with negative differential resistance. Consequently, many-body effects in the QD should be considered for an adequate description of the current. However, the main quantitative differences in the current, in the non-spin-polarized case, is shown to be given by taking the non-orthogonality into account. Actually, a comparison of the amplitudes of the currents with and without the overlap shows a difference of the order of one to two magnitudes, where the non-orthogonal representation provides the smaller. This difference can be understood by that

the coupling between, say, the left contact and the QD is not given by just the matrix element $v_{LD\sigma}$, as within the orthodox transfer Hamiltonian approach, but by $V_{LD\sigma} = v_{LD\sigma} + \mathcal{O}^{-1}_{LD\sigma}\Delta_{\sigma 0}$, where $\mathcal{O}^{-1}_{LD\sigma} \approx -\mathcal{O}_{LD\sigma}/(1 - |\mathcal{O}_{LD\sigma}|^2 - |\mathcal{O}_{RD\sigma}|^2)$ has the opposite sign of $v_{LD\sigma}$ and, therefore, *decreases* the coupling strength. The comparison of the J-V characteristics for orthogonal and non-orthogonal cases, given in Fig.1 of Ref. [27], shows that the current starts to grow at much smaller voltage in the orthogonal case than in the non-orthogonal, whereas for the solution of quasi-classical wave functions [83, 84] the discrepancy is even more drastical. Thus we conclude that, when interpreting experimental results in terms of theoretical predictions given within the non-orthogonal representation the effective widths and/or heights of the tunnel barriers are thinner and/or lower than without the non-orthogonality.

Chapter 6

Some recent results

THE THREE PRECEDING chapters have very much been devoted to theoretical techniques. There were discussions about transport theory for mesoscopic systems and there were some extensive parts on the theoretical treatment of QD. Some examples have also been provided. Apart from one of the examples, the character of these was to make evident that the developed theory is relevant for investigations of transport in QD systems. However, once this is done we should move on and apply the techniques to new systems. In the present chapter we briefly discuss a way to produce highly spin dependent currents, alternative to that presented in Paper V, and some new results on coupled QD.

6.1 Alternative opportunity to induce spin-dependent transport

There are numbers of examples of how to provide highly spin dependent tunnel currents [44, 60, 79, 91] and magneto-transport [20, 32, 46, 67, 80, 82] in mesoscopic systems. In addition, there are many suggestions of spin-filter devices [19, 21, 28, 50, 70, 72]. In most of these reports, magnetic fields have been used to provide a spin-current through the devices, applied either directly over the device or to polarize the leads only. On the contrary, the possibility of creating a highly spin polarized current without using magnetic fields has, so far, been a peripheral topic. However, by exploiting a combination of spin-splitting of the resonant level induced by the Rashba effect and the spin blockade phenomenon, it was proposed in Ref. [50] that a more than 99.9% spin polarized current can be achieved in a triple barrier resonant tunneling diode.

Another alternative can actually be found in theory presented in Sec. 5.2.3. Indeed, the spin dependent renormalization of the QD levels given in Eq. (5.39),

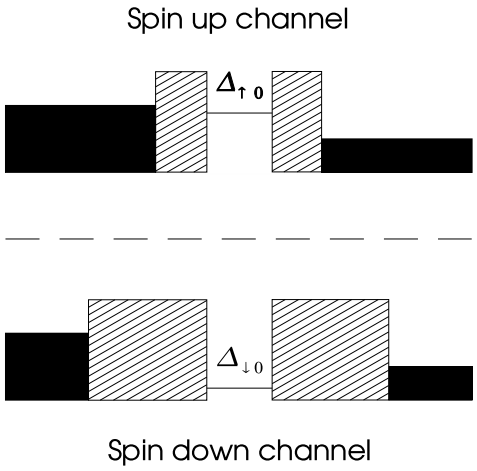

Figure 6.1: A model of the potential profiles for the two spin-channels.

rewritten here for convenience,

$$\Delta_{\sigma 0} - \Delta^0_{\sigma 0} = \sum_k V_{Dk\bar{\sigma}} V_{kD\bar{\sigma}} \frac{f(\varepsilon_{k\bar{\sigma}}) - f(\Delta_{\bar{\sigma}0})}{\varepsilon_{k\bar{\sigma}} - \Delta_{\bar{\sigma}0}} \tag{5.39'}$$

does not only depend on the spin polarization in the contacts, as discussed in Paper V. Note that we have here also included the overlap between the contacts and the QD in the tunneling coefficients $V_{Dk\bar{\sigma}}$ and $V_{kD\bar{\sigma}}$. A closer look at Eq. (5.39') shows that, if we can manipulate the tunneling coefficients $V_{Dk\sigma},\ V_{kD\bar{\sigma}}$ to become different for spin $\uparrow$ and $\downarrow$, then the level $\Delta_{\uparrow 0} \neq \Delta_{\downarrow 0}$. All this with non-polarized contacts.

One, from theoretical aspects, simple way of making the tunneling coefficients spin dependent, is to let the tunnel barriers between the contacts and the QD for the two spin-channels be of different widths and/or heights. Being specific, suppose that the tunnel barriers for the spin $\uparrow$-channel are wider than for spin $\downarrow$, see Fig. 6.1. Then, because of the different overlaps for the two spin-channels, due to the different widths of the barriers, the tunneling probabilities of the spin-channels become non-equal. Hence, the spin $\downarrow$ level in the QD experiences a larger renormalization than the spin $\uparrow$ level does, i.e. $\Delta_{\downarrow 0} < \Delta_{\uparrow 0}$. Therefore, the spin $\uparrow$-channel acquires the larger contribution to the conductance, since the tunneling probability is larger in addition to that the corresponding QD level being closer to the equilibrium chemical potential μ (assuming the levels lying below μ). By making the ratio $w_\downarrow/w_\uparrow$ sufficiently large, where w_σ is the width of the tunnel barrier for the spin σ-channel, the contribution from the spin $\downarrow$ current can be made less than 0.05 % of the total current. Thus, a static spin-filter is constructed. Ideas similar to these are discussed in Paper VI together with first principles calculations on a system (Vac/Fe/Pd/Fe/Vac) which shows a magnetization of the Pd layers induced by the Fe layers and spin dependent widths of the tunnel bar-

riers. Moreover, results on the transport properties of the system are provided, calculated within the non-orthogonal theory developed in Chaps. 4 and 5.

6.2 Cluster approach to transport in nanostructures

It is known from experiments on GaAs-Al_xGa_{1-x}AS heterostructures [35] that the conductance exhibits periodic shifts in the Coulomb blockade oscillations as a consequence of a tunable coupling to a non-conducting QD, in a system of coupled QD. Thus, on the one hand, the transport properties of one QD can governed with help of another, which is coupled to the former. On the other hand, for sufficiently small sizes of the QD, the strong electron correlations become important. The perturbative treatment of the QD give wrong positions of the levels and, therefore, provides an unsatisfactory description of the weak coupling between the QD. Actually, if the system is constituted by one or several interacting regions, which may or may not have mutual interactions with each other, we can handle them within the same formalism. What should be done, on the other hand, is to substitute the system of interacting regions with an equivalent *effective* interacting region, call it effective QD. Then, this effective QD is thought of being attached to one, two or more external contacts. The non-equilibrium techniques that are described in Chaps. 4 and 5 are not tailor made for systems with a single QD attached to external contacts. Thus, our method allows to treat the system of coupled QD as one single entity, or as on artificial molecule. Therefore, our method should provide a more reliable and detailed picture of the transport in such systems.

Suppose that we have a number of QD which are interacting with each other. At first we disconnect this system from the external contacts, thus the system is isolated from the environment. In order to bring the system into an effective QD, we have to diagonalize the system of QD. In other words, we have to find the eigenstates and eigenenergies of the system. In the case with one single level QD, the states are $|0\rangle$, $|\uparrow\rangle$, $|\downarrow\rangle$ and $|\uparrow\downarrow\rangle$ and the diagonalization is trivial. With two or more QD in the system we have an empty state, and several one-, two-, three, $\cdots$

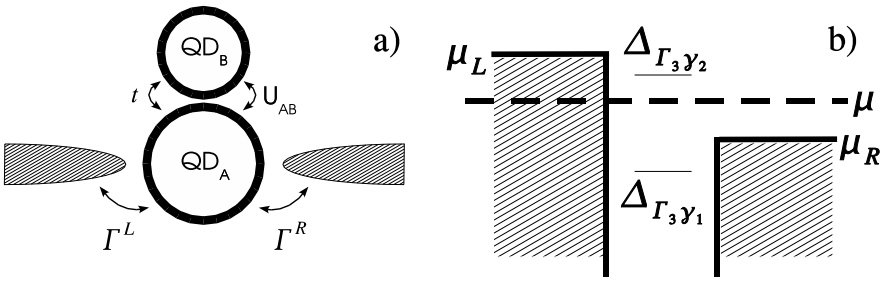

Figure 6.2: The system of the two coupled QD. a) The two QD interact via hopping t and inter-dot Coulomb repulsion U_{AB}. One of the QD is coupled to external contacts with strengths $\Gamma^{L/R}$ to the left/right contacts. b) In the diagonal representation of the coupled QD, an equivalent system is provided by an *effective* QD coupled to external contacts. In the effective QD the relevant levels are $\Delta_{\Gamma_3\gamma_i}$, $i = 1,2$.

Table 6.1: The three states of the two coupled QD, where $b = 2\varepsilon_A + U_A$, $\nu_\Gamma = \sqrt{[(E_{\Gamma_1} - b)/2]^2 + 2|t|^2}$, $u^\sigma_{i1} = (E_{\gamma_{i\sigma}} - \varepsilon_B)/\kappa_{1i}$, $|u^\sigma_{i2}|^2 = 1 - |u^\sigma_{i1}|^2$, $\kappa_{1i} = \sqrt{(E_{\gamma_{i\sigma}} - \varepsilon_B)^2 + |t|^2}$, $i = 1, 2$ and $\kappa_3 = \sqrt{(E_{\Gamma_3} - E_{\Gamma_2})^2 + 2|t|^2}$. The states $|\Phi^{(2)}_{S=0}) = [|\uparrow\rangle_A |\downarrow\rangle_B - |\downarrow\rangle_A |\uparrow\rangle_B]/\sqrt{2}$ and $|\Phi^{(2)}_{ex}) = |\uparrow\downarrow\rangle_A |0\rangle_B$.

N_{tot}	state	energy
1	$\|\gamma_{i\sigma}) = u^\sigma_{i1} \|\sigma\rangle_A \|0\rangle_B$ $+u^\sigma_{i2} \|0\rangle_A \|\sigma\rangle_B$	$E_{\gamma_{i\sigma}} = \frac{1}{2}\Big(\varepsilon_A + \varepsilon_B$ $+(-1)^i\sqrt{(\varepsilon_A - \varepsilon_B)^2 + \|t\|^2}\Big)$, $i = 1, 2$
2	$\|\Gamma_3) = -t^* \frac{\sqrt{2}}{\kappa_3} \|\Phi^{(2)}_{S=0})$ $+ \frac{E_{\Gamma_3} - E_{\Gamma_2}}{\kappa_3} \|\Phi^{(2)}_{ex})$	$E_{\Gamma_3} = \frac{E_{\Gamma_1} + b}{2} - \nu_\Gamma$

particle states. Once these states are found, the effective QD can be expressed in diagonal form in terms of Hubbard operators, i.e. $\mathcal{H}_{QD} = E_0 h^0 + \sum_i E_{\gamma_i} h^{\gamma_i} + \sum_i E_{\Gamma_i} h^{\Gamma_i} + \sum_i E_{\Lambda_i} h^{\Lambda_i} + \cdots$, where γ_i, Γ_i and Λ_i are the one-, two- and three-particle states, respectively. After the diagonalization, the initial Hamiltonian is rewritten, exactly, in terms of the new variables.

In Paper VII, we studied an example of two coupled QD which is diagonalized and expressed according to the procedure described above. In systems with two coupled QD there are two possible configurations. In one case the QD are put in series while the QD are in parallel alignment in the second. The latter possibility is illustrated in Fig. 6.2. Here, as well as in Paper VII, we have chosen to work with the latter configuration. Such a system is possibly a good candidate to work as a mesoscopic transistor, where the current through QD_A can be altered by varying the properties of QD_B, for example with an external gate voltage.

The two coupled QD interact via hopping of electrons between them and inter-dot Coulomb repulsion, see Fig. 6.2 a). The strengths of these interactions are denoted by t and U_{AB}, respectively. The intra-dot interaction we consider is the Coulomb repulsion. In QD_A we let the Coulomb repulsion, denoted by U_A, be finite whereas in QD_B it is infinite, $U_B = \infty$, thus excluding double occupancies of the levels in QD_B. For simplicity we have chosen U_{AB} sufficiently large, so that we can consider transitions between the two one-particle states and one specific two-particle state, see Table 6.1. In the absence of external magnetic fields, all states are spin-degenerate. Note, however, that the energies of the states explicitly depend on the hopping strength. In addition, for certain choices of the energies ε_A and ε_B, the one-particle states are quasi-degenerate with respect to the hopping. Here, $\varepsilon_{A/B}$ is the single-particle level in $\mathrm{QD}_{A/B}$.

Now, when the eigenstates of the isolated effective QD are known, we attach the external contacts via the couplings $\Gamma^{L/R}$. When no external field is applied, the system acquires the equilibrium chemical potential μ, c.f. Fig. 6.2 b). By applying a bias voltage, and assuming that it drops entirely over the effective QD, the (quasi-) chemical potential $\mu_{L/R}$ forms in the left/right contact. The energies

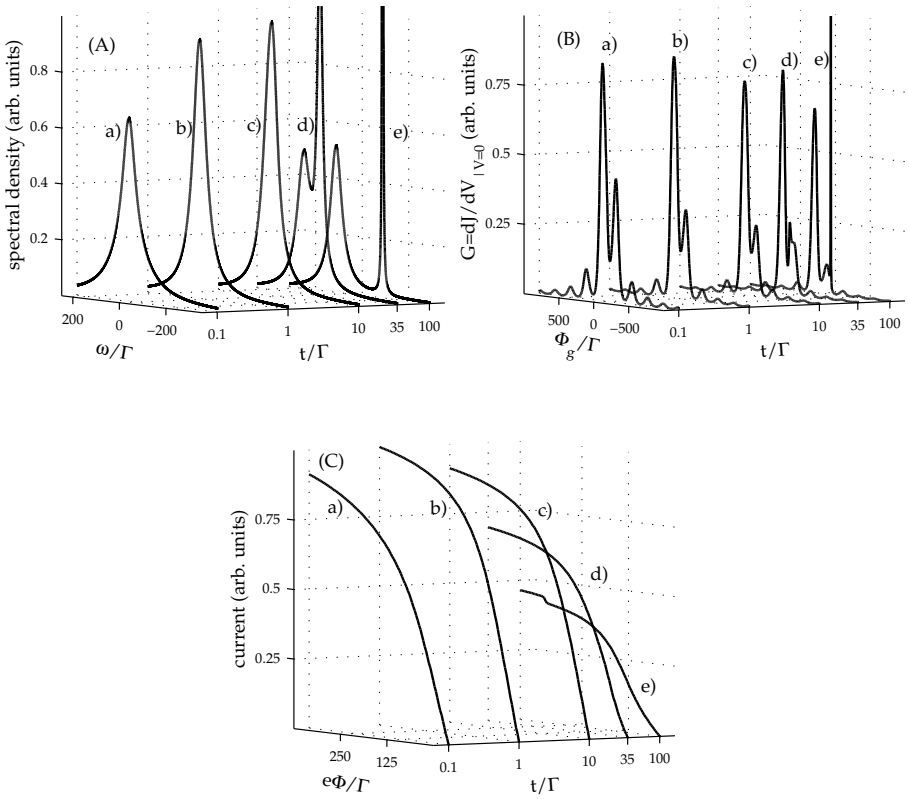

Figure 6.3: The local spectral density (A), the equilibrium conductance (B) and the $J-V$ characteristics of the coupled QD system as a function of the hopping t/Γ.

of the transitions $|\gamma_i\rangle \rightarrow |\Gamma_3\rangle\,,\ i=1,2$ are denoted by $\Delta_{\Gamma_3\gamma_i}$. It is clear that the system has different regimes depending on the hopping strength, since the one-particle energies $E_{\gamma_i\sigma},\ i=1,2$ split as the hopping $t\neq 0$. By investigating its behaviour through the dimensionless ratio t/Γ, where $\Gamma=\Gamma^L+\Gamma^R$, in principle, is the total width of the transitions due to the couplings with the contacts, we can distinguish between a weak and a strong coupling regime, i.e. in our case when $t/\Gamma\gg 10$ and $t/\Gamma\ll 10$, respectively. Indeed, in Fig. 6.3 (A) the local DOS of the coupled QD is plotted for five different hopping strengths. It becomes evident that, for a weak hopping $[t/\Gamma\in[0,10)]$ the transition $\Delta_{\Gamma_3\gamma_1}\approx\Delta_{\Gamma_3\gamma_2}$ see plots a)-c) in Fig. 6.3 (A), leading to that only one peak is observed in the local DOS. As the hopping becomes stronger the level splitting becomes more apparent, plot d)-e), and in the plot e) one of the levels has become almost localized with a large life time. Note that plot e) has a very similar structure to that shown in Fig. 5.2, however, with opposite order of the peaks. In the present case, though, the analysis is performed within the HIA for the effective QD GF. Hence, there is no spin-flip scattering process involved, in this case. Here, the strong peak

corresponds to the fact that the lower level is pushed far below the equilibrium chemical potential as t/Γ increases. Therefore, its interactions with the contact become smaller resulting in that the level becomes strongly localized.

The corresponding equilibrium conductances through the two transitions are shown in Fig. 6.3 (B). At first one notices the main conductance peaks, corresponding to the peaks in the spectral densities. However, in the conductance plots, it becomes clear that there are two transitions involved, since the main peaks actually are separated into two sub-peaks. Apart from this fact, one should also notice that there appear small resonances on each side of the main structures. These side-peaks arise since the transitions are strongly coupled due to the presence of the conduction electrons in the contacts. In Fig. 6.3 (C) the corresponding $J - V$ characteristics are provided. In the weak coupling regime the current growth resembles a single-level behaviour whereas in the strong coupling regime the separation of the levels creates a staircase structure in the $J - V$ characteristics. Note, however, that the steps in the current are not of equal heights, due to the many-body aspects of the system. A more detailed analysis of the coupled QD system can be found in Paper VII.

Summary

SOME QUESTIONS CONCERNING the transport through a QD coupled to external contacts have been posed and studied within a model theory. One important mechanism for tunneling has been explored, namely, the overlap between the states in the interacting region, i.e. the QD, and the contacts. It is clear to any reader that, in reality the system is not divided into several subsystems with their own states that may or may not penetrate into the other. This is simply a model description, however, it is a model which provides the essential physics of tunneling and, moreover, a model which supplies us with a simple framework for calculations of the current. It certainly also gives a comprehensible basis for the phenomenon itself.

An isolated QD carries a number of states and corresponding wave functions. If we describe this QD as a box with hard walls (infinitely high potential barriers), the wave functions are completely confined within the QD. There is no leakage out to the surroundings. Although a hard walled box may serve as good model description of the isolated QD, it does not correspond to any real situation. Actually, one should describe the isolated QD as a quantum well with barriers of finite heights and widths. At the far ends of the barriers we may have put contacts. Then, the wave functions do leak out, with an exponential decay, into the surrounding barriers. If the barrier widths are sufficiently large, the leakage of the wave functions into the contacts is negligible. By decreasing the barrier widths, hence putting the contacts closer, the leakage into the contacts eventually becomes large enough that the QD can no longer be treated as being isolated. Then, since the contacts also carries a number of states with corresponding wave functions, there arises a finite overlap of the states in the QD and the contacts. Hence, an electron located inside the QD is able to tunnel through the barriers into the contacts. By an external field (bias voltage, magnetic field etc.), the electron is forced to move along the direction imposed by the field, thus, a charge current is driven through the system.

Formally, the above discussion can be posed in the following sense. Suppose, at first, that the barrier widths are very large. Then, we can introduce local wave functions in the QD and the contacts, denoted by φ_n and ϕ_k, respectively. Because the wave functions are not completely confined in their corresponding domains, there is an overlap $\langle\varphi_n|\phi_k\rangle = \int \varphi_n^* \phi_k \mathrm{d}\mathbf{r} \neq 0$ them. Now, the parts of the wave

functions inside of the barriers depend directly on the heights and widths of the barriers. Thus, also the overlap $\langle\varphi_n|\phi_k\rangle$ depends on these properties of the barriers. Therefore, if the potential profile of the system is known, we can calculate the current through the system, for instance using Eqs. (4.28), (4.31) and (4.33). On the other hand, if the current through the system is measured in an experiment, then by assuming a specific form of the potential profile (thus assuming a specific set of wave functions for the QD and the contacts) the effective heights and widths of the barriers can be calculated, using the same formulas. In a sense, it is bad that we have to make assumptions about the system in order to calculate its properties. Nevertheless, this is the best we can do, since we anyway cannot take a walk in the system and see how it actually looks. The conclusion then is that we have presented a model theory that can be used both for evaluations of the transport in a given system and for interpretations of experimental results on transport.

It should be noticed that the theory is not only valid for transport through a QD attached to external contacts but, in principle, for any kind of mesoscopic system. Indeed, any system that may be thought of being constituted of a number of subsystems, somehow interacting with each other, can be treated within the formalism provided in Chaps. 3 and 4. Although the examples were directed towards QD coupled to contacts, there was never made an assumption that one of the parts has to be a QD. Therefore, a second conclusion is that the presented theory can be used in nanotransport in general.

Another issue that was included into the formalism was that, the overlaps (non-orthogonality) between the states in the QD and leads also were reflected in the (anti-) commutation relations between the electron operators. By construction of the operators [for instance, as in Eqs. (4.15) and (4.16)], the overlap of the states in the different subsystems became directly linked to the (anti-) commutators between them and, therefore, also made contributions to the tunneling coefficients in the formulas for the currents. These additional contributions serve to include a higher degree of non-linearity in the bias voltage dependence of the current, reflecting many experimental situations. Furthermore, by resolving the total current into quantities for the tunnel and displacement current, it was readily shown that the non-orthogonality gave rise to a contribution to the displacement current which is absent whenever the non-orthogonality is neglected. Thus, a third conclusion is that the orthodox transfer Hamiltonian formalism has been generalized to include more information about the actual system under investigation. In this respect, we have also taken a further step towards quantitative computations of the transport, in real systems.

Finally, in Chap. 5 we studied correlations between the states in a QD. By introducing many-body states and thus diagonalizing the Hamiltonian for the QD, we had the opportunity of investigation the properties of the QD without being disturbed by the intra-dot Coulomb interactions. Actually, in this formulation the propagator (GF) of the QD was presented in a diagrammatic expansion solely in terms of the interactions with the electrons in the contacts. From a practical point of view, this is a very pleasant situation since all assumptions concerning the strength of the interactions in the QD can be made in advance and do not have to be imposed as a final step by taking any limits of any kinds. Because of this,

we do not have to handle involved expressions in the intermediate derivation steps. However, one should note that within the used diagrammatic technique, each diagram may be quite cumbersome to handle. Nevertheless, since the procedure is straight forward (it is like a machinery), one does not have to make any decisions on what kinds of decouplings that are relevant in the specific problem that is considered. Everything is laid out automatically, nothing is lost by chance, and all that has to be done is to evaluate the importance of each diagram.

We would like to draw the attention to that, since the Hamiltonian describing the interacting region is put into a diagonal form, it does not matter whether the *effective* interacting region consists of one, two or more QD or similar structures. By the diagonalization, the interacting region is directly expressed in terms of many-body states. Thus the formal use of Hubbard operators, or other similar theoretical tools, is reasonable and rather natural. Therefore, we can conclude that the technique thus presented in Chap. 5 is general and formally appears exactly in the same form for any diagonal system.

What's next?

The first thing to discuss concerns the transport theory. In formulating it, we borrowed some ideas from an already existing method. Then, the formalism was generalized by including the non-orthogonality that, for simplicity, usually is neglected. In principle then, the generalization ought to give a better description of the transport properties of the system. However, one work for the future is to establish a parameter domain in which the theory is reliable and in which one can be certain that the physical properties are not violated. Outside this domain there should be a complimentary description in order to provide a full understanding of the intrinsic phenomenon of transport in mesoscopic systems.

The second thing to note concerns the description of the QD. At present, we have formulated and described strong correlations between the states in the QD. However, at all times the QD has been assumed to be in the mixed valence regime. All discussions about many-body effects, such as the Kondo effect, has been suppressed since they seem to be more or less irrelevant in this parameter range. On the other hand, all details about the Kondo effect are not yet resolved and it would probably be an rewarding task to try to complete the picture within a many-body formulation. Actually, we have performed the diagrammatic expansion up to the order where the Kondo contributions become visible (J. Fransson, unpublished). On the other hand, in order to provide the community with any deeper understanding of the spin-flip scattering processes involved, further rather complicated and deep calculations have to be carried out.

Lastly, let us discuss spin dependent transport. In Paper V we presented a spin dependent renormalization of the QD levels which, in turn, can be used for the construction of magnetic sensor devices. Magnetic sensors may have lots of applications in the technology that will replace todays electronics. Todays electronics devices are based upon the motion of electronic charges and has nothing, or very little, to do with the spin degree of freedom that electrons carry. For a deeper understanding of the mechanisms for spin dependent transport, it is desirable to work within a many-body approach since within it, and only

within such an approach, can one be sure of finding new correlation effects not yet found. This statement is neither very radical nor controversial, since every physicist knows this fact. However, most theoreticians turn away from it due to its inherited complications, both in the theoretical framework as well as in the analysis of the results. Also, in some special cases it is sufficient to work within the single-particle picture and, for these particular cases, why use a canon to kill a mosquito? On the contrary, this is a very simplistic view of science. As we have shown, there are effects that will not be provided within the fly swatter (single-particle) techniques. In order to find out about these, and others, there simply is no other choice than to employ more sophisticated (many-body) methods. Nature is complex and therefore its description necessarily is complicated.

Appendix A

Diagram technique

HERE, WE GIVE A more detailed discussion of the diagram technique that was briefly introduced in Sec. 5.2.1. However, just as in Sec. 5.2.1 we focus on the particular form of the QD GF that is being used and, for simplicity, we disregard the non-orthogonality between the states in the leads and the QD. For further details and a more general account of the diagram technique we refer to Refs. [75, 76].

The fundamental equation of motion for the QD GF

$$G_{\sigma\sigma'}(t,t') = (-i)\langle \mathrm{T} X^{0\sigma}(t) X^{\sigma' 0}(t')\rangle_U \equiv (-i)\frac{\langle \mathrm{T} S X^{0\sigma}(t) X^{\sigma' 0}(t')\rangle}{\langle \mathrm{T} S\rangle} \tag{A.1}$$

is given by

$$\begin{aligned}\left(i\frac{\partial}{\partial t} - \Delta^0_{\sigma 0}(t) - \Delta U_{\sigma 0}(t)\right) G_{\sigma\sigma'}(t,t') - U_{\sigma\bar{\sigma}}(t) G_{\bar{\sigma}\sigma'}(t,t') &= \delta(t-t') P_{\sigma\sigma'}(t) \\ &+ \sum_k v^*_{k\sigma}(t)(-i)\langle \mathrm{T}(h^0 + h^\sigma)(t) c_{k\sigma}(t) X^{\sigma' 0}(t')\rangle_U \\ &+ \sum_k v^*_{k\bar{\sigma}}(t)(-i)\langle \mathrm{T} Z^{\bar{\sigma}\sigma}(t) c_{k\bar{\sigma}}(t) X^{\sigma' 0}(t')\rangle_U . \end{aligned} \tag{A.2}$$

The appearance of the source fields $\Delta U_{\sigma 0}(t) = U_\sigma(t) - U_0(t)$ and $U_{\sigma\bar{\sigma}}(t)$ in Eq. (A.2) is due to the temporal derivative $i\partial/\partial t \mathrm{T} S X^{0\sigma}(t) = \mathrm{T} S[X^{0\sigma}, \mathcal{H} + \mathcal{H}'(t)]$ in the QD GF. In the equation of motion for the QD GF the three operator quantities

$$(-i)\langle \mathrm{T}(h^0 + h^\sigma)(t) c_{k\sigma}(t) X^{\sigma' 0}(t')\rangle_U$$

$$(-i)\langle \mathrm{T} Z^{\bar{\sigma}\sigma}(t) c_{k\bar{\sigma}}(t) X^{\sigma' 0}(t')\rangle_U$$

appear. These can be rewritten in terms of $G_{\sigma\sigma'}(t,t')$ and functional derivatives thereof. By considering the variation $\delta F_{k\sigma\sigma'}$ of the mixed GF $F_{k\sigma\sigma'}(t,t') = (-i)\langle \mathrm{T} c_{k\sigma}(t) X^{\sigma' 0}(t)\rangle_U$ with respect to the source field $U_\xi(t'')$, one finds that [75, 76]

$$(-i)\langle \mathrm{T} Z^\xi(t'') c_{k\sigma} X^{\sigma' 0}(t')\rangle_U = \left(\langle \mathrm{T} Z^\xi(t'')\rangle_U + i\frac{\delta}{\delta U_\xi(t'')}\right) F_{k\sigma\sigma'}(t,t'). \tag{A.3}$$

The mixed GF is given by

$$F_{k\sigma\sigma'}(t,t') = \int_{t_0}^{t_0-i\beta} v_{k\sigma}(t) g_{k\sigma}(t,s) G_{\sigma\sigma'}(s,t')\mathrm{d}s. \tag{A.4}$$

For a shorter notation we introduce $V_\sigma(t,t') = \sum_k v^*_{k\sigma}(t) v_{k\sigma}(t') g_{k\sigma}(t,t')$ and put $R_{\sigma\sigma'}(t) = i[\delta_{\sigma\sigma'}\delta/\delta U_{00}(t) + \delta/\delta U_{\sigma'\sigma}(t)]$. We also define $P_\sigma(t) \equiv P_{\sigma\sigma}(t)$ and $R_\sigma(t) \equiv R_{\sigma\sigma}(t)$. Thus, the exact equation of motion for the QD GF can be written

$$\begin{aligned}\left(i\frac{\partial}{\partial t} - \Delta^0_{\sigma 0}(t) - \Delta U_{\sigma 0}(t)\right) G_{\sigma\sigma'}(t,t') - U_{\sigma\bar\sigma}(t) G_{\bar\sigma\sigma'}(t,t') &= \delta(t-t') P_{\sigma\sigma'}(t) \\ &+ [P_\sigma(t) + R_\sigma(t)] \int_{t_0}^{t_0-i\beta} V_\sigma(t,s) G_{\sigma\sigma'}(s,t')\mathrm{d}s \\ &+ [P_{\sigma\bar\sigma}(t) + R_{\sigma\bar\sigma}(t)] \int_{t_0}^{t_0-i\beta} V_{\bar\sigma}(t,s) G_{\bar\sigma\sigma'}(s,t')\mathrm{d}s,\end{aligned} \tag{A.5}$$

completely expressed in terms of the QD GF and functional derivatives thereof. Physical information about the QD is obtained from Eq. (A.5) by applying the functional derivatives up to the desired order in the interactions V_σ and thereafter letting the source fields, that are not actually applied to the system, $U_\xi(t) \to 0$. In this limit, all quantities that do not conserve the longitudinal component of the total spin vanish, although their functional derivatives may not. Thus, in the final expression of the QD GF, i.e. when the limit $U_\xi(t) \to 0$ has been taken, one can just discard terms containing locators and cumulants of the transition $|\sigma\rangle \to |\bar\sigma\rangle$ and its opposite.

When applying the functional derivatives on the QD GF it should be noticed that it is composed by the product of its locator $D_{\sigma\sigma}(t,t')$ and the cumulant $P_{\sigma\sigma}(t)$, that is, $G_{\sigma\sigma'}(t,t') = D_{\sigma\sigma''}(t,t') P_{\sigma''\sigma'}(t')$. In addition, not only the locator is subject to the functional derivative but also the end-factor $P_{\sigma''\sigma'}(t')$. Hence, varying the QD GF yields $\delta G_{\sigma\sigma'} = (\delta D_{\sigma\sigma''}) P_{\sigma''\sigma'} + D_{\sigma\sigma''}(\delta P_{\sigma''\sigma'})$. The locator matrix D should satisfy the relation $DD^{-1} = I = D^{-1}D$ which implies that $\delta(DD^{-1}) = (\delta D)D^{-1} + D(\delta D^{-1}) = 0$. This results in

$$\begin{aligned} R_{ss'}(t'') D_{\sigma\sigma'}(t,t') &= -i \sum_{\sigma_1\sigma_2} \int_{t_0}^{t_0-i\beta} D_{\sigma\sigma_1}(t,t_1) \\ &\quad \times \Gamma_{\sigma_1\sigma_2}(t_1,t_2; R_{ss'}(t'')) D_{\sigma_2\sigma'}(t_2,t')\mathrm{d}t_1\mathrm{d}t_2, \end{aligned} \tag{A.6}$$

where we have introduced the vertex function

$$\Gamma_{\sigma_1\sigma_2}(t_1,t_2; R_{ss'}(t'')) \equiv \left(\delta_{ss'}\frac{\delta}{\delta U_{00}(t'')} + \frac{\delta}{\delta U_{s's}(t'')}\right) D^{-1}_{\sigma_1\sigma_2}(t_1,t_2). \tag{A.7}$$

The general vertex function can be expanded further by introducing the zero vertex

$$\Gamma^0_{\sigma_1\sigma_2}(t_1,t_2;R_{ss'}(t'')) \equiv \left(\delta_{ss'}\frac{\delta}{\delta U_{00}(t'')}+\frac{\delta}{\delta U_{s's}(t'')}\right)d^{-1}_{\sigma_1\sigma_2}(t_1,t_2), \tag{A.8}$$

where $d_{\sigma\sigma'}(t,t')$ is the locator of the isolated QD, and the self-operator

$$\begin{aligned} S_{\sigma_1\sigma_2}(t_1,t_2) &\equiv P_{\sigma_1\sigma_2}(t_1)V_{\sigma_2}(t_1,t_2) \\ &-i\int_{t_0}^{t_0-i\beta} V_{\sigma_3}(t_1,t_3)D_{\sigma_3\sigma_4}(t_3,t_4)\Gamma_{\sigma_4\sigma_2}(t_4,t_2;R_{\sigma_3\sigma_1}(t_1))\mathrm{d}t_3\mathrm{d}t_4. \end{aligned} \tag{A.9}$$

In this expression summation over the spin-indices σ_3, σ_4 is understood. The zero locator $d_{\sigma\sigma'}(t,t')$ satisfies the equation

$$\left(i\frac{\partial}{\partial t}-\Delta^0_{\sigma 0}-\Delta U_{\sigma 0}(t)\right)d_{\sigma\sigma'}(t,t')-U_{\sigma\bar\sigma}(t)d_{\bar\sigma\sigma}(t,t')=\delta(t-t') \tag{A.10}$$

and it is easy to verify that

$$\Gamma^0_{\sigma_1\sigma_2}(t_1,t_2;R_{ss'}(t''))=(\delta_{ss'}\delta_{\sigma_1\sigma_2}-\delta_{\sigma_1 s}\delta_{\sigma_2 s'})\delta(t-t'). \tag{A.11}$$

Thus

$$\begin{aligned} \Gamma_{\sigma_1\sigma_2}(t_1,t_2;R_{ss'}(t'')) &= (\delta_{ss'}\delta_{\sigma_1\sigma_2}-\delta_{\sigma_1 s}\delta_{\sigma_2 s'})\delta(t-t') \\ &-iR_{ss'}(t'')S_{\sigma_1\sigma_2}(t_1,t_2). \end{aligned} \tag{A.12}$$

Resolving the vertex in the self-operator, ones arrives at a perturbation series in terms of the interaction $V_\sigma(t)$, by successively applying the functional derivatives to the locators and cumulants.

The functional derivative of the end-factor $R_{ss'}(t'')P_{\sigma\sigma'}(t)$ is given by

$$\begin{aligned} R_{ss'}(t'')P_{\sigma\sigma'}(t) &= \langle \mathrm{T}[\delta_{ss'}h^0+Z^{s's}](t'')[\delta_{\sigma\sigma'}h^0+Z^{\sigma'\sigma}](t)\rangle_U \\ &-P_{ss'}(t'')P_{\sigma\sigma'}(t) \end{aligned} \tag{A.13}$$

It is readily seen that $R_\sigma(t^+)P_\sigma(t')=\langle \mathrm{T}(h^0+h^\sigma)(t)(h^0+h^\sigma)(t')\rangle_U - P_\sigma(t^+)P_\sigma(t')$. In contrast, the transverse functional derivative $R_{\sigma\bar\sigma}(t^+)P_{\bar\sigma\sigma}(t')=iK_{\bar\sigma\sigma}(t^+,t')-P_{\sigma\bar\sigma}(t^+)P_{\bar\sigma\sigma}(t')$, where

$$K_{\bar\sigma\sigma}(t^+,t')=(-i)\langle \mathrm{T}Z^{\bar\sigma\sigma}(t^+)Z^{\sigma\bar\sigma}(t')\rangle_U \equiv (-i)\frac{\langle \mathrm{T}SZ^{\bar\sigma\sigma}(t^+)Z^{\sigma\bar\sigma}(t')\rangle}{\langle \mathrm{T}S\rangle}.$$

The bare Bose-like GF $K_{\bar\sigma\sigma}(t^+,t')$ satisfies the equation

$$\left(i\frac{\partial}{\partial t}-\Delta^0_{\sigma\bar\sigma}(t^+)-\Delta U_{\sigma\bar\sigma}(t^+)\right)K_{\bar\sigma\sigma}(t^+,t')\delta(t^+-t')[P_{\bar\sigma}(t^+)-P_\sigma(t^+)], \tag{A.14}$$

where we have discarded propagators like $(-i)\langle \mathrm{T}h^{\sigma}(t^{+})Z^{\sigma\bar{\sigma}}(t')\rangle_{U}$ since they only give contributions for functional derivatives that are irrelevant for $K_{\bar{\sigma}\sigma}(t^{+},t')$, in this approximation.

The general structure of the QD GF equation of motion can now be found as

$$\left(i\frac{\partial}{\partial t}-\Delta^{0}_{\sigma 0}(t)-\Delta U_{\sigma 0}(t)\right)G_{\sigma\sigma'}(t,t')-U_{\sigma\bar{\sigma}}(t)G_{\bar{\sigma}\sigma'}(t,t')=\mathbb{P}_{\sigma}(t,t') + \int_{t_0}^{t_0-i\beta}\Sigma_{\sigma}(t,s)G_{\sigma\sigma'}(s,t')\mathrm{d}s, \tag{A.15}$$

where the dressed cumulant

$$\begin{aligned}\mathbb{P}_{\sigma}(t,t') &= \delta(t-t')P_{\sigma}(t) \\ &\quad + \sum_{s}\int_{t_0}^{t_0-i\beta} V_{s}(t,t_1)D_{s}(t_1,t')\mathrm{d}t_1 R_{\sigma s}(t^{+})P_{s\sigma'}(t')\end{aligned} \tag{A.16}$$

and the self-energy

$$\begin{aligned}\Sigma_{\sigma}(t,t') &= P_{\sigma}(t^{+})V_{\sigma}(t,t') \\ &\quad -i\sum_{s}\int_{t_0}^{t_0-i\beta} V_{s}(t,t_1)D_{s}(t_1,t_2)\Gamma_{s\sigma}(t_2,t';R_{\sigma s}(t^{+}))\mathrm{d}t_1\mathrm{d}t_2.\end{aligned} \tag{A.17}$$

Acknowledgments

FROM THE FIRST DAY as a Ph.D. student I've been both terrified and happy of the way of life that I've chosen, for what can I do in physics that it's worth devoting my life to??? Almost from the beginning I've had very much help and guidance from Igor Sandalov who's been my supervisor, although it never became formal. I thank you very much for letting me asking all these questions about things I probably was supposed to know about, for letting me say things that wasn't correct, for helping me out when I was completely stuck in the problems with Green functions and diagram techniques, and for correcting all stupid mistakes that I sent to you in all possible and impossible times. Most of the times I've enjoyed working with you, when I wasn't struggling in vain with the Hubbard operators. I've learned so many things, how to work theoretically and to focus on the things that one can do with pencil and paper, and how to realize which things that cannot be delivered from a purely pencil-and-paper-theoretical point of view. Thanks a lot Igor.

In order to put together the stuff I've been doing, Olle Eriksson has been an invaluable help. When there were so many thing that I wanted to write in the papers, Olle made some cuts here and there to make the papers look like being scientific. Good for me. But, apart from being a good mentor in writing papers, Olle has also been an encouraging and understanding person which I'm very grateful to have had around. Almost always he's been able to spend some time for my questions and concerns. For that matter, he's the professor that invited me for pike fishing on several occasions, and he let me catch more fish all times but one [and that particular occasion was very painful;-)]. Thanks a lot Olle.

Then, I want to thank my formal supervisor, Börje Johansson. Imagine this, you have established a group of people that are doing computational physics. Then comes this student to apply for a graduate student position. The student is very stubborn in making analytical theoretical work, however, the student doesn't know a thing about quantum mechanics. On the other hand, the student talks about some skills in mathematics and classical physics. Yet, you offer this student a position in your group and, thereto, letting the door open for virtually anything. I'm very happy that you let me come along and I sincerely hope that I haven't made you disappointed. Thanks a lot Börje.

Fysik IV is very pleasant planet to live on. There's always something going

on and there's always someone to talk to when you drown in problems, or, when you just want to talk away a couple of minutes. Unfortunately I don't know all (around 40) members in the group, but I thank you all. Especially, I want to thank Elisabeth Sjöstedt, Lars Nordström, Massimiliano Colarieti-Tosti, Urban Lundin, Erik Holmström, Anna Delin, Anders Niklasson, Susanne Mirbt, Mattias Klintenberg, Olivier Bengone Håkan Hugosson and Biplap Sanyal for all your encouragements and beliefs in me. What could be a better help than good people to rely on? Thank you. I also want to thank Susanne Mirbt for good conversations about science and other things. Bettan and Urban also read and commented on the manuscript. A special thank to Bettan and Mamo for listening to me during the hard times the last one and a half year. Thanks a lot Fysik IV.

I also thank Stiftelsen Anna-Maria Lundins stipendiefond for providing me money to conferences and work on four continents.

SLUTLIGEN SKALL SJÄLVKLART inte släkt och vänner glömmas bort. Utan någon hemmavid som tror på mig och i dåliga tider får mig att inse mina förtjänster, skulle det här arbetet antagligen gått mycket dåligt. Jag har nog varit trälig ibland, men på något märkligt sätt har du stått ut med allt. Tack så mycket Johanna. Mina barn, Eugenia och Elmer, har såklart inte bidragit med något sådant men utan dem skulle det varit svårt att koppla bort arbetet med jämna mellanrum. Alltså får de en skopa tack också.

Nää mamma, kvantprickar är inte något som katterna ligger på. Med tiden har ni blivit mer och mer intresserade av det jag sysslar med, låt vara att vi lämnat fysiken därhän för det mesta. De senaste åren har ni kommit med mycken uppmuntran och många frågor om hjälp. Tack så mycket mamma och pappa.

Tack så mycket Sofia, svärmor, Otto, svärfar, svågrar och svägerskor för att ni trott på mig och haft förståelse under mina perioder av sämre humör. Jag skyller allt på avhandlingen. Jag skall skriva en till bara för att ha något att skylla på i fortsättningen.

Andreas, min speciella kamrat. Tack så oerhört mycket för allt lyssnande på mina utläggningar om sakernas varande, tack för din omtanke och medmänsklighet under de lätta och svåra tiderna. Tack för din uppriktiga vänskap.

Johan, Christina, Pelle och Annika - ni har lyssnat på mitt prat om fysik, skrivande med mera. Tack för ert tålamod och vänskap.

Jag vill också uppmärksamma att mina el-tele-lärare Anders Gustafsson och Janne Sällberg var de första som fick mig att inse kunnandets njutningen.

Så var det slut då. De som ovan glömts bort får känna sig medräknade i mitt allmänna och aldrig sinande tackande. Avhandlingen är klar. Lite sorgligt känns det, men förbannat skönt.

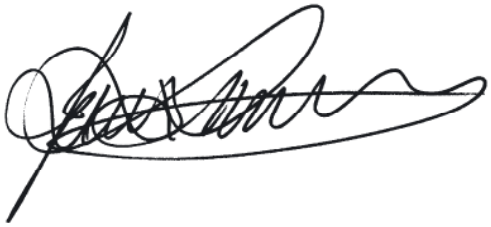

Jonas Fransson

Uppsala, September 23, 2002

BIBLIOGRAPHY

[1] A.A. Abrikosov. *Physics*, **2**, 5, (1965).

[2] A.A. Abrikosov. *Introduction to the Theory of Normal Metals*. (Academic Press, Inc., New York, 1972).

[3] A.A. Abrikosov, L.P. Gorkov, and I.E. Dzyaloshiski. *Methods of Quantum Field Theory in Statistical Mechanics*. (Dover Publications Inc., New York, 1975).

[4] M.P. Anantram and S. Datta. *Phys. Rev. B*, **51**, 7632, (1995).

[5] P.W. Anderson. *Phys. Rev.*, **124**, 41, (1961).

[6] A.F. Barabanov, K.A. Kikoin, and L.A. Maksimov. *Teor. Mat. Fiz.*, **20**, 364, (1974).

[7] A.F. Barabanov, K.A. Kikoin, and L.A. Maksimov. *Teor. Mat. Fiz.*, **25**, 87, (1974).

[8] A.F. Barabanov, K.A. Kikoin, and L.A. Maksimov. *Solid State Commun.*, **15**, 977, (1975).

[9] A.F. Barabanov, K.A. Kikoin, and L.A. Maksimov. *Solid State Commun.*, **18**, 1527, (1976).

[10] J. Bardeen. *Phys. Rev. Lett.*, **6**, 57, (1961).

[11] D. Bohm. *Quantum Theory*. (Prentice Hall Inc., New York, 1951).

[12] R. Büttiker, Y. Imry, R. Landauer, and S. Pinhaus. *Phys. Rev. B*, **31**, 6207, (1985).

[13] C. Caroli, R. Combescot, P. Nozieres, and D. Saint-James. *J. Phys. C*, **4**, 916, (1971).

[14] L.L. Chang, L. Esaki, and R. Tsu. *Appl. Phys. Lett.*, **24**, 593, (1974).

[15] M.H. Cohen, L.M. Falicov, and J.C. Philips. *Phys. Rev. Lett.*, **8**, 316, (1962).

[16] S. Datta. *Electronic Transport in Mesoscopic Systems*. (Cambridge University Press, Cambridge, 1995).

[17] S.T. Dembinski. *Physica*, **30**, 1217, (1964).

[18] F.J. Dyson. *Phys. Rev.*, **102**, 1217, (1956).

[19] A.L. Efros, E.I. Rashba, , and M. Rosen. *Phys. Rev. Lett.*, **87**, 206601.

[20] J.C. Egues. *Phys. Rev. Lett.*, **80**, 4578, 1998.

[21] J.C. Egues, C. Gould, G. Richter, and L.W. Molenkamp. *Phys. Rev. B.*, **64**, 195319, 2001.

[22] L. Esaki. *Phys. Rev.*, **109**, 603, (1958).

[23] L.D. Faddeev. *Sov. Phys. JETP*, **12**, 1014, (1961).

[24] D.K. Ferry and S.M. Goodnick. *Transport in Nanostructures*. (Cambridge University Press, 1997).

[25] J. Fransson, O. Eriksson, B. Johansson, and I. Sandalov. *Physica B*, **272**, 28, (1999).

[26] J. Fransson, O. Eriksson, and I. Sandalov. *submitted to Phys. Rev. B*.

[27] J. Fransson, O. Eriksson, and I. Sandalov. *Physical Review B*, **64**, 153403, (2001).

[28] M.J. Gilbert and J.P. Bird. *Appl. Phys. Lett.*, **77**, 1050.

[29] A. Groshev, T. Ivanov, and V. Valtchinov. *Phys. Rev. Lett.*, **66**, 1082, (1991).

[30] S. Haraichi, T. Wada, S.M. Gordwadkar, K. Ishiia, and H. Hiroshima. *J. Vac. Sci. Technol. B*, **5**, 1406, (1997).

[31] H. Haug and A.-P. Jauho. *Quantum Kinetics in Transport and Optics of Semi-Conductors*. (Springer-Verlag, Heidelberg, 1998).

[32] T. Hayashi, M. Tanaka, and A. Asamitsu. *J. Appl. Phys.*, **87**, 4673, 2000.

[33] M.H. Hettler. *Phys. Rev. Lett.*, **74**, 4907, (1995).

[34] A.C. Hewson. *The Kondo Problem to Heavy Fermions*. (Cambridge University Press, paperback edition, 1997).

[35] F. Hofmann, T. Heinzel, D.A. Wharam, and J.P. Kotthaus. *Phys. Rev. B*, **51**, 13872, (1995).

[36] J. Hubbard. *Proc. Roy. Soc. A*, **276**, 238, (1963).

[37] J. Hubbard. *Proc. Roy. Soc. A*, **277**, 237, (1963).

[38] Y.A. Izyumov, B.M. Letfulov, and E.V. Shipitsyn. *J. Phys: Condensed Matter*, **6**, 5137, (1994).

[39] Y.A. Izyumov, B.M. Letfulov, E.V. Shipitsyn, M. Bartkowiak, and K.A. Chao. *Phys. Rev. B*, **46**, 15697, (1992).

[40] Y.A. Izyumov, B.M. Letfulov, E.V. Shipitsyn, and K.A. Chao. *Int. J. Mod. Phys. B*, **6**, 3479, (1992).

[41] Y.A. Izyumov and Y.N. Skryabin. *Statistical Mechanics of Magnetically ordered systems*. (Consultants Bureau, New York, 1989).

[42] A.-P. Jauho. *cond-mat/9711141*, (1997).

[43] A.P. Jauho, N.S. Wingreen, and Y. Meir. *Phys. Rev. B*, **50**, 5528, (1994).

[44] M. Johnson. *Phys. Rev. B*, **58**, 9635, 1998.

[45] W. Jones and N.H. March. *Theoretical Solid State Physics*. (Dover Publications Inc., New York, 1985).

[46] M. Julliere. *Phys. Lett*, **54A**, 225, 1975.

[47] L.P. Kadanoff and G. Baym. *Quantum Statistical Mechanics*. (Benjamin, New York, 1962).

[48] L.V. Keldysh. *Sov. Phys. JETP*, **20**, 1018, (1965).

[49] C. Kittel. *Quantum Theory of Solids*. (Wiley, New York, 1963).

[50] T. Koga, J. Nitta, H. Takayanagi, and S. Datta. *Phys. Rev. Lett.*, **88**, 126601.

[51] J. Kondo. *Progr. Theor. Phys.*, **32**, 37, (1964).

[52] R. Kubo. *J. Phys. Soc. Japan*, **12**, 570, (1957).

[53] J.G. Kushmerick, D.B Holt, J.C. Yang, J. Naciri, M.H. Moore, and R. Shashidhar. *Phys. Rev. Lett.*, **89**, 086802, (2002).

[54] C. Lacroix. *J. Phys. F*, **11**, 2389, (1981).

[55] L.D. Landau and E.M. Lifschitz. *Quantum Mechanics (Non-relativistic theory), third ed.* (Pergamon Press, Oxford, 1977).

[56] R. Landauer. *IBM J. Res. Develop.*, **1**, 223, (1957).

[57] R. Landauer. *Phil Mag.*, **21**, 863, (1970).

[58] D.C. Langreth. Linear and nonlinear response theory with applications. In J.T. Devreese and V.E. van Doren, editors, *Nato Advanced Study Institute*, volume 17 of *Series B: Physics*. (Plenum, New York, 1976).

[59] A.I. Larkin and K.A. Matveev. *Sov. Phys. JETP*, **66**, 580, (1987).

[60] *Appl. Phys. Lett.*, **77**, 3630, 2000.

[61] O. Madelung. *Introduction to Solid-State Theory*. (Springer-Verlag, Berlin-Heidelberg-New York, 1978).

[62] G.D. Mahan. *Many-Particle Physics*. (Plenum, New York, second edition, 1990).

[63] R.D. Mattuck. *A Guide to Feynman Diagrams in the Many-Body Problem*. (Dover Publications Inc., New York, 1992).

[64] Y. Meir and N.S. Wingreen. *Phys. Rev. Lett.*, **68**, 2512, (1992).

[65] Y. Meir, N.S. Wingreen, and P.A. Lee. *Phys. Rev. Lett.*, **66**, 3048, (1991).

[66] Y. Meir, N.S. Wingreen, and P.A. Lee. *Phys. Rev. Lett.*, **70**, 2601, (1993).

[67] J.S. Moodera, L.R. Kinder, T.M. Wong, and R. Meservey. *Phys. Rev. Lett.*, **74**, 3273, 1995.

[68] T. Oguchi. *Phys. Rev.*, **117**, 117, (1960).

[69] P. Pals and A. MacKinnon. *J. Phys: Condensed Matter*, **8**, 5401, (1996).

[70] G. Papp and F.M. Peeters. *Appl. Phys. Lett.*, **78**, 2184, 2001.

[71] S.H. Persson and L. Olofsson. *Appl. Phys. Lett.*, **74**, 2546, (1999).

[72] P. Recher, E.V. Sukhorukov, and D. Loss. *Phys. Rev. Lett.*, **85**, 1962, 2000.

[73] A.E. Ruckenstein and S. Schmitt-Rink. *Phys. Rev. B*, **38**, 7188, (1988).

[74] A.E. Ruckenstein and S. Schmitt-Rink. *Int. J. Mod. Phys. B*, **3**, 1809, (1989).

[75] I. Sandalov, B. Johansson, and O. Eriksson. *cond-mat/0011259*, (2001).

[76] I. Sandalov, U. Lundin, and O. Eriksson. *cond-mat/0011260*, (2001).

[77] I. Sandlov and V.I. Filatjev. *Physica B*, **162**, 139, (1990).

[78] J. Schwinger. *Proc. Natl. Acad. Sci. U.S.*, **37**, 452, (1951).

[79] M. Sharma, J.H. Nickel, T.C. Anthony, and S.X. Wang. *Appl. Phys. Lett.*, **77**, 2219, 2000.

[80] M. Sharma, S.X. Wang, and J.N. Nickel. *Phys. Rev. Lett.*, **82**, 616, 1999.

[81] A. Sillbille, J.F. Palmier, H. Wand, and F. Mollet. *Phys. Rev. Lett.*, **64**, 52, (1990).

[82] H.-S. Sim, G. Ihm., N. Kim, and K.J. Chang. *Phys. Rev. Lett.*, **87**, 146601, 2001.

[83] J.G. Simmons. *J. Appl. Phys.*, **34**, 1793, (1963).

[84] J.G. Simmons. *J. Appl. Phys.*, **34**, 1828, (1963).

[85] T.C.L.G. Sollner, W.D. Goodhue, P.E. Tannenwald, C.D. Parker, and D.D. Peck. *Appl. Phys. Lett.*, **43**, 588, (1983).

[86] H. Suhl. *Phys. Rev.*, **138**, A515, (1965).

[87] R. Tsu and L. Esaki. *Appl. Phys. Lett.*, **22**, 562, (1973).

[88] A.M. Tsvelick and P.B. Wiegmann. *Adv. Phys.*, **32**, 453, (1983).

[89] C.M. Varma and Y. Yafet. *Phys. Rev. B*, **13**, 2950, (1976).

[90] B. Wang, J. Wang, and H. Guo. *Phys. Rev. Lett.*, **82**, 398, (1999).

[91] J. Wang, P.P. Freitas, and E. Snoeck. *Appl. Phys. Lett.*, **79**, 4553, 2001.

[92] N.S. Wingreen, A.-P. Jauho, and Y. Meir. *Phys. Rev. B*, **48**, 8487, (1993).

[93] K. Yosida. *Theory of Magnetism*. (Springer-Verlag, Berlin-Heidelberg-New York, 1996).

[94] J.Q. You, C.-H. Lam, and H.Z. Zheng. *Phys. Rev. B*, **62**, 1978, (2000).

[95] C. Zener. *Proc. Roy. Soc.*, **A145**, 523, (1943).

[96] J.M Ziman. *Electrons and Phonons*. (Oxford Univeristy Press, Inc., New York, 1960).